VNIVERSIDAD DE SALAMANCA
Departamento de Medicina

Microambiente y lesión ósea en el mieloma múltiple:

Papel de las células *stem*mesenquimales y nuevos fármacos

Antonio García Gómez

2012

CIC Centro de Investigación del Cáncer
CSIC Consejo Superior de Investigaciones Científicas
IBSAL Instituto de Investigación Biomédica de Salamanca

Dª.Mercedes Garayoa Berrueta,Doctora en Ciencias Biológicas e Investigadora del Centro de Investigación del Cáncer de Salamanca.

D. Fermín Martín Sánchez-Guijo,Profesor Asociado de la Facultad de Medicina de la Universidad de Salamanca y Médico Adjunto del Servicio de Hematología del Hospital Universitario de Salamanca.

D. Jesús Fernando San Miguel Izquierdo, Catedrático de Hematología de la Facultad de Medicina de la Universidad de Salamanca, Jefe de Servicio de Hematología del Hospital Universitario de Salamanca e Investigador del Centro de Investigación del Cáncer de Salamanca.

CERTIFICAN:

Que el trabajo realizado bajo nuestra dirección por **D.Antonio García Gómez** titulado: *Microambiente y lesión ósea en el mieloma múltiple: papel de las células "stem" mesenquimales y nuevos fármacos*, reúne las condiciones de originalidad y calidad científica requeridas para optar al grado de Doctor por la Universidad de Salamanca.

Y para que así conste a los efectos oportunos, firmamos el presente certificado en Salamanca, a 15 de noviembre de 2012.

Fdo.:

Dra. Mercedes Garayoa Berrueta

Dr. Fermín Martín Sánchez Guijo

Prof. Dr. Jesús San Miguel Izquierdo

Este trabajo ha sido financiado con las siguientes ayudas:

- Proyecto del Centro en Red de Medicina Regenerativa y Terapia Celular de Castilla y León "Estudio de las células mesenquimales en el mieloma múltiple: papel en la patogenia de la enfermedad y en el desarrollo de la lesión lítica y perspectivas en terapia celular"
- Proyecto Acción Estratégica en Salud del Ministerio Español de Ciencia e Innovación – Instituto de Salud Carlos III (PI081825) "Estudio de la eficacia y mecanismo de acción de fármacos anti-mieloma conespecial incidencia sobre el microambiente de la médula ósea"
- Red Temática de Investigación Cooperativa en Cáncer (RD06/0020/0006)
- Proyecto de la Fundación de Investigación Médica Mutua Madrileña (AP27262008) "Estudio de la eficacia y mecanismo de acción de fármacos inhibidores de tirosina quinasas sobre las células mielomatosas y el microambiente de la médula ósea"
- Beca de la Fundación Española de Hematología y Hemoterapia "Identificación y estudio de posibles dianas terapéuticas en el mieloma múltiple a partir de sistemas de co-cultivo de células mielomatosas y células *stem*mesenquimales de la médula ósea"

Agradecimientos

Aunque resulta difícil, intentaré resumir en unas pocas líneas a todos aquellos que han contribuido por su apoyo y dedicación a que esta Tesis se pudiera hacer realidad.

En primer lugar, agradecer al Dr. Jesús San Miguel la oportunidad que me brindó para formar parte de su grupo, así como por transmitir su experiencia, su filosofía de trabajo y su pasión por la investigación.

A la Dra. Mercedes Garayoa, por compartir su tiempo, sus conocimientos y su entusiasmo científico, por su confianza, por hacer cada día de trabajo más fácil, y por haber guiado mis primeros pasos en el mundo de la investigación.

Al Dr. Fermín Sánchez-Guijo, por su constante disposición a solucionar cualquier problema y por ampliar siempre el punto de vista científico.

A todos y cada uno de mis compañeros del *Laboratorio 12*, por crear un ambiente de trabajo ideal, por la infinidad de ayuda y consejos recibidos, por compartir tantos momentos, buenos y no tan buenos, y por crecer conmigo durante estos años.

A mis compañeros del *Laboratorio de Terapia Celular*, por su disposición a echar una mano siempre, su cercanía y su invariable buen humor.

A mis compañeros del *Laboratorio 2, y 15*, por toda la ayuda y los consejos que han hecho que muchos experimentos tengan éxito.

A todos mis compañeros del CIC, por el tiempo, la confianza y las metas que hemos compartido y por todo lo que me han enseñado.

Al Dr. Javier de las Rivas, por su paciencia, su tiempo y por haberme acercado al mundo de la bioinformática de una forma tan familiar.

Al Dr. Juan Blanco y a todos los facultativos del *Servicio de Traumatología y del Servicio de Hematología del Hospital de Salamanca* que han formado parte de la cadena para que cada una de las muestras llegara a nuestras manos. Y por supuesto, a cada uno de los donantes y de los pacientes.

Al *Banco de Tumores del CIC* y a la *Unidad de Imagen del CIMA*, porque sin ellos serían imposibles las evidencias *in vivo* de nuestros estudios.

A las entidades que han dado soporte económico a esta Tesis: al Ministerio de Ciencia e Innovación, a la Fundación Mutua Madrileña, a la Red de Terapia Celular de Castilla y León y a la Red Temática de Investigación Cooperativa en Cáncer, así como a la Fundación Española de Hematología y Hemoterapia.

A todas las personas que se han cruzado conmigo a lo largo de esta etapa en Salamanca y que me han ayudado a conocerme más, por todos los buenos momentos que hemos compartido y por los que quedan. A mis amigos de la infancia, con los que tengo la suerte de seguir creciendo, por demostrarme que siempre están ahí.

A mi familia, que me ha hecho ser quien soy, por todos los valores que me han transmitido, su preocupación y apoyo incondicional.

A todos ellos, **muchas gracias de corazón.**

Índice

Abreviaturas

Ag	Antígeno
AID	*Activation-inducedcytidinedeaminase*
Akt	*v-akt murine thymoma viral oncogene*
ALP	*Alkaline phosphatase*
APC	*Adenomatosis polyposiscoli*
APRIL	*A proliferation-inducing ligand*
ATP	*Adenosine triphosphate*
ATP6i	*T-cell, immune regulator 1, ATPase, H^+ transporting, lysosomal V0 subunit A3*
BAD	*BCL2-associated agonist of cell death*
BAFF	*B-cell activating factor*
Bcr-Abl	*Breakpoint cluster region-Abelson tyrosine-protein kinase*
bFGF	*Basic fibroblast growth factor*
BGLAP	*Gamma-carboxyglutamic acid-containing protein/Osteocalcin*
BIRC2/3	*Baculoviral IAP repeatcontaining 2/3*
BP	Bisfosfonatos
c-fos	*FBJmurineosteosarcoma viraloncogenehomolog*
c-fms	*Colonystimulating factor 1 receptor*
c-jun	*Jun oncogene*
c-Kit/CD117	*Kit oncogene*
c-Src	*v-src sarcoma (Schmidt-Ruppin A-2) viral oncogenehomolog (avian)*
CAII	*Carbonicanhidrase II*
CAMDR	*Cell Adhesion-Mediated Drug Resistance*
CD138	*Syndecan-1*
CD44	*CD44 molecule (Indian blood group) / Hyaluronate receptor*
CDF	Célula dendrítica folicular
CFU-F	Unidad formadora de colonia fibroblástica
CG	Centro germinal
CMHII	Complejo mayor de histocompatibilidad de clase II
COLIA1	*Collagen I type A1*
CMM	Célula de mieloma
CP	Célula plasmática
CPL	Célula progenitora linfoide
CPM	Célula progenitora mieloide
CSH	Célula *stem* hematopoyética

CSM	Célula *stem*mesenquimal
CSMd	Célula stemmesenquimal procedente de un donante sano
CSMp	Célula stemmesenquimal procedente de un paciente con mieloma
CTX	C-terminal cross-linking telopeptide of type-I collagen
CXCR4	*Chemokine (C-X-C motif) receptor 4*
CYLD	*Cylindromatosis (turban tumor syndrome)*
DASH	*Fibroblast activation protein*
DKK1	*Dickkopf homolog 1*
EFNB2	*Ephrin-B2*
EGFR	*Epidermalgrowth factor receptor*
EphB4	*EPH receptor B4*
ERE	Evento relacionado con el esqueleto
Erk1/2	*Extracellularsignal-regulatedkinase 1/2*
FGFR3	*Fibroblastgrowth factor receptor 3*
FLIP	*FLICE-like inhibitory protein*
FN	*Fibronectin*
Fzd	*Frizzled receptor*
GMSI	Gammapatía monoclonal de significado incierto
GSK3β	*Glycogensynthasekinase 3 beta*
HGF	*Hepatocytegrowth factor*
HSP90	*Heatshockprotein 90*
ICAM1/CD54	*Intercellularadhesionmolecule 1*
IDO	*Indole 2,3-dioxygenase*
IGF1	*Insulingrowth factor 1*
IgH	*Heavy chainimmunoglobulin*
IL1β	*Interleukin 1 beta*
IL3	*Interleukin 3*
IL6	*Interleukin 6*
IL7	*Interleukin 7*
IMiDs	*Immunomodulatorydrugs*
IP	Inhibidores del proteasoma
IRF4	*Interferonregulatory factor 4*
JAK	*Janus kinase*
KRAS	*v-Ki-ras2 Kirsten rat sarcoma viral oncogene homolog*
LEF1	*Lymphoidenhancer-binding factor 1*
LFA1 (CD18) (ITGB2)	*Lymphocyte function-associated antigen 1 / Integrin beta 2*
LMA	Leucemia mieloide aguda
LMC	Leucemia mieloide crónica
LRP5/6	*Low density lipoprotein receptor-related protein 5/6*

M-CSF	*Macrophagecolony-stimulating factor 1*
MAF	*v-mafmusculoaponeuroticfibrosarcomaoncogenehomolog (avian)*
MAPK	*Mitogen-activatedproteinkinase*
MCL1	*Myeloid cell leukemia sequence 1 (BCL2-related)*
MIP1α	*Macrophageinflammatoryprotein 1 alpha*
MM	Mieloma múltiple
MMP1/9	*Matrix metalloproteinase 1/9*
MMSET	*Multiple myeloma SET domainproteincontainingprotein type III*
MO	Médula ósea
MUC1	*Mucin 1, cellsurfaceassociated*
MYC	*v-mycmyelocytomatosis viral oncogenehomolog (avian)*
NFATc1	*Nuclear factor of activated T-cells cytoplasmiccalcineurin-dependent 1*
NFκB	*Nuclear factor kappa B*
NO	*Nitric oxide*
NRAS	*Neuroblastoma RAS viral (v-ras) oncogenehomolog*
NTX	*N-terminal cross-linking telopeptide of type-I collagen*
OAFs	*Osteoclastactivatingfactors*
OB	Osteoblasto
OC	Osteoclasto
OPG	*Osteoprotegerin*
OSCAR	*Osteoclastassociated receptor*
Osx	*Osterix*
P1NP	*Procollagen type-I N-terminal propeptide*
PDGFRα/β	*Platelet derived growth factor receptor alpha/beta*
PI3K	*Phosphatidylinositol-3 kinase*
PKC	*Proteinkinase C*
pOB	Precursor de osteoblasto
pOC	Precursor de osteoclasto
PTEN	*Phosphatase and tensinhomolog*
PTHrP	*Parathyroid hormone-relatedprotein*
PU.1	*Spleen focus forming virus (SFFV) proviral integration oncogene spi1*
RANK	*Receptor of NFκB*
RANKL	*RANK ligand*
RB1	*Retinoblastoma 1*
RC	Remisión completa
RCB	Receptor de célula B
RHAMM (CD168)	*Hyaluronan-mediated motility receptor*
Runx2/Cbfa1	*Runt-related transcription factor 2/Core-binding factor alpha 1*
SCID	*Severe combined immunodeficiency*
SDF1α	*Stromal derived growth factor 1 alpha*

SBF	Suero Bovino Fetal
sFRP2/3	*Secreted frizzled related protein 2/3*
SG	Supervivencia global
SLE	Supervivencia libre de enfermedad
SMD	Síndromes mielodisplásicos
SPARC	*Secreted protein, acidic, cysteine-rich/Osteonectin*
SPP1	*Secretedphosphoprotein 1/Osteopontin*
STAT3	*Signal transducer and activator of transcription 3*
TACI	*Transmembrane activator and CAML interactor*
TCF7	*Transcription factor 7 (T-cell specific, HMG-box)*
TGFβ	*Transforming growth factor beta*
TNFα	*Tumor necrosis factor α*
TP53	*Tumor protein p53*
TRAF3/6	*TNF receptor-associated factor 3/6*
TRAIL	*TNF-related apoptosis inducing ligand*
TRAP	*Tartrate resistant acid phosphatase*
uPA	*Urokinase-type plasminogenactivator*
VCAM1 (CD106)	*Vascular celladhesionmolecule 1*
VEGF	*Vascular endothelialgrowth factor*
VEGFR1/2	*Vascular endothelial growth factor receptor 1/2*
VLA4 (CD49d-CD29) (ITGA4-ITGB1)	*Very late antigen 4* *Integrin alpha 4/beta 1*
VLA5 (CD49e-CD29) (ITGA5-ITGB1)	*Very late antigen 5 (fibronectin receptor)* *Integrin alpha 5/beta 1*
VTNR (CD51-CD61) (ITGAV-ITGB3)	*Vitronectin receptor* *Integrin alpha V/beta 3*
Wnt	*Wingless signaling*
Wnts	*Wingless-type MMTV integration site family members*

OPEN ACCESS Freely available online

PLoS one

Dasatinib as a Bone-Modifying Agent: Anabolic and Anti-Resorptive Effects

Antonio Garcia-Gomez[1,2,3], Enrique M. Ocio[1,3], Edvan Crusoe[1,3], Carlos Santamaria[2], Pilar Hernández-Campo[2], Juan F. Blanco[3], Fermin M. Sanchez-Guijo[2,3], Teresa Hernández-Iglesias[1], Jesús G. Briñón[4], Rosa M. Fisac-Herrero[5], Francis Y. Lee[6], Atanasio Pandiella[1,3], Jesús F. San Miguel[1,2,3], Mercedes Garayoa[1,2,3]*

1 Centro de Investigación del Cáncer, IBMCC, Universidad de Salamanca-CSIC, Salamanca, Spain, **2** Centro en Red de Medicina Regenerativa y Terapia Celular de Castilla y León, Salamanca, Spain, **3** Hospital Universitario de Salamanca-IBSAL, Salamanca, Spain, **4** Departamento de Biología Celular y Patología, Facultad de Medicina, Universidad de Salamanca, Salamanca, Spain, **5** Servicio de Hematología, Hospital General de Segovia, Segovia, Spain, **6** Bristol-Myers Squibb Pharmaceutical Research Institute, Princeton, New Jersey, United States of America

Abstract

Background: Bone loss, in malignant or non-malignant diseases, is caused by increased osteoclast resorption and/or reduced osteoblast bone formation, and is commonly associated with skeletal complications. Thus, there is a need to identify new agents capable of influencing bone remodeling. We aimed to further pre-clinically evaluate the effects of dasatinib (BMS-354825), a multitargeted tyrosine kinase inhibitor, on osteoblast and osteoclast differentiation and function.

Methods: For studies on osteoblasts, primary human bone marrow mensenchymal stem cells (hMSCs) together with the hMSC-TERT and the MG-63 cell lines were employed. Osteoclasts were generated from peripheral blood mononuclear cells (PBMC) of healthy volunteers. Skeletally-immature CD1 mice were used in the *in vivo* model.

Results: Dasatinib inhibited the platelet derived growth factor receptor-β (PDGFR-β), c-Src and c-Kit phosphorylation in hMSC-TERT and MG-63 cell lines, which was associated with decreased cell proliferation and activation of canonical Wnt signaling. Treatment of MSCs from healthy donors, but also from multiple myeloma patients with low doses of dasatinib (2–5 nM), promoted its osteogenic differentiation and matrix mineralization. The bone anabolic effect of dasatinib was also observed *in vivo* by targeting endogenous osteoprogenitors, as assessed by elevated serum levels of bone formation markers, and increased trabecular microarchitecture and number of osteoblast-like cells. By *in vitro* exposure of hemopoietic progenitors to a similar range of dasatinib concentrations (1–2 nM), novel biological sequelae relative to inhibition of osteoclast formation and resorptive function were identified, including F-actin ring disruption, reduced levels of c-Fos and of nuclear factor of activated T cells 1 (NFATc1) in the nucleus, together with lowered cathepsin K, αVβ3 integrin and CCR1 expression.

Conclusions: Low dasatinib concentrations show convergent bone anabolic and reduced bone resorption effects, which suggests its potential use for the treatment of bone diseases such as osteoporosis, osteolytic bone metastasis and myeloma bone disease.

Citation: Garcia-Gomez A, Ocio EM, Crusoe E, Santamaria C, Hernández-Campo P, et al. (2012) Dasatinib as a Bone-Modifying Agent: Anabolic and Anti-Resorptive Effects. PLoS ONE 7(4): e34914. doi:10.1371/journal.pone.0034914

Editor: Micah Luftig, Duke University Medical Center, United States of America

Received July 13, 2011; **Accepted** March 8, 2012; **Published** April 23, 2012

Funding: This work was supported by grants from the Spanish Ministry of Science and Innovation – ISCIII (PI081825); Mutua Madrileña Medical Research Foundation (AP27262008); Centro en Red of Regenerative Medicine and Cellular Therapy from Castilla y León, Consejería de Sanidad JCyL – ISCIII; the Cooperative Research Thematic Network in Cancer (RTICC; RD06/0020/0006 and RD03/0020/0041); and Spanish FIS (PS09/01897). AG-G and CS are supported by the Centro en Red of Regenerative Medicine and Cellular Therapy from Castilla y León Project. The funders had no role in study design, data collection and analysis, decision to publish, or preparation of the manuscript.

Competing Interests: FYL is an employee of Bristol-Myers Squibb. This does not alter the authors' adherence to all the PLoS ONE policies on sharing data and materials. There are no patents or products in development to declare.

* E-mail: mgarayoa@usal.es

Introduction

Bone mass is regulated by the balance of bone formation and bone resorptive rates. Alteration of this balance by increased number and activity of bone-resorbing osteoclasts (OCs) and/or reduced differentiation and impaired activity of bone-forming osteoblasts (OBs), leads to pathological states of bone loss. That is the case of bone diseases such as osteoporosis, osteolytic bone metastasis and multiple myeloma bone disease. In osteoporosis, a prevalent disease of postmenopausal women and elderly patients, bone resorption exceeds that of bone formation resulting in a systemic impairment of bone mass, strength, and microarchitecture [1]. This highly increases the propensity of fragility fractures, most commonly occurring in the spine, hip or wrist. Also, many solid tumors (prostate, breast, lung, colon, renal), commonly metastasize to bone. When this occurs, tumor cells mobilize

cellular and extracellular matrix bone components to ultimately promote bone invasion and enhance tumor growth, which leads to deregulated bone remodeling and as a consequence, devastating skeletal complications [2,3]. Furthermore, multiple myeloma (MM) is a hematological malignancy primarily developing within the bone marrow as a consequence of the abnormal expansion of clonal plasma cells. Interestingly, one major (in up to 80% of MM patients) clinical symptom associated with this disease is the development of osteolytic lesions as a result of increased bone resorption and marked impairment of bone formation. The interactions of myelomatous cells with the bone marrow microenvironment are thought to be critical in the development of MM bone disease, and the diverse interplaying cellular and molecular components have been extensively studied recently [4–6]. Of interest, isolated mesenchymal osteoprogenitor cells from the bone marrow of myeloma patients have been reported to show distinct gene expression profile and also reduced osteogenic potential as compared to those from healthy donors [7,8]. All these low bone mass pathologies (osteoporosis, osteolytic bone metastasis and myeloma bone disease) cause skeletal fragility and are commonly associated to skeletal related events including pathological fractures, severe bone pain, hypercalcemia and spinal cord and nerve compression. These events can severely compromise the quality of life of patients and even result in significant mobidity and increased risk of death. This emphasizes the need to identify and develop new bone-targeted pharmacological agents which may prevent, reduce or even reverse these pathological conditions of bone loss in the above mentioned diseases.

Specific tyrosine kinases have been proposed as potential targets for anti-tumor therapy. Imatinib mesylate (STI-571) is a tyrosine kinase inhibitor which was originally approved as a first-line treatment for chronic myeloid leukemia because of its capacity to inhibit the Bcr-Abl kinase activity of Philadelphia$^+$ cells [9]. Additional tyrosine kinases with oncogenic potential also inhibited by imatinib include c-Kit, the platelet-derived growth factor receptors: PDGFR-α and PDGFR-β, and the c-Fms receptor [9,10], which account for the anti-tumor effect of imatinib in several types of solid tumors. Interestingly, evidence has accumulated for a direct effect of imatinib in the skeleton with increased trabecular bone volume and bone mineral density in imatinib-treated patients [11,12]. In *vitro* studies showed that imatinib suppressed OB proliferation and stimulated osteogenic gene expression and mineralization majorly by inhibiting PDGFR function [11,13]. Moreover, imatinib has a potent inhibitory effect on OC bone resorption and stimulates apoptosis of mature OCs [14].

Dasatinib (BMS-354825) is a novel oral bioactive multitargeted tyrosine kinase inhibitor which was developed as a second-generation drug rationally designed for the use against imatinib-resistant leukemias [15]. The target tyrosine kinase profile of dasatinib partially overlaps that of imatinib but presenting much higher potency, and is also broader, including the Src family kinases [10]. Dasatinib is now being evaluated in Phase II trials in a variety of tumor types, including prostate, breast, colorectal and lung cancer [16]. However, taking into account the aforementioned skeletal effects of imatinib, it was expected that dasatinib might be even more effective in inhibiting osteoclastogenesis and promoting bone formation. In fact, it has already been reported that dasatinib inhibits OC formation and resorption capacity, mainly by its potent inhibition of c-Fms on OC progenitors [17,18]. Also, recent data of dasatinib effect enhancing osteoblastogenesis from mesenchymal progenitors have been reported [19-21]; other authors, however, have claimed an inhibitory effect on OB differentiation for this agent in similar settings [22]. In the present study we provide *in vitro* evidences of the effect of low dasatinib concentrations in enhancing differentiation and function of mesenchymal osteoprogenitors from both healthy donors, and interestingly, also from myeloma patients. This anabolic bone effect of dasatinib was also observed in the *in vivo* setting after administration of relatively low dasatinib doses to skeletally-immature mice to avoid the inhibitory effects of the agent on OCs and OC precursors and thus targeting endogenous osteoprogenitor cells. Besides, within the same low nanomolar range of dasatinib concentrations, we show *in vitro* data of additional mechanisms of dasatinib inhibitory effect on OC differentiation [diminished expression of c-Fos and reduced levels of nuclear factor of activated T cells 1 (NFATc1) in the nuclear compartment], and on OC function (F-actin ring disruption and lowered $\alpha V\beta 3$ integrin, CCR1 and cathepsin K expression). Taken together, our data support the overall bone anabolic effects of dasatinib, with a double component of enhancement of OB differentiation and function together with inhibition of osteoclastogenesis and bone resorption, exerted within a similar concentration range. Potential therapeutic implications of dasatinib for the treatment of specific bone disorders are also discussed.

Methods

Participants

Samples from the bone marrow of 10 healthy donors and 10 newly diagnosed MM patients (stages I to III) were used in this study after informed and written consent of participants. Approval of the study was granted by the Institutional Review Board of the CIC, IBMCC (University of Salamanca-CSIC, Spain), and research was conducted following principles in the Declaration of Helsinki.

Reagents and immunochemicals

Dasatinib was provided by Bristol-Myers Squibb Company (Stamford, CT, USA). For *in vitro* assays, dasatinib was reconstituted in dimethyl sulfoxide (DMSO; Merck, Hohenbrunn, Germany) at a stock concentration of 100 mM and stored at $-20^{\circ}C$; further dilutions were made in tissue culture medium at the time of use. Recombinant human PDGF-BB, macrophage colony-stimulating factor (M-CSF) and receptor activator of NF-κB ligand (RANKL) were purchased from Peprotech (London, UK), while stem cell factor (SCF) was obtained from Strathmann (Hamburg, Germany). Primary antibodies for immunoblotting, immunohistochemical and flow cytometry analyses were directed against: PDGFR-β, phospho-PDGFR-β (Tyr857), Erk1/2, phospho-Erk1/2 (Thr202/Tyr204), NFATc1, histone H1 and cathepsin K, purchased from Santa Cruz Biotechnology (Santa Cruz, CA, USA); phospho-c-Fms (Tyr723), phospho-c-Kit (Tyr719), c-Src, phospho-Src (Tyr416), p38 MAPK, phospho-p38 MAPK (Thr180/Tyr182), Akt, phospho-Akt (Ser473), phospho-β-catenin (Thr41/Ser45), PU.1 and c-Fos, from Cell Signaling Technology (Danvers, MA, USA); CD51/61 and CD191, from R&D Systems (Minneapolis, MN, USA); c-Kit and nucleoporin p62, from BD Biosciences (Bedford, MA, USA); α-tubulin, from Calbiochem (Darmstadt, Germany); dephospho-β-catenin (aa 35–50), from Enzo Life Sciences (Plymouth Meeting, PA, USA), and T-cell factor 4 (Tcf4), from Upstate (Millipore, Billerica, MA, USA). All cell culture media and reagents were purchased from Gibco (Paisley, UK). Trypan Blue Solution 0.4% was delivered by Sigma-Aldrich (St. Louis, MO, USA), and the alamarBlue reagent by Invitrogen (Carlsbad, CA, USA).

Cell lines

The human mesenchymal stem cell (MSC) line immortalized by expression of the telomerase reverse transcriptase gene (hMSC-TERT) was a generous gift from Dr D Campana (Department of Oncology and Pathology, St Jude Children's Research Hospital, Memphis, TN, USA) [23]. The human osteosarcoma cell line MG-63 was obtained from the American Type Culture Collection (CRL-1427; LGC Promochem, London, UK), and used as an osteoblast-like cell line [24]. Cell lines were grown in RPMI 1640 medium (hMSC-TERT) or DMEM medium (MG-63) supplemented with 10% heat-inactivated fetal bovine serum (FBS), 100 U/mL penicillin and 100 μg/mL streptomycin. All cell types were cultured at 37°C in a humidified atmosphere in the presence of 5% CO_2–95% air.

Primary mesenchymal stem cells and osteoprogenitor cells

Primary MSCs from BM samples of healthy donors (n = 10) and MM patients (n = 10) were generated as described by Garayoa et al. [25]. Briefly, mononuclear cells from bone marrow samples were isolated using Ficoll-Paque density gradient centrifugation (ρ 1.073; GE Healthcare, Uppsala, Sweden), cultured in DMEM with 10% FBS, 100 U/mL penicillin, 100 μg/mL streptomycin and 2 mM L-glutamine for four days and selected by their adherence to plasticware. The culture medium was replaced twice weekly until MSC cultures were approximately 90% confluent or had been in culture for a maximum of 21 days; at that point, cells were trypsinized (0.05% Trypsin-EDTA) and expanded in a 1:3 ratio. At passage 3, selected MSCs from both origins were tested to meet definition criteria according to the recommendations of the International Society for Cellular Therapy [26] and experiments were performed.

To induce *ex vivo* differentiation to OBs, the growth medium of MSCs at 80–90% confluence was replaced by an osteogenic differentiation medium consisting of α-MEM supplemented with 10% FBS, 10 mM β-glycerol phosphate, 50 μg/mL ascorbic acid and 10 nM dexamethasone (all additives from Sigma-Aldrich). MSCs were grown in the osteogenic medium for 7 (early stage of OB differentiation), 14 (pre-OB stage) or 21 days (fully differentiated OBs), replacing the medium every 3 or 4 days, in the absence or presence of specified concentrations of dasatinib.

Cell proliferation and viability assays

To test whether dasatinib affected the growth capacity of the MSC/OB lineage, the hMSC-TERT and MG-63 cell lines were seeded in 6-well plates at 10^4 cells/cm^2 or 2.5×10^3 cells/cm^2, respectively, and incubated for 7 days in the absence or presence of different dasatinib concentrations. Cells were then trypsinized (0.05% Trypsin-EDTA) and counted using a Trypan Blue solution and a haemocytometer. The alamarBlue reagent was used to examine cell viability of the hMSC-TERT and primary MSCs from myeloma patients at different time points and dasatinib concentrations along the osteogenic differentiation process, as by manufacturers instructions.

In addition, to check whether changes in the number of viable cells were due to diminished proliferative capacity or apoptotic effects of the drug, the hMSC-TERT cell line was stained with PKH67 (Sigma-Aldrich), a green fluorescent cell tracker that is retained in the cell membrane and thus can be used for monitoring proliferation based on dye dilution with each cell division. After PKH67 labeling, cells were seeded in 6-well plates at 10^4 cells/cm^2 and incubated for 7 days in the osteogenic differentiation medium in the presence or absence of dasatinib. At the end of the culture period, cells were trypsinized and incubated with phycoerythrin (PE) conjugated Annexin-V and 7-amino-actinomycin D (7-AAD) [Becton Dickinson (BD) Biosciences, Bedford, MA, USA] for complementary apoptosis/necrosis information. The cells were acquired using a FACSCalibur flow cytometer, and data were analyzed using the ModFit program to determine the number of cell divisions and the percentage of cells in each division (compared with undivided colcemid-treated cultures) or the Paint-A-Gate program for percentages of apoptotic cells (BD Biosciences).

Western blotting analyses

Protein lysates were generated and western blotting procedures were performed as previously described [27]. For subcellular fractionation of proteomic samples, the Qproteome Cell Compartment kit was used (Qiagen GmbH, Hilden, Germany).

Detection of PDGFR-β, phospho-PDGFR-β (Tyr857), c-Kit, phospho-c-Kit (Tyr719), c-Src, phospho-Src (Tyr416), Erk1/2, phospho-Erk1/2 (Thr202/Tyr204), p38 MAPK, phospho-p38 MAPK (Thr180/Tyr182), Akt, phospho-Akt (Ser473), phospho-c-Fms (Tyr723), PU.1, NFATc1, c-Fos, cathepsin K, phospho-β-catenin (Thr41/Ser45), dephospho-β-catenin (aa 35–50), histone H1 and α-tubulin was performed by a standard procedure, using primary and appropriate horseradish peroxidase-conjugated secondary antibodies and a luminol detection system with *p*-iodophenol enhancement for chemiluminescence.

To analyze the effect of dasatinib on PDGFR-β, c-Kit and c-Src tyrosine kinases, the hMSC-TERT and MG-63 cell lines were first incubated with different concentrations of dasatinib for 6 hours and then treated with 10 ng/mL PDGF-BB or 50 nM SCF for 20 minutes prior to protein isolation. To test the effect of dasatinib on c-Fms, c-Kit and c-Src, OC progenitors were incubated with dasatinib for 2 hours and then treated with 50 ng/mL M-CSF or 50 nM SCF for 20 minutes prior to protein isolation.

Alkaline phosphatase and Runx2 activities and mineralization assay

Primary MSCs were cultured in 12-well plates in MSC medium until reaching ~80% confluency. Cells were then changed to the osteogenic differentiation medium in the presence or absence of dasatinib (2 or 5 nM) for 7 or 21 days, at which times the alkaline phosphatase (ALP) activity, or the Runx2 activity and mineralization assays were performed.

To measure ALP activity, cells were washed in phosphate-buffered saline (PBS), lysed in ice-cold lysis buffer and protein content determined using the Micro BCA assay kit (Pierce, Rockford, IL). ALP activity was determined by specific hydrolysis of *p*-nitrophenylphosphate into *p*-nitrophenol (Sigma-Aldrich) and quantified by OD reading at 405 nm in triplicate using a microplate reader (Asys UVM340, Biochrom, Eugendorf, Austria). Values were referred to the total protein content of the sample.

When determining Runx2 activity, protein nuclear extracts were prepared using the Qproteome Cell Compartment kit. Quantification of Runx2 activation was performed with the ELISA based Trans-AM (AML-3/Runx2) kit as per manufacturer instructions.

For quantitative analysis of alizarin red staining (ARS), we used the method described by Gregory et al. [28]. Briefly, cells were fixed with 10% ice-cold phosphate-buffered formaldehyde for 10 minutes, rinsed with distilled water and stained with 40 mM alizarin red (pH 4.2) for 20 minutes at room temperature. After several washes to reduce non-specific ARS, stained cultures were photographed with an Olympus DP70 camera on an Olympus 31 inverted microscope. Dye was extracted by acetic acid incubation

and sample heating, and measured in triplicate at 405 nm in 96-well plates.

Real-time RT-PCR analysis

To evaluate the effect of dasatinib on the expression of bone formation markers throughout their osteogenic differentiation, MSCs from MM patients or healthy donors were cultured for 7 or 14 days in the osteogenic differentiation medium in the presence or absence of the drug. Total RNA was isolated using the Rneasy Mini kit (Qiagen GmbH, Hilden, Germany). Reverse transcription was performed with 1.0 μg RNA in the presence of random hexamers and 100 U of SuperScript RNase H reverse transcriptase (Invitrogen). For PCR reactions we used the Step One Plus Real-Time PCR System and TaqMan Gene Expression Assays (Applied Biosystems, Foster City, CA, USA) according to manufacturer's instructions. Assay IDs were: *ALP*, Hs00758162_m1; *COL1A1*, Hs01076777_m1, *Osterix*, Hs00541729_m1, and *Runx2*, Hs01047976_m1. Experiments were performed in duplicate for both the target and the endogenous gene (GAPDH) used for normalization. Relative quantification of the target gene expression was calculated by the comparative threshold cycle (Ct) method: $2^{-\Delta\Delta Ct}$ where $\Delta Ct = Ct_{\text{target gene}} - Ct_{\text{GAPDH}}$ and $\Delta\Delta Ct = \Delta Ct_{\text{dasatinib-treated samples}} - \Delta Ct_{\text{samples in absence of dasatinib}}$.

In vivo model

For *in vivo* studies, dasatinib powder was dissolved in sterile 80 mM citric acid pH 2.1 to make a 10 mg/mL stock solution and then further dilutions were made in 80 mM sodium citrate pH 3.1. Thirty 5-week-old female CD1 healthy mice were housed at our Animal Care Facility. At this age, healthy CD1 mice are skeletally immature and show very active bone formation and minimal bone resorption, and this model was chosen so that the effect of dasatinib on bone could be majorly ascribed to its action on OBs and not to inhibition of OC formation and function. Animals were divided into three groups (n = 10 in each group) receiving: a) 80 mM sodium citrate pH 3.1 as vehicle; b) a lower dasatinib dose of 2.5 mg/kg, and c) a higher dasatinib dose of 10 mg/kg. Treatment was administered by oral gavage in 0.01 mL volume, in a BID regimen (twice a day), 5 days/week in an attempt to maintain the dasatinib concentration range throughout the day. Serum samples were collected at the beginning of the experiment, and also after 3 and 7 weeks of dasatinib treatment (n = 7 per group). Three to 5 animals per group were sacrificed after 3 and 7 weeks of treatment, and both femurs were dissected for microtomographic imaging (micro-CT), histological and immunohistochemical analyses. All animal experiments were conducted according to Institutional Guidelines for the Use of Laboratory Animals of the University of Salamanca, after acquiring permission from the local Ethical Committee for Animal Experimentation, and in accordance with current Spanish laws on animal experimentation.

Osteocalcin and ALP (as markers of new bone formation) as well as TRAP5b levels (the active isoform of TRAP, specifically expressed by OCs, and thus reflecting OC number and activity), were quantified in collected sera. Markers of bone metabolism were measured by dedicated ELISAs according to manufacturers guidelines [Alkaline phosphatase (Sigma-Aldrich), Mouse osteocalcin (Biomedical Technologies, Stoughton, MA, USA) and Mouse TRAP Assay (Immunodiagnostic Systems, Boldon, UK)]. For statistical analysis, values for a determined serum marker (e. g. osteocalcin) at each point (control, 3 and 7 weeks of treatment) were normalized for every individual animal to its own osteocalcin level at the beginning of the experiment, and plotted as fold change.

To assess bone morphology and microarchitecture, 10% formalin-fixed femurs were analyzed by a micro-CT system (MicroCATII; Siemens, Knoxville, TN, USA) at 75.0 kVp and 250.0 uA. Seven hundred X Ray projections were acquired during a 200° rotation around the sample, with 1250 ms camera exposure time per projection at full resolution (512×512). The reconstruction of the 3D image was done using COBRA V6.1.8 (Exxim Computing Corporation, Pleasanton, CA, USA) with a final resolution of 10.4 μm/voxel. The post-processing, rendering and generation of the cross sections of the samples was done using Amira (Visage Imaging, San Diego, CA, USA). Analysis of microarchitectural trabecular bone morphology in the distal femur was performed using CT-Analyser software (SkyScan, Kontich, Belgium). Quantitative bone determined parameters were the bone perimeter per area ratio (B Pm/B Ar; mm^{-1}), trabecular number (Tb N; mm^{-1}) and trabecular separation (Tb Sp; mm).

In parallel, other femurs were also processed for histologic and/or immunohistochemical studies following standard procedures. Briefly, specimens were fixed in 10% formalin for 24 h, decalcified in Osteosoft bone decalcifying solution (Merck KGaA, Darmstadt, Germany) for 5 days and embedded in paraffin. Samples were cut into 3-μm-thick sections and stained with H&E for bone histologic evaluation or either used for immunohistochemical studies. In the latter case, antigen retrieval was carried out in a Pascal pressure chamber (Dako, Glostrup, Denmark) at 90°C for 20 minutes using a Tris-EDTA buffer pH 9.0, and then tissue endogenous peroxidase activity was quenched with a 3% H_2O_2 solution for 10 minutes. Sections were incubated overnight with an anti-Tcf4 antibody at 4°C and 1:20 working dilution, followed by incubation with EnVision anti-mouse complexes (Dako). The peroxidase activity was shown using 3,3′-diaminobenzidine+ (DAB+; Dako) as a chromogen. Finally, sections were washed in water, lightly counterstained with hematoxylin, dehydrated and mounted in DPX. Histologic and immunostained sections were observed with an Olympus BX51 microscope and photographed with a Olympus DP70 camera. Tcf4 is an activating transcription factor which cooperatively interacts with Runx2/Cbfa1 to stimulate osteoblast-specific osteocalcin expression [29], and thus can be used as a bona fide marker for OB cells.

Osteoclast differentiation and pit formation assays

Peripheral blood monocuclear cells (PBMCs) from 6 healthy donors were obtained by density gradient centrifugation using Ficoll-Paque (ρ 1.073; GE Healthcare), and cultured overnight at 0.5×10^6 cells/cm^2 in α-MEM medium supplemented with 10% FBS and 100 U/mL penicillin and 100 μg/mL streptomycin. After removal of non-adherent cells, the remainder were maintained in the same medium but with additional 50 ng/mL RANKL and 25 ng/mL M-CSF in the absence or presence of dasatinib at indicated times and doses. The medium was replaced twice weekly and cultures under each condition were performed in quadruplicate from PBMCs of at least three different donors.

To evaluate the effect of dasatinib on OC formation, cells were stained for tartrate-resistant acid phosphate (TRAP; leukocyte acid phosphatase kit, Sigma), according to the manufacturer's instructions after 21 days of culture. Using a Leica DMI6000 B inverted microscope, TRAP+ cells containing three or more nuclei were enumerated with the aid of a 1×1 mm^2 grid (five randomly selected fields/well) and photographed with a Leica DFC350FX camera.

To test the effect of dasatinib on the bone resorption capacity of OCs, PBMCs at 0.6×10^6 cells/well were seeded on calcium-coated slides (Becton Dickinson) in 200 μl of OC medium supplemented with 5 ng/mL TGF-β1 (Peprotech) and 1 μM

dexamethasone for 17 days [30]. The medium was changed twice weekly by semi-depletion in the absence or presence of indicated concentrations of dasatinib. At the end of the assay, cells were removed with a 0.1% Triton X-100 solution and resorption pits were photographed using a Leica DFC350FX camera mounted on a Leica DMI6000 B microscope. The total resorbed area per well was calculated using the Adobe Photoshop histogram function (Adobe Photoshop CS2, 9.0.2). Assays were performed in triplicate for each condition using PBMCs from five healthy volunteers.

Flow cytometry on osteoclast cells

After 2 weeks of osteoclastogenic differentiation in the absence or presence of dasatinib, pre-OBs were trypsinized (0.25% Trypsin-EDTA) and resuspended in Dulbecco's PBS. Cells were stained with anti-CD51/61-PE ($\alpha V\beta 3$ integrin-PE conjugated Mouse IgG_1) or anti-CD191-APC (CCR1-allophycocyanin conjugated Mouse IgG_{2B}) for 15 minutes and subsequently with 7-AAD for 5 minutes. After washes, cells were acquired on a FACSCalibur flow cytometer using the CellQuest program and analyzed with the Infinicyt software 1.3 (Cytognos, Salamanca, Spain). Specific staining for CD51/61 or CD191 was evaluated on 7-AAD^- viable cells.

Actin ring formation assay

PBMCs were seeded at 0.5×10^6 cells/cm^2 on cover slips and cultured in the specified osteoclastogenic medium for 12–14 days in the presence or absence of the drug. At this point, pre-OCs were fixed in 2% paraformaldehyde for 20 minutes, permeabilized with 0.1% Triton X-100 and blocked in 5% bovine serum albumin in PBS. Cover slips were then incubated with rhodamine-conjugated phalloidin (1:200; Invitrogen) for 20 minutes to visualize F-actin, and stained with DAPI to make nuclei evident. After a final rinse, cover slips were mounted with an aqueous mounting medium (Vector Laboratories, Burlingame, CA, USA), and the distribution of the F-actin ring was observed with a Leica DMI6000 B microscope and photographed with the Leica DFC350FX camera. Assays were performed in triplicate for each condition using PBMCs from at least three different healthy volunteers.

Statistical analysis

Each assay was performed at least three times. Quantitative data were expressed as mean ± SD or SEM, as specified. Statistical comparisons using the non-parametric Mann-Whitney *U*-test were considered statistically significant for values of $p<0.05$ (SPSS Statistics 15.0, Chicago, IL, USA).

Results

Dasatinib inhibits PDGFR-β, c-Kit and c-Src phosphorylation and modulates downstream signaling on osteoprogenitor cells

We first examined the effect of dasatinib on two tyrosine kinases, PDGFR-β and c-Src, which are described targets for dasatinib and with known involvement in mesenchymal stem cell/osteoblast (MSC/OB) proliferation and function. PDGF is mitogenic to mesenchymal cells while inhibiting OB differentiation and bone matrix formation [31,32], and targeted deletion of PDGFR-β in murine mesenchymal cells also stimulates OB differentiation and function [33]. On the other hand, knockdown of Src expression has also been shown to enhance OB differentiation and function [19,34]. Serum-starved hMSC-TERT and MG-63 cell lines (respectively representing the multipotent MSCs and the differentiated OBs), were exposed to PDGF-BB in the absence or presence of escalating doses of dasatinib to check for potential differences in sensitivity due to their differentiation status. As illustrated in Figure 1A, PDGF-BB exposure markedly increased PDGFR-β tyrosine phosphorylation in both cell lines, and dasatinib strongly diminished PDGF-stimulated PDGFR-β activation. PDGF-BB treatment also increased basal p-Y416 of c-Src, ascribable to PDGFR-β activation and its interaction with the Src family kinases [35]. Dasatinib treatment only partially abrogated both basal and PDGF-induced c-Src activation in the hMSC-TERT, while inhibition of c-Src phosphorylation was more pronounced in the MG-63 cell line (Figure 1A). We also show that both cell lines express c-Kit, the stem cell factor (SCF) receptor for which dasatinib also presents inhibitory activity [10,36]. SCF-induced c-Kit phosphorylation is efficiently diminished by dasatinib in both cell lines (Figure 1A).

To gain some insight into the mechanisms underlying the effect of dasatinib on these cells, we explored the activation status of key molecules in signaling pathways downstream the affected tyrosine kinases, such as: Erk1/2, Akt, and p38 mitogen activated protein kinase (MAPK). As observed in Figure 1B, dasatinib inhibits PDGF-induced Akt activation in the hMSC-TERT and even more effectively in the MG-63 cell line. Inhibition of PDGF-induced PI3-kinase/Akt activation has been shown to promote osteogenic differentiation and mineralized-matrix production in osteogenic cultures [11,37], and a similar effect could be expected from dasatinib in our experimental settings. On the other hand, dasatinib induced a remarkable inhibition of Erk 1/2 phosphorylation only in the MG-63 cell line and failed to modulate p38 activation in neither cell line. Although activation of Erk 1/2 and p38 have been reported to promote OB differentiation and matrix mineralization through Osterix [38,39], at least in our experimental settings, dasatinib does not seem to stimulate the osteogenic differentiation and function by similar molecular mechanisms.

Dasatinib inhibits osteoprogenitor cell and osteoblast proliferation

OBs are derived from precursor MSCs, a process which implies reduction of their proliferative and stem cell self-renewal capacities while acquisition of OB-specific features and lineage commitment [31]. We therefore first tested the effect of dasatinib on the growth rate and viability of OB cells and their mesenchymal progenitors. As seen in Figure 2A, the number of cells in both the hMSC-TERT and MG-63 cultures was progressively reduced with increasing doses of dasatinib. We further studied the effect of increasing dasatinib concentrations on the number of viable cells at different times along the osteogenic differentiation process. A dose and time-dependent reduction on the number of viable cells was observed as referred to the absence of the drug (control) at each time point, which was especially evident at the end of the differentiation period (21 days) and with dasatinib concentrations $\geq$10 nM (Figure 2B). Also, OBs derived from primary MSCs resulted more sensitive to higher dasatinib doses than OBs derived from the hMSC-TERT cell line (Figure 2B, left graph *vs* right graph), with no significant differences in the number of viable OBs derived from MM patients and healthy donors (data not shown).

It is likely that the reduced number of viable cells in osteogenic cultures after dasatinib treatment could be majorly ascribed to reduced cell proliferation and/or increased apoptosis. Using the hMSC-TERT cell line and a 7-day culture period, we show that dasatinib effect until a 50 nM dose was mainly due to a reduced proliferative capacity (Figure 2C, left) as assessed by reduced number of cell divisions when increasing dasatinib concentration. The percentage of apoptotic and/or necrotic hMSC-TERT cells,

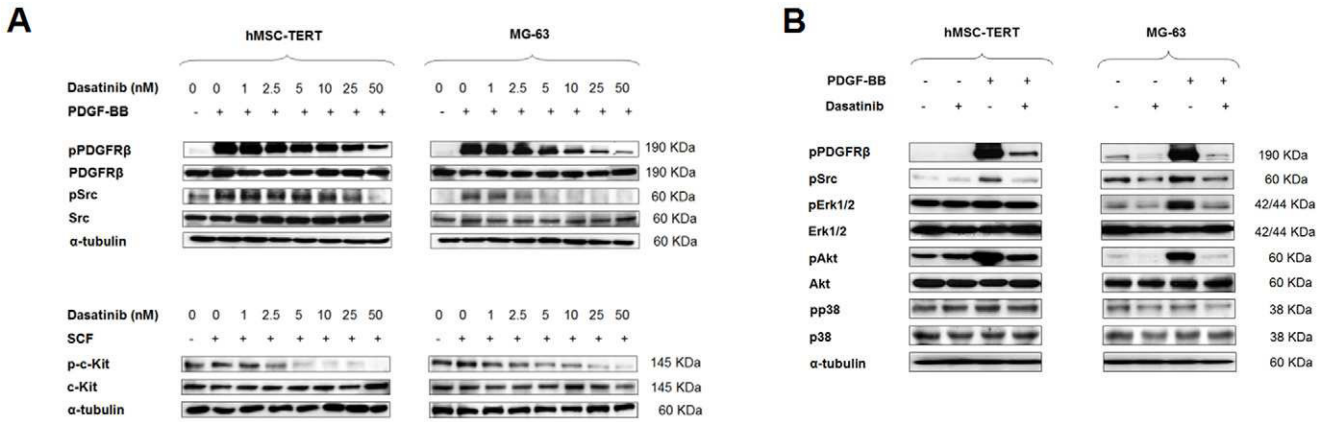

Figure 1. Dasatinib inhibits PDGFR-β, c-Kit and c-Src phosphorylation in mesenchymal and osteoblast-like cell lines. (A) Mesenchymal (hMSC-TERT) and osteoblast-like (MG-63) cell lines were pretreated with different concentrations of dasatinib for 6 hours and then exposed to PDGF-BB or SCF for 20 minutes before protein lysates were generated. Immunoblotting with specific antibodies against total and phosphorylated PDGFR-β, c-Kit and c-Src were performed. (B) Modulation of downstream signaling after dasatinib treatment. Similarly to experimental conditions in (A), the hMSC-TERT and the MG-63 cell lines were pretreated with 50 nM dasatinib for 6 hours, stimulated with PDGF-BB for 20 minutes and then cell harvested for protein isolation. Immunoblotting is shown for total and phosphorylated forms of PDGFR-β, c-Src, Erk 1/2, Akt and p38 mitogen activated protein kinase (MAPK).
doi:10.1371/journal.pone.0034914.g001

however, was only slightly increased within the mentioned dasatinib doses (Figure 2C, right). Our results are therefore consistent with those of other authors which have found that dasatinib inhibits osteoprogenitor cell proliferation [19] and induces apoptosis with higher doses of the drug (≥100 nM) [20].

Importantly, the number of viable cells in OBs derived from primary MSCs (either from MM patients or healthy donors) after the 21-day differentiation period was more pronouncedly diminished as compared to OBs derived from the hMSC-TERT cell line (Figure 2B, left graph *vs* right graph). This issue should be taken into account if dasatinib is used for the treatment of human primary osteoprogenitor cells, in order to achieve a compromise between dasatinib inhibition of cell proliferation and its osteogenic potential. In fact, the use of high dasatinib concentrations might have been the reason why some authors failed to observe an osteogenic effect on human MSCs with this drug [22]. In the light of these observations and for next experiments, we decided to restrict the use of dasatinib concentrations to the low nanomolar range (≤5 nM).

Low dasatinib concentrations promote osteogenic differentiation, alkaline phosphatase and Runx2/Cbfa1 activities and matrix mineralization

Since OB maturation implies a balance between proliferation and differentiation, it could be hypothesized that inhibition of osteoprogenitor proliferation by dasatinib would correlate with an enhanced osteogenic differentiation. We evaluated whether dasatinib was capable of modulating osteogenic gene expression in OBs derived from primary MSCs at the selected low concentrations (2–5 nM). Expression of bone-formation markers such as alkaline phosphatase (ALP), collagen I type A 1 (COLIA1) and the transcription factors Runx2/Cbfa1 and Osterix was evaluated by real time RT-PCR and analyzed at either day 7 or 14 of the differentiation process [40]. Figure 3A shows that dasatinib clearly increased the expression of the osteogenic genes to levels higher than those observed in the same conditions but in absence of the drug (control). Interestingly enough, this effect was not restrained to MSCs from healthy volunteers, but MSCs from myeloma patients also responded to dasatinib in a similar way (Figure 3A), thereby supporting the osteoblastogenic therapeutic potential of dasatinib in this disease.

We also examined the biological effect of dasatinib in promoting osteogenic differentiation by measuring ALP and the transcription factor Runx2/Cbfa1 activities as well as mineralized-matrix formation, in OBs differentiated from primary MSCs and from the hMSC-TERT cell line. Dasatinib (at 2 nM or 5 nM) was added to the osteogenic medium at the initiation of OB differentiation, and ALP and Runx2/Cbfa1 activities were measured as surrogates of OB activity at day 7 and 14, respectively. Dasatinib significantly and dose-dependently increased ALP activity even in OBs derived from primary MSCs (Figure 3B, upper). Also Runx2/Cbfa1 activity measured in nuclear lysates of pre-OBs was augmented in the presence of dasatinib, although the increase was not statistically significant in OBs derived from healthy donors (Figure 3B, lower). To estimate matrix mineralization, alizarin red staining and dye quantification were performed after a 21-day osteogenic differentiation of MSCs. Under the aforementioned conditions, OBs derived from the hMSC-TERT cell line underwent a clear dose-dependent increase in mineralization (Figure 3C, left); a slight but reproducible trend towards increased matrix mineralization was also observed in OBs derived from primary MSCs from healthy volunteers and myeloma patients, although it did not reach significance in the latter (Figure 3C, right).

The Wnt/β-catenin signaling pathway is known to play a key role in the osteogenic differentiation of mesenchymal progenitors and in normal skeletal development [41]. Therefore, we examined whether the activity of dasatinib in our experimental setting was accompanied by downstream activation of the canonical Wnt signal transduction. As observed in Figure 3D by immunoblot analysis, dasatinib clearly induced accumulation of the active dephosporylated form of β-catenin in the nuclear compartment, whereas levels of the inactive phosphorylated form in the cytoplasm were reduced. Taken together, our data show that the MSC/OB lineage expresses tyrosine kinases such as PDGFR-β, c-Src, and c-Kit, whose activation can be partially inhibited by low doses of dasatinib (≤5 nM). Within the same range of dasatinib concentrations, these effects are associated with activation of canonical Wnt signaling.

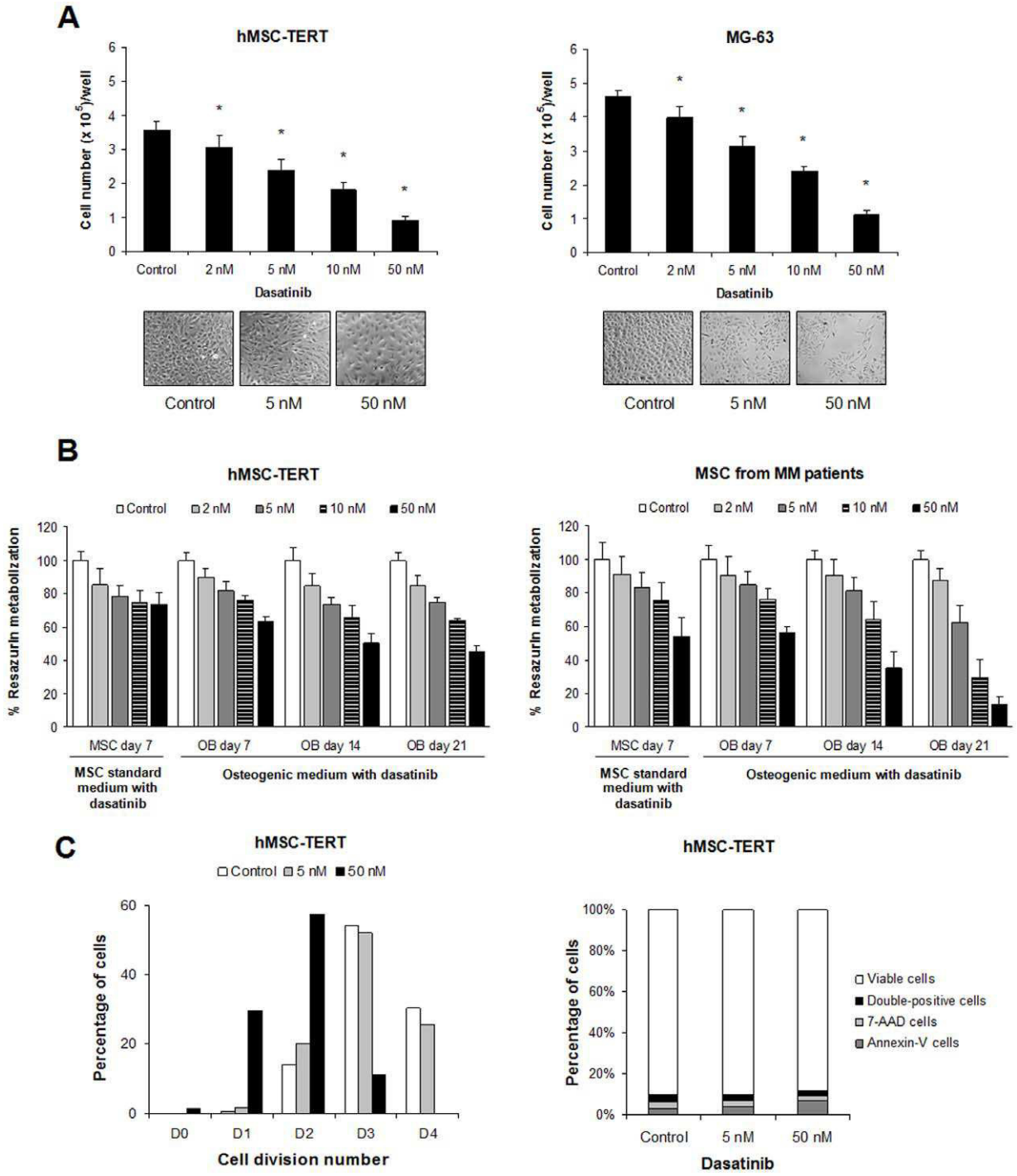

Figure 2. Dasatinib reduces the number of viable cells by inhibition of mesenchymal and OB cell proliferation. (A) Dasatinib decreases the number of MSC and OB cells in culture. The hMSC-TERT and the MG-63 cell lines were cultured for 7 days in maintenance medium in the absence or presence of increasing dasatinib concentrations, and then the number of cells at each condition was counted with a haemocytometer and a Trypan Blue solution. Representative micrographs are shown. (B) Dasatinib reduced the number of viable cells in osteogenic cultures in a time and concentration-dependent manner. MSCs were maintained in osteogenic medium for 7, 14 or 21 days in the presence of different dasatinib concentrations, and percentage of viable cells was evaluated with the alamarBlue assay on OBs derived from the hMSC-TERT (left) and from primary MSCs from MM patients (right). Data are expressed as the mean ± SD from three experiments. Statistically significant differences from control are indicated as $*P<0.05$. (C) Dasatinib (5–50 nM) reduces the number of cell divisions in the hMSC-TERT cell line (left) but does not induce apoptosis (right). MSCs were stained with PKH67 and cultured in osteogenic medium for 7 days in the absence or presence of dasatinib; at the time of collection, cells were also stained with Annexin-V-PE and 7-AAD and analyzed by flow cytometry.
doi:10.1371/journal.pone.0034914.g002

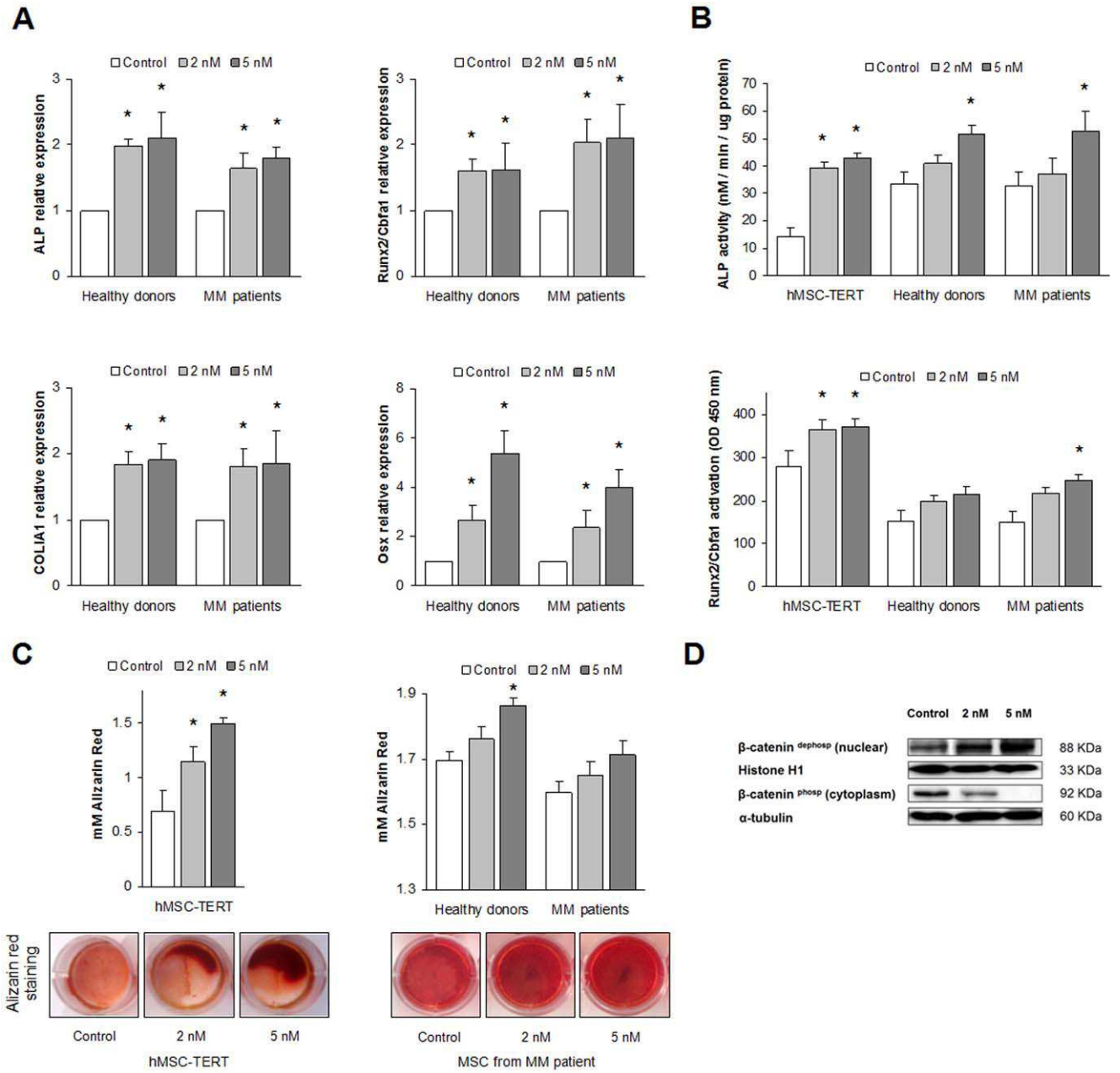

Figure 3. Dasatinib promotes osteogenic differentiation of MSCs from MM patients and healthy donors and of the hMSC-TERT cell line. (A) Dasatinib upregulates the expression of bone-formation markers in the osteogenic differentiation process. Primary MSCs from MM patients and healthy donors were cultured in osteogenic medium in the presence (2–5 nM) or absence of dasatinib, and total RNA was isolated on days 7 and 14. Real-time qRT-PCR was used to determine the expression of several OB related markers: ALP was determined at day 7, whereas the transcription factors Runx2/Cbfa1 and Osterix (Osx), and collagen I type A 1 (COLIA1) were measured at day 14. Expression levels for each gene were normalized to GAPDH expression and referred to those in the absence of dasatinib. Graphs illustrate mean values from samples from 5 healthy donors and 5 MM patients ± SEM (*bars*) *$P<0.05$. (B) Dasatinib increases ALP and Runx2/Cbfa1 activities in osteoprogenitor cells. In the hMSC-TERT cell line and in primary hMSCs derived from three myeloma patients and three healthy donors, ALP activity was measured at day 7 (upper graph) and Runx2/Cbfa1 activity was measured at day 14 (lower graph) after the addition of dasatinib to the osteogenic differentiation medium. Data are represented as the mean ± SD from three experiments. (C) Dasatinib (2–5 nM) augments bone matrix mineralization in OBs derived from the hTERT-MSC cell line (left) or MSCs from healthy donors and myeloma patients (right), as assessed by alizarin red staining quantification. Data are represented as the mean ± SD from three experiments with the hMSC-TERT cell line, and as the mean (5 MM patients and 5 healthy donors) ± SEM in experiments with primary MSCs. Statistically significant differences from controls are indicated as *, where $P < 0.05$. Micrographs show matrix mineralization after alizarin red staining of correspondent differentiated OBs. (D) Both dephospho- and phospho-β-catenin levels were determined by immunoblotting in cytosolic or nuclear lysates of pre-OBs differentiated from the hMSC-TERT cell line in the absence or presence of dasatinib. Histone H1 and α-tubulin were used as loading controls for nuclear or cytosolic protein fractions.
doi:10.1371/journal.pone.0034914.g003

Dasatinib promotes osteoblast differentiation *in vivo*

Consistent with our *in vitro* findings, we corroborated the bone anabolic properties of dasatinib in the *in vivo* setting. To better discern the putative bone formation effect of dasatinib from its known inhibitory activity on OC formation and function, we used skeletally-immature 5 week-old healthy mice which present very active bone formation and minimal bone resorption. Two different doses of dasatinib (2.5 mg/kg *vs* 10 mg/kg) administered twice-a-day (BID) and two periods of dasatinib treatment (3 *vs* 7 weeks) were compared in order to evaluate potential osteogenic/anti-proliferative activities of the drug on endogenous osteoprogenitor cells, as we had observed *in vitro* for primary MSCs. Being ALP an early marker of bone formation, Figure 4A shows that ALP levels in serum were significantly increased in mice treated with both doses of dasatinib after 3 weeks of treatment, whereas ALP levels remained unaffected with respect to vehicle-treated animals at longer treatment periods. Relative to osteocalcin (also a bone formation marker, but expressed at later stages of OB differentiation), significant increases in serum were observed for both doses of dasatinib after 3 weeks and even further increments were attained in a 7-week period. Minimal differences were found in osteocalcin serum levels between the 2.5 mg/kg BID and 10 mg/kg BID doses, neither after 3 weeks nor after 7 weeks of treatment, which probably reflects a near to plateau-effect on osteocalcin induction with the doses in our study. Due to the use of young healthy mice with limited OC function, no changes on levels of TRAP5b (a surrogate marker for OC number) were measured between baseline and after 3 or 7 weeks of treatment (Figure 4C). This is in accordance with a very scarce presence of OCs observed in the histological sections from femurs of control animals along the experiment (data not shown).

The effects of both doses of dasatinib were also evaluated by quantitative micro-CT scanning of distal femurs of treated mice. As observed in Figure 4D, dasatinib treatment led to a marked increase in trabecular microarchitecture of cancellous bone in a dose- and time-dependent manner. This effect was associated to significant increases of trabecular number (Tb N; mm^{-1}) and of the ratio of bone perimeter per bone area (B Pm/B Ar; mm^{-1}), together with decreased trabecular separation (Tb Sp; mm) compared with vehicle-treated animals (Figures 4E-G). The effects of dasatinib on increased trabecular structures were more pronounced for the 10 mg/kg BID and the 7-week period treatment as compared to the rest of the experimental conditions. The increased trabecular number was equally apparent by histologic observation of newly formed trabeculae at the epiphyseal plate (Figure 4H), and also correlated with increased number and intensity of staining of Tcf4 positive OB-like cells lining the trabecular borders (Figure 4I). The transcriptional activation of target genes by Tcf transcription factors mediates the activation of the canonical Wnt/β-catenin signalling pathway, which is essential in OB differentiation [41]. Specifically, within the Tcf family members, Tcf4 is the one most abundantly expressed in OB cell lines and primary human MSCs [42]; therefore, the increased number and intensity of Tcf4 positive cells may well reflect an increased number of active OBs after dasatinib treatment.

Dasatinib inhibits osteoclast formation and activity

We first confirmed the inhibitory effect of dasatinib in osteoclastogenesis (Figure 5A) and OC function (Figure 5B), as has already been reported for this drug [17,18]. For this purpose, PBMCs from healthy volunteers were incubated in an M-CSF/RANKL-containing medium for 21 days, and dasatinib was added throughout the differentiation process or on days 7–21 or 14–21. As seen in Figure 5A, when dasatinib was present for 21 days, it markedly reduced OC numbers in a dose-dependent fashion (IC_{50} = 2.16 nM; $P<0.05$ at ≥1 nM *vs.* control). When dasatinib was added to early OC progenitors (day 7) or to committed OC precursors (day 14) it was also effective in reducing osteoclastogenesis, although higher doses were required: IC_{50} = 3.14 nM; $P<0.05$ at ≥2.5 nM *vs* control (7–21 days); IC_{50} = 5.62 nM; $P<0.05$ at ≥ 2.5 nM *vs* control (14–21 days). Notably, the number of OCs was markedly reduced at higher doses of dasatinib (Figure 5A, e.g., ≥5 nM dasatinib, 1–21 days). This could be explained by a toxic effect of dasatinib on OC progenitors at those doses, but it may well also reflect that dasatinib is targeting essential pathways for OC viability.

Figure 5B shows the area of resorptive pits. Progressive substantial reductions of resorbed lacunae were observed with increasing dasatinib concentrations, resorption being almost completely abrogated at a concentration of 2.5 nM. Of note, this effect of dasatinib on OCs is achieved within similar low doses of dasatinib (low nanomolar range) as for its activity in promoting *in vitro* osteogenic differentiation from mesenchymal precursors. Thus, *in vitro* doses of 2–2.5 nM dasatinib on OCs are sufficient for inhibition of OC formation to a 20% of the control and to reduce the resorptive activity further to a 5% of the control, and would not interfere with the osteogenic activity of this compound.

Mechanism of action of dasatinib on osteoclasts

We first assessed that the low concentrations of dasatinib capable of reducing OC formation and resorption in our previous experiment (1–2 nM) were also effective in inhibiting the activation of the M-CSF receptor, c-Fms, in OCs (as is shown in Figure 6A). Since M-CSF and RANKL are the two main proliferation and survival factors involved in osteoclastogenesis from monocyte/macrophage precursors, the c-Fms kinase has been considered as a major target of dasatinib on OCs [17,18].

However, since dasatinib is capable of inhibiting OC formation when not present throughout the differentiation process but also at later stages of OC differentiation (days 7–21 and 14–21; Figure 5A), together with the fact that OC resorption is more effectively reduced than OC formation (Figure 5A *vs* 5B), indirectly suggests that inhibition of additional tyrosine kinases other than c-Fms, are also contributing to dasatinib effects on this cell type. Figure 6A shows that in OC precursors, even at doses as low as 1 or 2 nM, dasatinib is capable of inhibiting the activation of two other tyrosine kinases, such as c-Src and c-Kit. The c-Src kinase is an essential molecule for OC resorption, intervening in the αVβ3 integrin outside-in signaling in the sealing zone between the OC and the bone matrix [43]; in accordance with these observations, c-Src $^{-/-}$ mice show an osteopetrotic phenotype with OCs unable to form ruffled borders despite a normal morphological appearance [44]. Thus, inhibition of this tyrosine kinase by dasatinib would greatly compromise OC functionality. On the other hand, the ligand for c-Kit, the SCF, has been shown to be mitogenic for OC precursors and to promote mature OC activity [45]. Inhibition of signaling through c-Kit by dasatinib may therefore also play a role in inhibition of osteoclastogenesis and diminished OC resorption.

Besides, when analyzing the expression of several key molecules implicated in OC commitment/differentiation/function, we were able to identify further and novel consequences of dasatinib treatment on this cell type. As shown in Figure 6B, in early OC progenitors (day 4 since initiation of *in vitro* differentiation) dasatinib does not affect levels of PU.1, which is a transcription factor that regulates the commitment of myeloid cells to common progenitors for macrophages and OCs [45]. At a later stage of OC

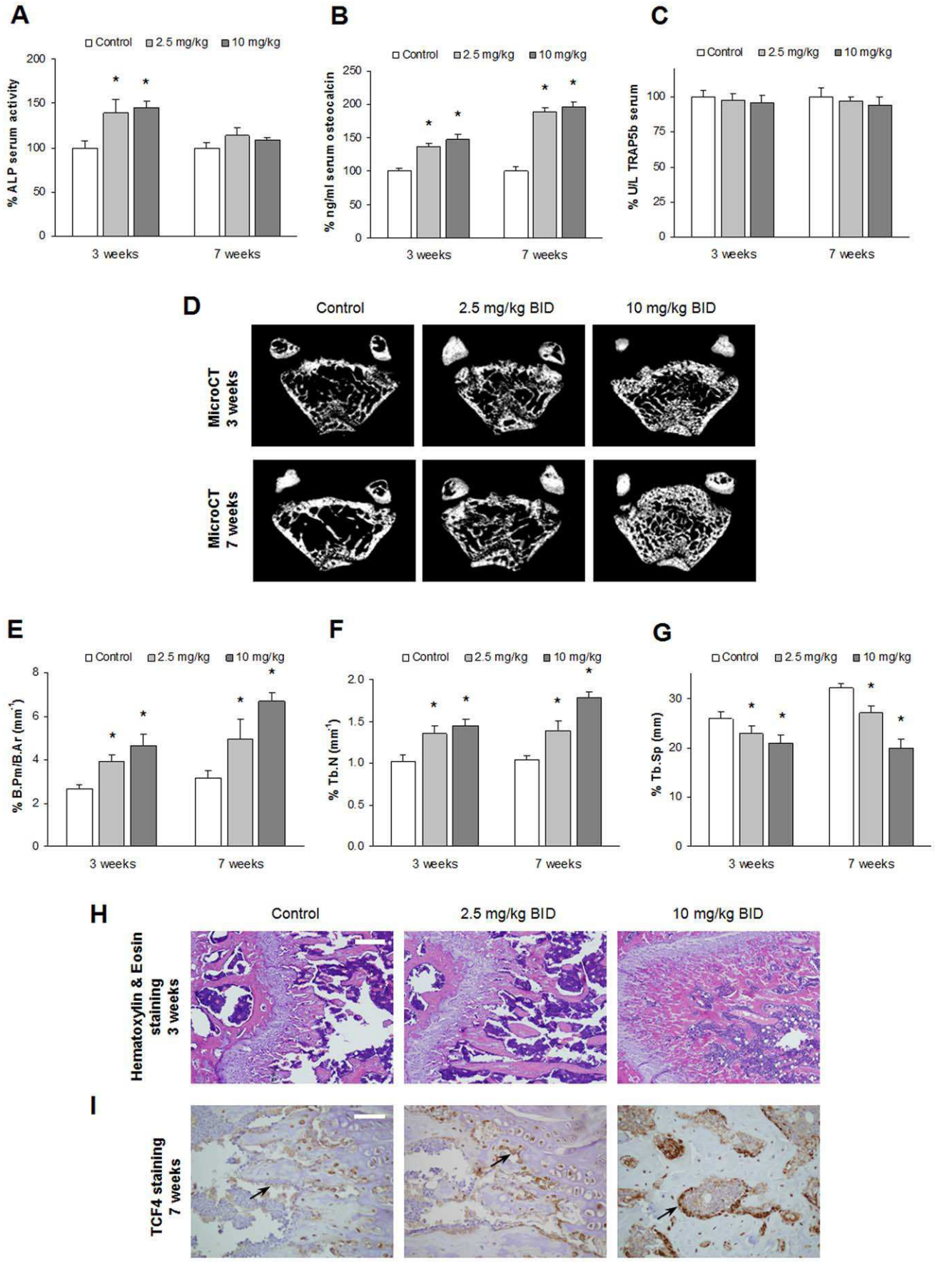
A
Control
2.5 mg/kg
10 mg/kg
% ALP serum activity
200
150
100
50
0
3 weeks
7 weeks
B
Control
2.5 mg/kg
10 mg/kg
% ng/ml serum osteocalcin
250
200
150
100
50
0
3 weeks
7 weeks
C
Control
2.5 mg/kg
10 mg/kg
% U/L TRAP5b serum
100
75
50
25
0
3 weeks
7 weeks
D
Control
2.5 mg/kg BID
10 mg/kg BID
MicroCT 3 weeks
MicroCT 7 weeks
E
Control
2.5 mg/kg
10 mg/kg
% B.Pm/B.Ar (mm-1)
8
6
4
2
0
3 weeks
7 weeks
F
Control
2.5 mg/kg
10 mg/kg
% Tb.N (mm-1)
2.0
1.5
1.0
0.5
0.0
3 weeks
7 weeks
G
Control
2.5 mg/kg
10 mg/kg
% Tb.Sp (mm)
30
20
10
0
3 weeks
7 weeks
H
Control
2.5 mg/kg BID
10 mg/kg BID
Hematoxylin & Eosin staining 3 weeks
I
TCF4 staining 7 weeks

Figure 4. Dasatinib promotes trabecular bone formation *in vivo*. (A, B, C) Five-week-old CD1 mice were treated with vehicle (control) or with dasatinib in a 2.5 mg/kg BID or a 10 mg/kg BID regimen for 3 or 7 weeks, and serum levels were determined for ALP (A), osteocalcin (B) or TRAP5b (C) before initiation of the experiment and at each time point. Graphs are plotted as mean values of fold change from baseline levels for the mentioned factors in sera ± SEM (*bars*). *, $P<0.05$ indicates significant differences between levels for each time and dose of dasatinib and untreated mice at the same conditions (control). (D) Representative micro-CT analyses of equivalent cross-sections of distal femurs are shown for each dasatinib concentration and time of treatment. (E, F, G) Trabecular bone morphometric parameters from micro-CT images were quantitated by CT-Analyser software for bone perimeter per area (E), trabecular number (F) and trabecular separation (G). *, $P<0.05$ relative to vehicle control at each time-point; n = 3 femurs per group. (H) Representative femur sections treated with both dasatinib doses for 3 weeks and stained with hematoxylin and eosin. Bar = 50 μm. (I) Representative images of Tcf4 immunohistochemistry in dasatinib-treated femurs for 7 weeks. OB-like cells immunostained for Tcf4 can be observed lining the trabeculae (arrows). Bar = 12.5 μm.
doi:10.1371/journal.pone.0034914.g004

differentiation (day 7), dasatinib treatment is associated with a slight inhibition of p-Erk 1/2, and specifically, a marked reduction of c-Fos levels. Notably, c-Fos is a key regulator of OC differentiation and is clearly required for osteoclastogenesis [45,46]. Mice lacking c-Fos develop osteopetrosis due to defective OC differentiation, whereas the number of macrophages increases [46,47]. We also show that NFATc1, a major transcription factor integrating RANKL signaling in terminal differentiation of OCs [45,48] is retained in the cytoplasmic fraction while nuclear NFATc1 levels are diminished after dasatinib treatment for 7 days (Figure 6B). NFATc1 requires dephosphorylation and nuclear translocation to activate the transcription of OC-specific genes [49], and thus the diminished transcriptional activity of NFATc1 would likely contribute to the inhibitory effects of dasatinib in OC differentiation. Besides, in late OC precursors (day 14, prefusion OCs and multinucleated OCs), dasatinib treatment reduces the expression of cathepsin K, which is the major cysteine protease in OCs implicated in degradation of organic cellular matrix during bone resorption [43]; therefore, our data provide another mechanism by which dasatinib may inhibit OC resorption.

Furthermore, dasatinib treatment on OCs was also associated to a clear reduced expression of the αVβ3 integrin and of CCR1 (Figure 7A, B), and to disruption or even absence of the F-actin ring in most multinucleated OC precursors (Figure 7C). The αVβ3 integrin mediates the interactions between OCs and the extracellular matrix, and is therefore implicated in cell adhesion, regulation of OC migration and bone resorption [43]. The reduced levels of αVβ3 together with inhibition of c-Src activation, would likely account for the disruption of the F-actin ring, which is necessary for the maintenance of the sealing zone and an effective bone resorption [50]. Also, CCR1 is the major receptor for CCL3 (MIP-1α), a pro-inflammatory cytokine that induces osteoclastogenesis and stimulates OC activity [51–53]. It is therefore conceivable that downregulation of CCR1 by dasatinib would further sustain dasatinib inhibitory effects in OC formation and resorption. Taken together, we could say that at very low concentrations (1–2 nM) dasatinib is capable of targeting various tyrosine kinases (including c-Fms, c-Src, c-Kit), which by several avenues lead to a profound inhibition of osteoclastogenesis and of OC function.

Discussion

Mesenchymal stem cells from the bone marrow may under specific conditions differentiate into osteoblasts, adipocytes, chondrocytes, tenocytes, skeletal myocytes and cells of visceral mesoderm [54,55]. Considerable interest has been raised in recent years for the use of MSCs for repair and regeneration of a number of tissues including bone [56–59]. Moreover, the possibility of pharmacologic agents targeting this population of progenitor cells to specifically enhance their differentiation into the osteogenic

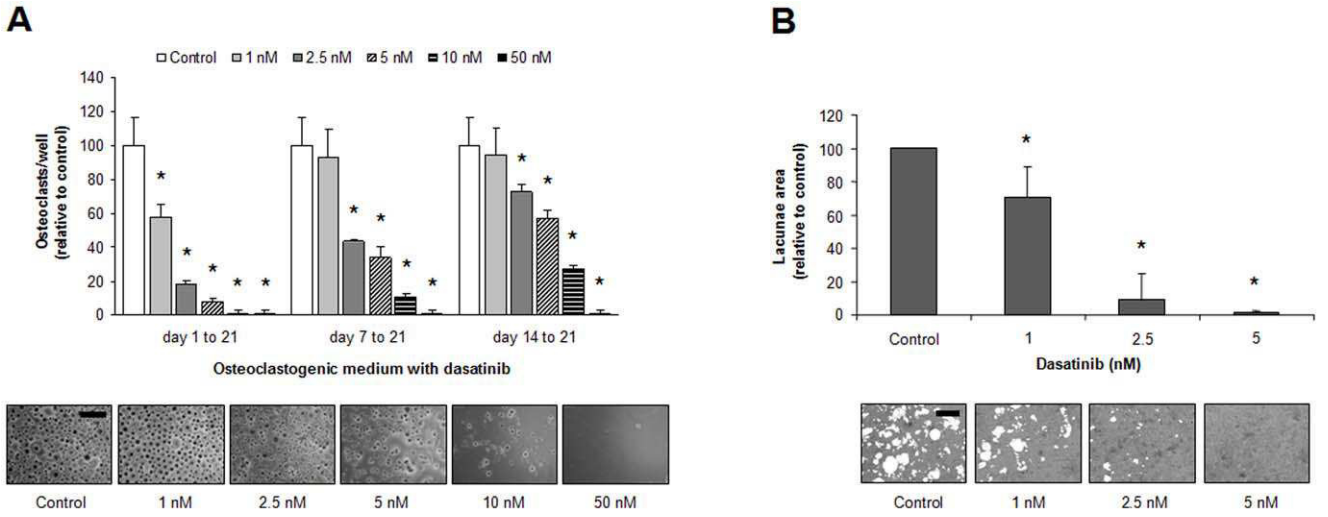

Figure 5. Dasatinib treatment inhibits OC formation and resorption activity. (A) PBMCs from healthy donors were cultured in medium containing M-CSF/RANKL for 21 days in the absence or presence of dasatinib for the indicated times, and OCs were counted (as assessed by TRAP+ staining and the presence of more than three nuclei). Representative micrographs of TRAP staining for OCs treated with dasatinib for 3 weeks are shown. *Bar* = 0 μm. (B) OCs were generated on calcium-coated slides, and the effect of different dasatinib concentrations on OC resorption was evaluated by calculation of the total area of resorbed lacunae. Graphs represent mean values of samples from OCs derived from three healthy donors ± SEM (*bars*). *, $P<0.05$ indicates significant differences between dasatinib-treated cultures and untreated control at the same conditions. Representative micrographs of resorbed lacunae on the calcium-coated wells are shown. *Bar* = 30 μm.
doi:10.1371/journal.pone.0034914.g005

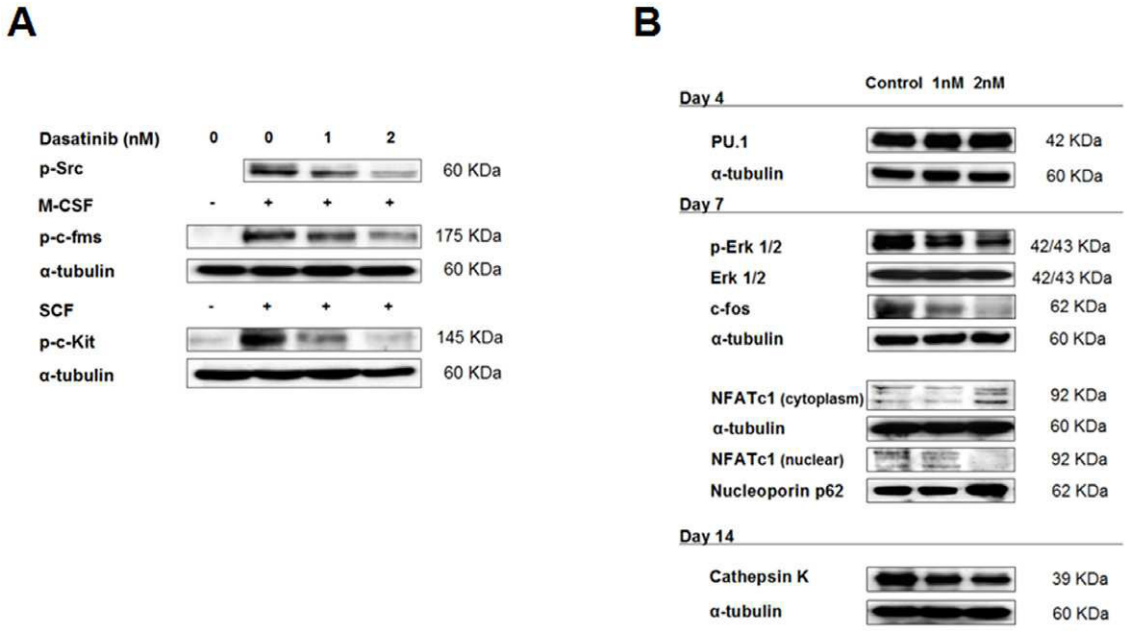

Figure 6. Dasatinib regulates the expression of important molecules/factors for OC formation, differentiation and activity. (A) Dasatinib inhibits c-Fms, c-Src, and c-Kit tyrosine kinase phosphorylation in committed OC precursors. PBMCs were differentiated in osteoclastogenic medium for 7 days, pretreated with 1 nM or 2 nM dasatinib or vehicle, and exposed to 50 ng/mL M-CSF or 50 nM SCF for 20 minutes prior to protein isolation. Immunoblotting with specific antibodies was performed as indicated. (B) PBMCs were maintained in osteoclastogenic medium for indicated times in absence or presence of 1 nM or 2 nM dasatinib. Immunoblots are shown for PU.1, Erk1/2, p-Erk1/2, c-Fos, NFATc1 (both in nuclear and cytoplasmic protein fractions) and cathepsin K.
doi:10.1371/journal.pone.0034914.g006

lineage, further expands their potential as a strategy for bone regenerative medicine.

In concordance with these expectations and also in line with previous data from other groups [19–21], we were able to observe that dasatinib treatment effectively promoted the osteogenic differentiation of mesenchymal progenitors (both primary bone marrow MSCs and the hMSC-TERT cell line) as observed by increased ALP and Runx2 activities, augmented matrix mineralization and elevated expression levels of genes associated with OB differentiation (Runx2/Cbfa1, Osterix, ALP and COLIA1). We have also shown that MSCs and OBs express various tyrosine kinases such as PDGFR-β, c-Src and c-Kit, and although with some differences in sensitivity between MSCs or differentiated OBs, dasatinib at low concentrations (≤5 nM) was capable of partially inhibiting their phosphorylation. It is likely, therefore, that concomitant inhibition of these three kinases might be mediating the osteogenic differentiation in our experimental conditions. Other authors have linked the enhanced OB differentiation of dasatinib to its inhibitory activity on the c-Src kinase [19,20] and on the Abl kinase [19]. We and others have shown that dasatinib promotion of OB differentiation and function relies on inhibition of cell proliferation at lower doses [19] and to

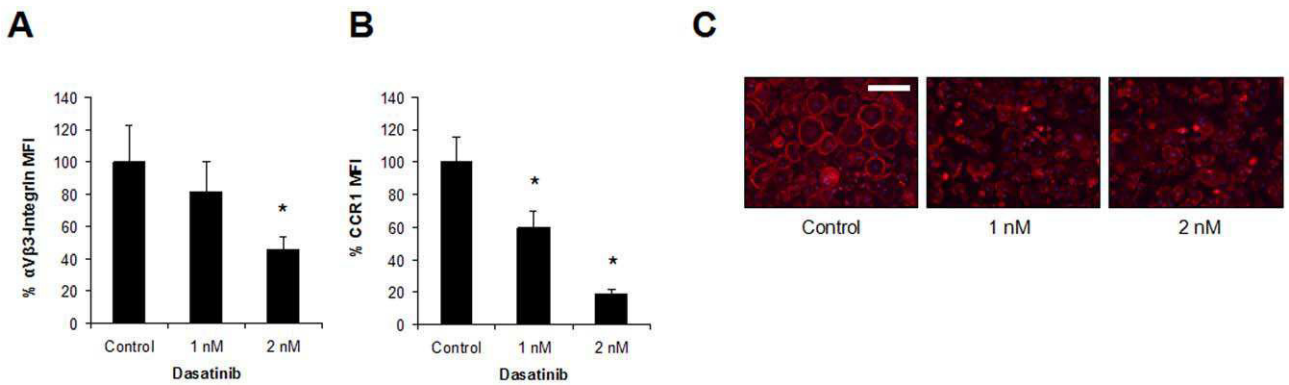

Figure 7. Further consequences of dasatinib treatment on OC function. Expression of αVβ3-integrin (CD51/61) (A) and CCR1 (CD191) (B) was evaluated by flow cytometry in pre-OCs after culture in an osteoclastogenic medium in the absence or presence of dasatinib for 2 weeks. Graphs represent the mean values of the median fluorescence intensity (MFI) percentage from OCs derived from three healthy donors ± SD (*bars*). *, $P<0.05$ indicates significant differences between dasatinib-treated cultures and untreated control. (C) The integrity of the F-actin ring in multinucleated OC precursors (obtained like in A and B) was evaluated by phalloidin-rhodamine staining, whereas nuclei were visualized with DAPI. Representative micrographs for each condition are reported. Bar = 50 μm.
doi:10.1371/journal.pone.0034914.g007

induction of apoptosis with higher doses of the drug [20]. Since we observed that primary MSCs (both from normal donors and myeloma patients) are more sensitive to this effect of dasatinib than the hMSC-TERT cell line, it is worth to mention that if dasatinib is used in the clinical setting to pursue an osteogenic effect, special precaution should be taken to achieve a compromise within reduced osteoprogenitor cell numbers and enhanced osteogenic differentiation.

Interestingly, and in support of our *in vitro* observations on the osteogenic promotion activity of dasatinib, these effects were also reflected in our *in vivo* model. Specifically, 5-week-old skeletally-immature mice with very active bone formation and minimal bone resorption were used, so that the effect of dasatinib on bone could be majorly ascribed to its action on OBs and not to inhibition of OC formation and function. Our data showed that both doses of dasatinib were associated with significant increases of trabecular architecture parameters (as calculated from micro-CT analyses) and a higher number of trabeculae on histologic sections of cancellous bone in distal femurs. Although the increased trabecular structures could also result from the inhibitory effect of dasatinib on OC formation and resorption, the augmented serum levels of bone formation markers (ALP, osteocalcin), the increased number and activation of OB-like cells (as observed by Tcf4 immunostaining), together with absence of significant changes in serum TRAP5b levels (as a surrogate for OC number), lead us to conclude that in our model the augmented trabecular formation after dasatinib treatment is majorly attributable to increased OB formation and activity rather than to an inhibitory effect on OCs. It should also be noted that both doses used in our *in vivo* study are relatively low as compared to those used for this drug in mouse models of tumor malignancies, and near the considered minimum efficacious doses of dasatinib (1.25 mg/kg BID or 2.5 mg/kg once a day) [60]. From preliminary studies (data not shown), we know that levels of bone formation markers (ALP, osteocalcin) were not increased as compared to controls in mice treated with a higher dose of dasatinib (25 mg/kg, BID, 5 days/week), which in line with our *in vitro* studies, highlights the importance of maintaining a low and constant concentration of dasatinib to promote the osteogenic differentiation of osteoprogenitors. It should be mentioned that in another model of physiological bone turnover, skeletally-mature 9-month-old rats were treated with a dasatinib dose of 5 mg/kg once a day (thus quantitatively equivalent to our low dose of 2.5 mg/kg on a BID regimen). Serum OB markers were not significantly altered in this study [61], and increases in tibial trabecular bone volume in the rat model were attributed to dasatinib inhibition of OC activity. This discrepancy in both *in vivo* models may be explained by species differences in sensitivity of osteoprogenitor cells to dasatinib, but also likely to differences in experimental models. Consequently with our observations, the capacity of dasatinib to target bone marrow MSCs and to promote their osteogenic differentiation could be used in the biologic repair of skeletal defects of traumatic origin. For instance, dasatinib could be used as an adjuvant therapy to promote endogenous MSC osteogenic differentiation and accelerate bone fracture healing and bone implant fixation. Moreover, dasatinib treatment after establishment of MSC-based bone grafts could improve bone repair and regeneration in the field of orthopaedic surgery.

On the other hand, we were able to confirm the inhibitory effects of dasatinib on osteoclastogenesis and OC resorption *in vitro* [17,18]. These effects were achieved at very low doses (1–2 nM), and in fact we showed that these concentrations were effective in inhibiting the activation of c-Fms, c-Src and c-Kit (Figure 6A) which are essential tyrosine kinases for OC differentiation and function. When analyzing the expression of several key molecules in the presence of these low dasatinib concentrations, we were able to identify further and novel consequences of dasatinib treatment which would probably contribute to inhibition of OC differentiation (such as reduced c-Fos levels and NFATc1 levels in the nuclear compartment, as well as diminished expression of the CCR1 receptor), and to impair OC resorption (reduced $\alpha v\beta 3$ integrin, CCR1 and cathepsin K protease expression, and F-actin ring disruption). Therefore, dasatinib treatment would by several mechanisms lead to a profound inhibition of OC formation and OC function. As previously mentioned, dasatinib inhibitory effect on OCs has also been shown in an *in vivo* model [61].

It is noteworthy to mention that our inhibitory *in vitro* effects of dasatinib on OC formation and function were achieved within the same low nanomolar range ($\leq$5 nM) of concentrations at which dasatinib promoted the *in vitro* osteogenic differentiation from mesenchymal precursors. Besides, those doses have been reported to be safe and therapeutically achievable in pharmacological studies [60,62]. In our *in vivo* model, we have shown effective bone anabolic effects targeting the osteoprogenitor population also at relatively low dasatinib concentrations (2.5 mg/kg–10 mg/kg) [60]. This likely suggests that there is a therapeutic dosage window of easily pharmacologically achievable low dasatinib concentrations in which concurrent bone formation would be enhanced and bone resorption would be impaired, thus making dasatinib a potential attractive pharmacological approach for the treatment of bone diseases coursing with bone loss and in which both of these processes are affected. In osteoporosis, progressive bone loss results because the osteoblastic activity cannot compensate for excessive bone resorption. Although the standard of care for osteoporosis patients has traditionally relied on anti-resorptive drugs [1,63], last decade advances in the knowledge of bone biology have highlighted the need for additional anabolic treatments in this disease, and several agents, including calcilytic drugs and antagonists of Wnt inhibitors (such as antibodies against sclerostin and anti-DKK1) are now being evaluated in clinical trials (reviewed in [1]). It can be envisioned that the simultaneous bone-forming and anti-resorptive effects of low doses of dasatinib may well be exploited for the treatment of this disease. Also, in osteolytic-type tumor metastases (most common in metastasis of breast, lung and renal cancer), the enhanced differentiation and resorption activity of OCs, is also accompanied by suppressed OB formation due to DKK-1 secretion from tumor cells [3,64]. Therefore, convergent anabolic and anti-resorptive activities of dasatinib could be investigated for beneficial impact as an adjuvant treatment besides regular tumor chemotherapy in metastatic skeletal osteolytic lesions.

The potential therapeutic use of dasatinib as an adjuvant therapy in myeloma-associated bone disease deserves a separate comment. The osteolytic lesions in MM are also characterized by augmented OC numbers and resorption and almost suppressed osteoblast OB differentiation and bone formation [5,65]. The interaction of myeloma cells with stromal and osteoprogenitor cells in the bone marrow leads to the overexpression of multiple OC activating factors (including RANKL, CCL3, IL-3, osteopontin, IL-6 and vascular endothelial growth factor; in turn, OCs also support myeloma proliferation and survival by production of myeloma growth factors such as IL-6, B-cell-activating factor, and a proliferation inducing ligand [4]. The very potent inhibitory effects of dasatinib on osteoclastogenesis and OC function [17,18] and our own data strongly support that dasatinib would greatly reduce OC numbers and resorption in the context of myeloma bone disease. Besides, we have shown that dasatinib treatment reduces CCR1 expression on late OC precursors (Figure 7B),

which is the major receptor for CCL3 (MIP-1α), a crucial stimulator of osteoclastogenesis and of OC function in MM [51,52]. This would therefore further support an inhibitory resorptive effect of dasatinib in the context of myeloma bone disease. On the other hand, reduced osteoblastogenesis in MM relies on abnormal (genetic, functional and phenotypical) properties and impaired osteogenic potential of osteoprogenitor cells from myeloma patients [7,25,66,67], together with production of multiple osteoblastogenesis inhibitors by myeloma cells and the microenviromental cells within the myelomatous bone [5,68,69]. Interestingly, in the present report we have shown that bone marrow MSCs from MM patients, although having a reduced osteogenic capacity [7] are also capable to respond to dasatinib and differentiate to OBs in a similar way as those from normal donors. Preclinical efficacy of dasatinib in multiple myeloma, with specific inhibition of proliferation of myeloma plasma cells and angiogenesis has already been reported [70]. It should be noted, however, that both the *in vitro* stimulatory action of dasatinib on MSCs from myeloma patients as well as its inhibitory effect on OC formation and function are attained at doses in the low nanomolar range (2–5 nM), which are subapoptotic for myeloma cells (IC_{50} = 25–100 nM) and for inhibition of angiogenesis (IC_{50} = 50 nM) [70]. Thererefore, if dasatinib at low doses is to be used in multiple myeloma for a beneficial effect on osteolytic lesions it should be added as a supportive therapy together with other pharmacological agents targeting myeloma growth. Current standard management of MM bone disease relies primarily on bisphosponates (pamidronate, ibandronate, zolendronic acid), which are strong bone-resorption inhibitors but do not stimulate bone formation [71], and may induce adverse side effects such as osteonecrosis of the jaw and renal impairment [72]. Although bisphosphonates are very effective in reducing skeletal complications, bone disease still progresses at a slower rate, which highlights the importance of the clinical incorporation of strategies that may not only impede bone degradation but also promote an anabolic bone effect in multiple myeloma [4,68]. In line with these treatments, our data strongly suggest that dasatinib at low doses may be a valuable adjuvant therapy for the treatment of myeloma-associated bone disease.

In summary, our results provide evidence that low dasatinib concentrations (2–5 nM) are capable of *in vitro* promoting the osteogenic differentiation and OB activity of primary MSCs, including those derived from MM patients. A bone anabolic effect of dasatinib was also observed in a skeletally-immature mouse model with relatively low doses of dasatinib (2.5 mg/kg BID and 10 mg/kg BID), as assessed by increased trabecular structures, elevated serum levels of bone building markers and higher number of active OBs; since no significant changes were found in sera for TRAP5b (a surrogate marker for the number of OCs), the increased bone trabeculae were ascribed to the promotion of OB differentiation and enhanced activity of endogenous mesenchymal progenitors. In addition, in the same range of low nanomolar concentrations, we showed that dasatinib is capable of hindering *in vitro* osteoclastogenesis and resorption activity and of inhibiting the activation of c-Fms, c-Src and c-Kit kinases. Some of the molecular mechanisms mediating these effects on the OC population have also been identified in this study, including some inhibiting OC differentiation (reduced c-Fos and nuclear NFATc1 levels) and function (reduced expression of αvβ3, CCR1, cathepsin K and F-actin ring disruption). Therefore, our data confirm and provide new insights of dasatinib at low doses as a bone modifying agent with convergent bone anabolic and anti-resorptive effects at therapeutically and safe achievable concentrations. Specifically, dasatinib at low concentrations might be used as an adjuvant therapy to promote the osteogenic differentiation of endogenous or ectopically implanted MSCs. Also, dasatinib holds promise to be therapeutically beneficial for bone disorders coursing with augmented bone resorption and inhibited bone formation, such as osteoporosis, osteolytic tumor metastasis and myeloma bone disease.

Acknowledgments

The authors thank Montserrat Martín, Susana Fraile (CIC-IBMCC), Isabel Isidro, Teresa Prieto, Almudena Martín and Sandra Muntión (Hospital Universitario de Salamanca), for their excellent technical work and expertise. We are also thankful to Drs Norma Gutiérrez and Lucía López, Hospital Universitario de Salamanca, for follow-up of MM patients participating in the study. We are indebted to Drs Carlos Ortiz de Solórzano and Laura Guembe, Centro de Investigación Médica Aplicada (CIMA) of the Universidad de Navarra (Spain), for micro-CT and immunohistochemical analyses, as well as to M[a] Victoria Barbado, Universidad de Salamanca, for histologic processing of undecalcified femur samples.

Author Contributions

Conceived and designed the experiments: AG-G EMO CS JFB FMS-G FYL AP JFSM MG. Performed the experiments: AG-G EC CS PH-C RMF-H MG. Analyzed the data: AG-G EMO AP MG. Contributed reagents/materials/analysis tools: CS JFB. Wrote the paper: AG FMS-G JFSM MG. Performed histological studies: TH-I JGB.

References

1. Rachner TD, Khosla S, Hofbauer LC (2011) Osteoporosis: now and the future. Lancet 377: 1276–1287.
2. Vallet S, Smith MR, Raje N (2010) Novel bone-targeted strategies in oncology. Clin Cancer Res 16: 4084–4093.
3. Weilbaecher KN, Guise TA, McCauley LK (2011) Cancer to bone: a fatal attraction. Nat Rev Cancer 11: 411–425.
4. Basak GW, Srivastava AS, Malhotra R, Carrier E (2009) Multiple myeloma bone marrow niche. Curr Pharm Biotechnol 10: 345–346.
5. Yaccoby S (2010) Advances in the understanding of myeloma bone disease and tumour growth. Br J Haematol 149: 311–321.
6. Fowler JA, Edwards CM, Croucher PI (2011) Tumor-host cell interactions in the bone disease of myeloma. Bone 48: 121–128.
7. Corre J, Mahtouk K, Attal M, Gadelorge M, Huynh A, et al. (2007) Bone marrow mesenchymal stem cells are abnormal in multiple myeloma. Leukemia 21: 1079–1088.
8. Todoerti K, Lisignoli G, Storti P, Agnelli L, Novara F, et al. (2010) Distinct transcriptional profiles characterize bone microenvironment mesenchymal cells rather than osteoblasts in relationship with multiple myeloma bone disease. Exp Hematol 38: 141–153.
9. Capdeville R, Buchdunger E, Zimmermann J, Matter A (2002) Glivec (STI571, imatinib), a rationally developed, targeted anticancer drug. Nat Rev Drug Discov 1: 493–502.
10. Karaman MW, Herrgard S, Treiber DK, Gallant P, Atteridge CE, et al. (2008) A quantitative analysis of kinase inhibitor selectivity. Nat Biotechnol 26: 127–132.
11. Fitter S, Dewar AL, Kostakis P, To LB, Hughes TP, et al. (2008) Long-term imatinib therapy promotes bone formation in CML patients. Blood 111: 2538–2547.
12. Vandyke K, Fitter S, Dewar AL, Hughes TP, Zannettino AC (2010) Dysregulation of bone remodeling by imatinib mesylate. Blood 115: 766–774.
13. O'Sullivan S, Naot D, Callon K, Porteous F, Horne A, et al. (2007) Imatinib promotes osteoblast differentiation by inhibiting PDGFR signaling and inhibits osteoclastogenesis by both direct and stromal cell-dependent mechanisms. J Bone Miner Res 22: 1679–1689.
14. Dewar AL, Farrugia AN, Condina MR, Bik To L, Hughes TP, et al. (2006) Imatinib as a potential antiresorptive therapy for bone disease. Blood 107: 4334–4337.
15. Olivieri A, Manzione L (2007) Dasatinib: a new step in molecular target therapy. Ann Oncol 18 Suppl 6: vi42–46.
16. Aguilera DG, Tsimberidou AM (2009) Dasatinib in chronic myeloid leukemia: a review. Ther Clin Risk Manag 5: 281–289.
17. Vandyke K, Dewar AL, Farrugia AN, Fitter S, Bik To L, et al. (2009) Therapeutic concentrations of dasatinib inhibit in vitro osteoclastogenesis. Leukemia 23: 994–997.

18. Brownlow N, Mol C, Hayford C, Ghaem-Maghami S, Dibb NJ (2009) Dasatinib is a potent inhibitor of tumour-associated macrophages, osteoclasts and the FMS receptor. Leukemia 23: 590–594.
19. Lee YC, Huang CF, Murshed M, Chu K, Araujo JC, et al. (2010) Src family kinase/abl inhibitor dasatinib suppresses proliferation and enhances differentiation of osteoblasts. Oncogene 29: 3196–3207.
20. Id Boufker H, Lagneaux L, Najar M, Piccart M, Ghanem G, et al. (2010) The Src inhibitor dasatinib accelerates the differentiation of human bone marrow-derived mesenchymal stromal cells into osteoblasts. BMC Cancer 10: 298.
21. Tibullo D, Barbagallo I, Giallongo C, La Cava P, Branca A, et al. (2011) Effects of second-generation tyrosine kinase inhibitors towards osteogenic differentiation of human mesenchymal cells of healthy donors. Hematol Oncol.
22. Jonsson S, Hjorth-Hansen H, Olsson B, Wadenvik H, Sundan A, et al. (2010) Second-generation TKI dasatinib inhibits proliferation of mesenchymal stem cells and osteoblast differentiation in vitro. Leukemia 24: 1357–1359.
23. Mihara K, Imai C, Coustan-Smith E, Dome JS, Dominici M, et al. (2003) Development and functional characterization of human bone marrow mesenchymal cells immortalized by enforced expression of telomerase. Br J Haematol 120: 846–849.
24. Wang L, Zhao G, Olivares-Navarrete R, Bell BF, Wieland M, et al. (2006) Integrin beta1 silencing in osteoblasts alters substrate-dependent responses to 1,25-dihydroxy vitamin D3. Biomaterials 27: 3716–3725.
25. Garayoa M, Garcia JL, Santamaria C, Garcia-Gomez A, Blanco JF, et al. (2009) Mesenchymal stem cells from multiple myeloma patients display distinct genomic profile as compared with those from normal donors. Leukemia 23: 1515–1527.
26. Dominici M, Le Blanc K, Mueller I, Slaper-Cortenbach I, Marini F, et al. (2006) Minimal criteria for defining multipotent mesenchymal stromal cells. The International Society for Cellular Therapy position statement. Cytotherapy 8: 315–317.
27. Maiso P, Carvajal-Vergara X, Ocio EM, Lopez-Perez R, Mateo G, et al. (2006) The histone deacetylase inhibitor LBH589 is a potent antimyeloma agent that overcomes drug resistance. Cancer Res 66: 5781–5789.
28. Gregory CA, Gunn WG, Peister A, Prockop DJ (2004) An Alizarin red-based assay of mineralization by adherent cells in culture: comparison with cetylpyridinium chloride extraction. Anal Biochem 329: 77–84.
29. Xiao G, Jiang D, Ge C, Zhao Z, Lai Y, et al. (2005) Cooperative interactions between activating transcription factor 4 and Runx2/Cbfa1 stimulate osteoblast-specific osteocalcin gene expression. J Biol Chem 280: 30689–30696.
30. Susa M, Luong-Nguyen NH, Cappellen D, Zamurovic N, Gamse R (2004) Human primary osteoclasts: in vitro generation and applications as pharmacological and clinical assay. J Transl Med 2: 6.
31. Chaudhary LR, Hofmeister AM, Hruska KA (2004) Differential growth factor control of bone formation through osteoprogenitor differentiation. Bone 34: 402–411.
32. Hock JM, Canalis E (1994) Platelet-derived growth factor enhances bone cell replication, but not differentiated function of osteoblasts. Endocrinology 134: 1423–1428.
33. Tokunaga A, Oya T, Ishii Y, Motomura H, Nakamura C, et al. (2008) PDGF receptor beta is a potent regulator of mesenchymal stromal cell function. J Bone Miner Res 23: 1519–1528.
34. Marzia M, Sims NA, Voit S, Migliaccio S, Taranta A, et al. (2000) Decreased c-Src expression enhances osteoblast differentiation and bone formation. J Cell Biol 151: 311–320.
35. Veracini L, Franco M, Boureux A, Simon V, Roche S, et al. (2005) Two functionally distinct pools of Src kinases for PDGF receptor signalling. Biochem Soc Trans 33: 1313–1315.
36. Bantscheff M, Eberhard D, Abraham Y, Bastuck S, Boesche M, et al. (2007) Quantitative chemical proteomics reveals mechanisms of action of clinical ABL kinase inhibitors. Nat Biotechnol 25: 1035–1044.
37. Kratchmarova I, Blagoev B, Haack-Sorensen M, Kassem M, Mann M (2005) Mechanism of divergent growth factor effects in mesenchymal stem cell differentiation. Science 308: 1472–1477.
38. Wang X, Goh CH, Li B (2007) p38 mitogen-activated protein kinase regulates osteoblast differentiation through osterix. Endocrinology 148: 1629–1637.
39. Choi YH, Gu YM, Oh JW, Lee KY (2011) Osterix is regulated by Erk1/2 during osteoblast differentiation. Biochem Biophys Res Commun 415: 472–478.
40. Kulterer B, Friedl G, Jandrositz A, Sanchez-Cabo F, Prokesch A, et al. (2007) Gene expression profiling of human mesenchymal stem cells derived from bone marrow during expansion and osteoblast differentiation. BMC Genomics 8: 70.
41. Clevers H (2006) Wnt/beta-catenin signaling in development and disease. Cell 127: 469–480.
42. Qiang YW, Hu B, Chen Y, Zhong Y, Shi B, et al. (2009) Bortezomib induces osteoblast differentiation via Wnt-independent activation of beta-catenin/TCF signaling. Blood 113: 4319–4330.
43. Vaananen HK, Laitala-Leinonen T (2008) Osteoclast lineage and function. Arch Biochem Biophys 473: 132–138.
44. Teitelbaum SL (2000) Bone resorption by osteoclasts. Science 289: 1504–1508.
45. Asagiri M, Takayanagi H (2007) The molecular understanding of osteoclast differentiation. Bone 40: 251–264.
46. Grigoriadis AE, Wang ZQ, Cecchini MG, Hofstetter W, Felix R, et al. (1994) c-Fos: a key regulator of osteoclast-macrophage lineage determination and bone remodeling. Science 266: 443–448.
47. Wang ZQ, Ovitt C, Grigoriadis AE, Mohle-Steinlein U, Ruther U, et al. (1992) Bone and haematopoietic defects in mice lacking c-fos. Nature 360: 741–745.
48. Takayanagi H (2007) The role of NFAT in osteoclast formation. Ann N Y Acad Sci 1116: 227–237.
49. Martinez-Martinez S, Rodriguez A, Lopez-Maderuelo MD, Ortega-Perez I, Vazquez J, et al. (2006) Blockade of NFAT activation by the second calcineurin binding site. J Biol Chem 281: 6227–6235.
50. Nakamura I, Duong le T, Rodan SB, Rodan GA (2007) Involvement of alpha(v)beta3 integrins in osteoclast function. J Bone Miner Metab 25: 337–344.
51. Han JH, Choi SJ, Kurihara N, Koide M, Oba Y, et al. (2001) Macrophage inflammatory protein-1alpha is an osteoclastogenic factor in myeloma that is independent of receptor activator of nuclear factor kappaB ligand. Blood 97: 3349–3353.
52. Lentzsch S, Gries M, Janz M, Bargou R, Dorken B, et al. (2003) Macrophage inflammatory protein 1-alpha (MIP-1 alpha) triggers migration and signaling cascades mediating survival and proliferation in multiple myeloma (MM) cells. Blood 101: 3568–3573.
53. Roodman GD, Dougall WC (2008) RANK ligand as a therapeutic target for bone metastases and multiple myeloma. Cancer Treat Rev 34: 92–101.
54. Charbord P (2010) Bone marrow mesenchymal stem cells: historical overview and concepts. Hum Gene Ther 21: 1045–1056.
55. Pittenger MF, Mackay AM, Beck SC, Jaiswal RK, Douglas R, et al. (1999) Multilineage potential of adult human mesenchymal stem cells. Science 284: 143–147.
56. Kagami H, Agata H, Tojo A (2011) Bone marrow stromal cells (bone marrow-derived multipotent mesenchymal stromal cells) for bone tissue engineering: basic science to clinical translation. Int J Biochem Cell Biol 43: 286–289.
57. Khosla S, Westendorf JJ, Modder UI (2010) Concise review: Insights from normal bone remodeling and stem cell-based therapies for bone repair. Stem Cells 28: 2124–2128.
58. Nandi SK, Roy S, Mukherjee P, Kundu B, De DK, et al. (2010) Orthopaedic applications of bone graft & graft substitutes: a review. Indian J Med Res 132: 15–30.
59. Mazo M, Gavira JJ, Abizanda G, Moreno C, Ecay M, et al. (2010) Transplantation of mesenchymal stem cells exerts a greater long-term effect than bone marrow mononuclear cells in a chronic myocardial infarction model in rat. Cell Transplant 19: 313–328.
60. Luo FR, Yang Z, Camuso A, Smykla R, McGlinchey K, et al. (2006) Dasatinib (BMS-354825) pharmacokinetics and pharmacodynamic biomarkers in animal models predict optimal clinical exposure. Clin Cancer Res 12: 7180–7186.
61. Vandyke K, Dewar AL, Diamond P, Fitter S, Schultz CG, et al. (2010) The tyrosine kinase inhibitor dasatinib dysregulates bone remodelling through inhibition of osteoclasts in vivo. J Bone Miner Res 25: 1759–1770.
62. Christopher LJ, Cui D, Wu C, Luo R, Manning JA, et al. (2008) Metabolism and disposition of dasatinib after oral administration to humans. Drug Metab Dispos 36: 1357–1364.
63. Sambrook P, Cooper C (2006) Osteoporosis. Lancet 367: 2010–2018.
64. Voorzanger-Rousselot N, Goehrig D, Journe F, Doriath V, Body JJ, et al. (2007) Increased Dickkopf-1 expression in breast cancer bone metastases. Br J Cancer 97: 964–970.
65. Roodman GD (2009) Pathogenesis of myeloma bone disease. Leukemia 23: 435–441.
66. Garderet L, Mazurier C, Chapel A, Ernou I, Boutin L, et al. (2007) Mesenchymal stem cell abnormalities in patients with multiple myeloma. Leuk Lymphoma 48: 2032–2041.
67. Wallace SR, Oken MM, Lunetta KL, Panoskaltsis-Mortari A, Masellis AM (2001) Abnormalities of bone marrow mesenchymal cells in multiple myeloma patients. Cancer 91: 1219–1230.
68. Yaccoby S (2010) Osteoblastogenesis and tumor growth in myeloma. Leuk Lymphoma 51: 213–220.
69. Giuliani N, Rizzoli V, Roodman GD (2006) Multiple myeloma bone disease: Pathophysiology of osteoblast inhibition. Blood 108: 3992–3996.
70. Coluccia AM, Cirulli T, Neri P, Mangieri D, Colanardi MC, et al. (2008) Validation of PDGFRbeta and c-Src tyrosine kinases as tumor/vessel targets in patients with multiple myeloma: preclinical efficacy of the novel, orally available inhibitor dasatinib. Blood 112: 1346–1356.
71. Rosen LS (2004) New generation of bisphosphonates: broad clinical utility in breast and prostate cancer. Oncology (Williston Park) 18: 26–32.
72. Terpos E, Sezer O, Croucher PI, Garcia-Sanz R, Boccadoro M, et al. (2009) The use of bisphosphonates in multiple myeloma: recommendations of an expert panel on behalf of the European Myeloma Network. Ann Oncol 20: 1303–1317.

Invest New Drugs
DOI 10.1007/s10637-012-9845-3

SHORT REPORT

RAF265, a dual BRAF and VEGFR2 inhibitor, prevents osteoclast formation and resorption. Therapeutic implications

Antonio Garcia-Gomez · Enrique M. Ocio · Atanasio Pandiella · Jesús F. San Miguel · Mercedes Garayoa

Received: 17 February 2012 / Accepted: 30 May 2012

Summary *Introduction* The RAS/RAF/MEK/ERK signaling pathway plays an important role in osteoclast (OC) differentiation and survival mediated by macrophage-colony stimulating factor (M-CSF). Also, vascular endothelial growth factor (VEGF) may greatly influence OC formation and resorption through VEGFR1 and VEGFR2. RAF265 is a novel, orally bioavailable dual inhibitor of RAF kinase and VEGFR2. *Methods* Effect of RAF265 on osteoclastogenesis from peripheral blood mononuclear cells (PBMCs) and OC resorption on calcium-coated wells was assessed by appropriate *in vitro* assays. Immunoblotting, real-time RT-PCR and flow cytometry were used to evaluate RAF265 mechanism of action. *Results* RAF265 significantly impaired *in vitro* differentiation of PBMCs to OCs induced by receptor activator of NF-kB ligand (RANKL) and M-CSF ($IC_{50}\cong 160$ nM). In parallel, RAF265 exerted a potent inhibition of OC resorptive capacity ($IC_{50}\cong 20$ nM). RAF265 treatment led to ERK inhibition and diminished expression of c-fos and NFATc1 (nuclear factor of activated T cells, calcineurin-dependent 1), which would likely account for inhibition of osteoclastogenesis. The reduced gene expression of aVb3 integrin, CCR1, cathepsin K, carbonic anhydrase II, matrix metalloproteinase 9, urokinase and tissue-type plasminogen activators, vacuolar H^+-ATPase subunit (ATP6V1A) and Rab7 GTPase would probably mediate RAF265 hindered resorption. RAF265 inhibitory effect on VEGFR2 (noticeable at 10–50 nM) was also found to be implicated in the potent inhibition of this agent on OC function. *Conclusions* We have found a new therapeutic application for RAF265 as an inhibitory agent of osteoclastogenesis and OC function, which might be useful for the treatment of skeletal disorders associated with increased bone resorption.

Keywords RAF265 · Osteoclast · Osteoclastogenesis · Resorption · VEGFR2 · BRAF

A. Garcia-Gomez · E. M. Ocio · A. Pandiella · J. F. San Miguel · M. Garayoa (✉)
Centro de Investigación del Cáncer, IBMCC (Universidad de Salamanca-CSIC),
Campus Miguel de Unamuno, Avda. Coimbra s/n,
37007 Salamanca, Spain
e-mail: mgarayoa@usal.es

A. Garcia-Gomez · J. F. San Miguel · M. Garayoa
Centro en Red de Medicina Regenerativa y Terapia Celular de Castilla y León,
Salamanca, Spain

A. Garcia-Gomez · E. M. Ocio · A. Pandiella · J. F. San Miguel · M. Garayoa
Hospital Universitario de Salamanca-IBSAL,
Salamanca, Spain

Introduction

RAF265 is a novel, orally bioavailable, small molecule inhibitor of RAF kinase and vascular endothelial growth factor receptor 2 (VEGFR2) [1, 2]. It exhibits potent *in vitro* inhibition of the three wild-type isoforms of RAF and of mutant $BRAF^{V600E}$ kinase activities (IC_{50} 3–60 nM) [1, 2], which translates into effective anti-proliferative activity in melanoma and colorectal cancer cell lines harboring activating BRAF mutations (IC_{50} 140–300 nM) [1]. RAF265 has also been

Published online: 07 July 2012

shown to achieve time and dose-dependent tumor regression in $BRAF^{V600E}$ melanoma and colorectal cancer xenograft models [1, 3], correlating with MEK/ERK pathway and cyclin D1 inhibition [4, 5]. RAF265 is currently undergoing a melanoma phase-I/II trial (RAF265-MEL01) with wild type and mutant BRAF patients included [2]. In relation to RAF265 VEGFR2 inhibitory properties, this compound has been shown to inhibit the proliferation of endothelial cells (IC_{50} 20–30 nM) [1], and these anti-angiogenic properties are also thought to indirectly mediate its antitumoral effects [6].

It is known that activation of the RAS/RAF/MEK/ERK pathway is a critical component of the macrophage colony stimulating factor (M-CSF)-promoted osteoclast (OC) differentiation and survival [7, 8]; in fact, MEK1/2 inhibitors have been proven to effectively reduce cytokine-induced osteoclastogenesis [9, 10]. Besides, there is now increasing evidence for VEGF playing a decisive role in OCs, directly enhancing their resorptive activity and survival [11–14], and supporting OC differentiation from precursors similarly to M-CSF [11, 12, 14]. These activities are being mediated by VEGFRs type 1 and 2 present in OCs and OC precursors [11–14]. In light of these observations, and since RAF265 targets both RAF kinase and VEGFR2, we investigated here whether RAF265 could modulate OC formation and/or activity, and also whether any such effects could be due to RAF and/or VEGFR2 inhibition of signal transduction.

Material and methods

In vitro osteoclast differentiation

Human OC precursors were prepared from peripheral blood mononuclear cells (PBMCs) from 6 healthy donors by Ficoll-Paque (ρ 1.073; GE Healthcare, Uppsala, Sweeden) density centrifugation. PBMCs were seeded at 0.5×10^6 cells/cm^2 and cultured overnight in α-MEM medium with 10 % FBS and 100 U/ml penicillin and 100 μg/ml streptomycin. After aspiration, remaining adherent cells were maintained in osteoclastogenic medium [the same medium supplemented with 50 ng/ml RANKL and 25 ng/ml M-CSF (both from Peprotech, London, UK), and with or without RAF265 at indicated doses. The medium was replaced twice per week during 14 days (pre-OCs) or 17–21 days (mature OCs). OCs were identified as tartrate-resistant acid phosphatase [TRAP; leukocyte acid phosphatase kit (Sigma, St Louis, MO, USA)] positive cells containing three or more nuclei.

RAF265 was provided by Novartis (Emeryville, CA, USA). Stock solutions (10 mM) were dissolved in dimethylsulfoxide, and further diluted in cell culture medium to achieve experimental concentrations.

Osteoclast resorption

PBMCs were seeded at 2×10^6 cells/cm^2 on calcium phosphate-coated wells (Becton Dickinson, Bedford, MA, USA) in osteoclastogenic medium for 17 days (adding 1 μM dexamethasone in the first 7 days). The medium was changed twice weekly by semi-depletion in the absence or presence of RAF265. When specifically evaluating RAF265 inhibition of VEGFR2 on OC resorption, either RAF265 or the human anti-VEGFR2 neutralizing antibody [10–100 ng/ml; R&D Systems (Minneapolis, MN, USA)] were added for comparison. At the end of the assay, cells were removed with a 0.1 % Triton X-100 solution and resorption pits were photographed. Resorbed area per well was calculated using the Adobe Photoshop histogram function (Adobe Photoshop CS2, 9.0.2).

Western blot analyses

Western blotting procedures followed standard techniques. To analyze the effect of RAF265 on VEGFR2 phosphorylation, pre-OCs were serum starved overnight, treated with RAF265 for 90 min and then stimulated with 50 ng/ml $VEGF_{165}$ (Peprotech) during 10 min prior to protein isolation. Primary antibodies used in this study were directed against: phospho-VEGFR2, phospho-Erk1/2, cathepsin K and NFATc1 (purchased from Santa Cruz Biotechnology, Santa Cruz, CA, USA), phospho-Src, PU.1 and c-fos (obtained from Cell Signaling Technology, Danvers, MA, USA) and α-tubulin (from Calbiochem, Darmstadt, Germany).

Flow cytometry assays

Pre-OCs differentiated in the absence or presence of RAF265 were detached by trypsinization and stained with anti-CD51/61-PE (αVβ3 integrin-phycoerythrin conjugated Mouse IgG_1) from R&D systems (Minneapolis, MN, USA) or anti-CD191-APC (CCR1-allophycocyanin conjugated Mouse IgG_{2B}) and subsequently with 7-Aminoactinomycin D (7-AAD) (Becton Dickinson). Cells were acquired on a FACSCalibur flow cytometer using the CellQuest program (Becton Dickinson) and analyzed with the Infinicyt software 1.3 (Cytognos, Salamanca, Spain) for specific staining of CD51/61 or CD191 on $7\text{-}AAD^-$ viable cells.

Real-time RT-PCR

Total RNA was isolated from differentiated OCs using the Rneasy Mini kit (Qiagen GmbH, Hilden, Germany) and subsequent reverse transcription was performed with 1.0 μg RNA in the presence of random hexamers and 100 U of SuperScript RNase H reverse transcriptase (Invitrogen, Carlsbad, CA, USA). TaqMan Gene Expression Assays (Applied

Biosystems, Foster City, CA) for CAII, MMP9, PLAU, PLAT, ATP6V1A and Rab7 were performed according to manufacturer's instructions. Relative quantification was calculated using the $2^{-\Delta\Delta Ct}$ values, where $\Delta Ct = Ct_{gene} - Ct_{GAPDH}$ and $\Delta\Delta Ct = \Delta Ct_{Raf265\text{-}treated\ samples} - \Delta Ct_{untreated\ samples}$. Each sample was performed in duplicate and the GADPH gene was used for normalization.

Statistical analyses

Each assay was performed at least three times using PBMCs from different individuals and triplicates were measured for each condition. Quantitative data are expressed as mean ± SD. Statistical comparisons were performed using the non-parametric Mann–Whitney U test (2 groups) and Kruskal-Wallis with Mann–Whitney U post-hoc test with Bonferroni´s adjustment (≥3 groups), and were considered significant for values of $p<0.05$ (SPSS Statistics 15.0, Chicago, IL, USA).

Results

We first examined the effect of RAF265 in a human OC formation system in which PBMCs were cultured in the presence of osteoclastogenic medium for 21 days. As observed in Fig. 1a, RAF265 significantly decreased the number of multinucleated TRAP+ cells in a dose-dependent manner ($IC_{50}\cong 160$ nM). This effect seemed not to be due to a cytotoxic effect of RAF265 on OC progenitors, since cell culture densities did not significantly vary even at higher concentrations of this compound (Fig. 1a and data not shown). It should be noted that this effect of RAF265 was accompanied by a potent reduction of OC activity as assessed by the decrease of the area of resorption lacunae when precursors were established on calcium phosphate-coated wells (Fig. 1b). This decrease of OC resorptive capacity was already evident at doses as low as 10 nM RAF265 ($IC_{50}\cong 20$ nM), and was almost completely abrogated at 50 nM. Therefore, pharmacologically relevant concentrations of RAF265 (personal communication from Novartis) are capable of significantly reducing the *ex vivo* formation and activity of human OCs from peripheral blood precursors.

To gain insight towards the mechanism of action of RAF265, key molecules implicated in the commitment/differentiation/function of OCs were analyzed by immunoblot, flow cytometry or real time RT-PCR along the differentiation process. While PU.1 levels at early stages of OC differentiation were not affected by RAF265, after 7 days of treatment there was a noticeable inhibition of Erk1/2 activation and reduced expression of c-fos and NFATc1 (nuclear factor of activated T cells, calcineurin-dependent 1) at 10–100 nM of RAF265 (Fig. 2a). RAF265 treatment of PBMCs for 14 days (pre-OCs) was also associated to a dose-dependent reduction of levels of αVβ3 integrin, CCR1 (receptor for CCL3, CCL5 and CCL7) and cathepsin K, although these effects were obtained at somewhat higher concentrations of RAF265 (100–500 nM) (Fig. 2a, b). At more mature OCs (17 days), gene expression of other molecules implicated in OC resorptive activity [such as carbonic anhydrase II (CAII), matrix metalloproteinase 9 (MMP9), urokinase and tissue-type plasminogen activators (uPA, tPA), the vacuolar-H^+-ATPase catalytic subunit A1 (ATP6V1A) and the small GTPase Rab7] was significantly diminished by RAF265 (starting at doses

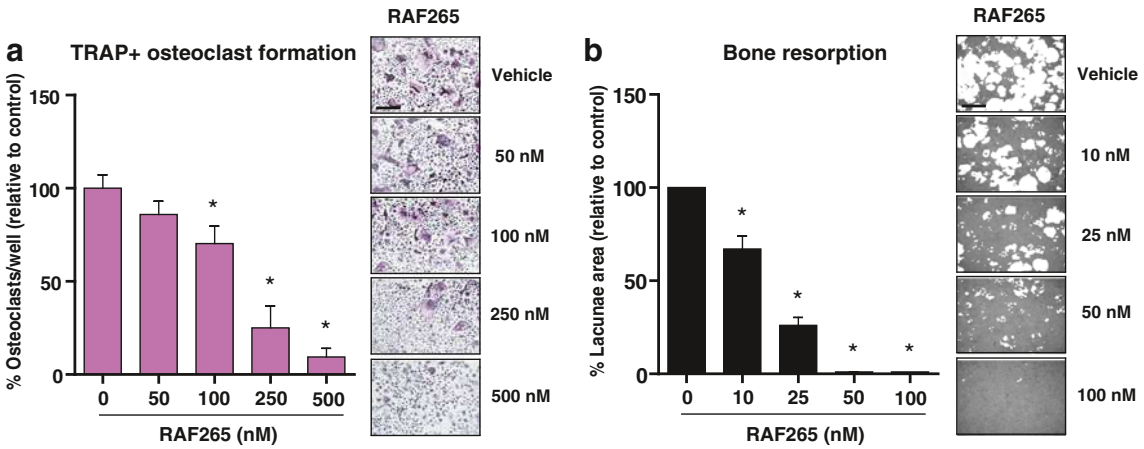

Fig. 1 RAF265 inhibits OC formation and fuction. **a.** RAF265 treatment inhibits OC formation in a dose-dependent manner. PBMCs from healthy donors were cultured in osteoclastogenic medium containing M-CSF and RANKL in the absence or presence of RAF265. OC formation was evaluated by TRAP+staining and enumeration of three or more nuclei. Representative micrographs of TRAP staining for OCs treated with RAF265 for three weeks are shown. *Bar*=30 μm. **b.** RAF265 potently inhibited the area of resorption. OCs were generated on calcium-coated slides for 17 days and the area of resorbed lacunae was measured. *Bar*= 30 μm. Graphs represent mean values of samples from OCs derived from four healthy donors ± SD (*bars*). *, $p<0.05$ indicates significant differences between RAF265 treated cultures and untreated control

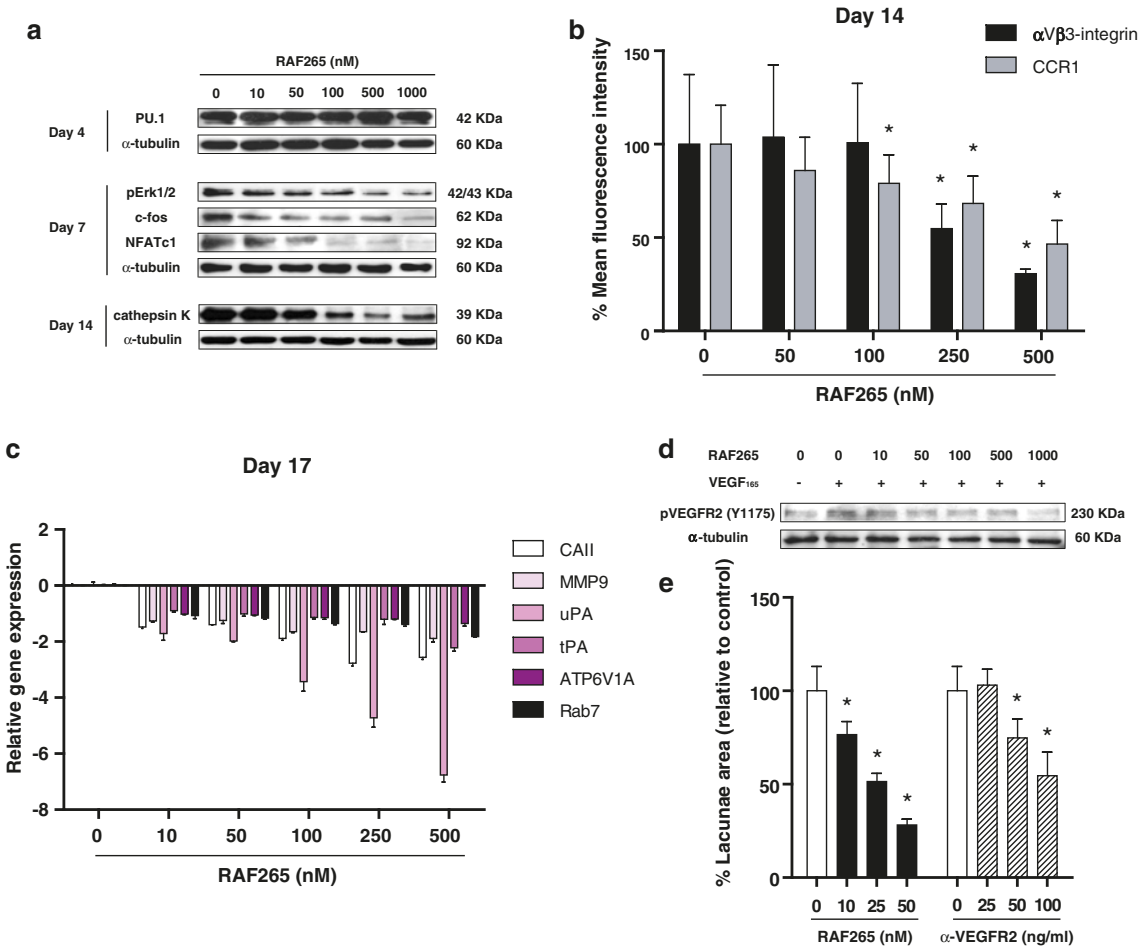

Fig. 2 Raf265 mechanism of action. **a.** Immunoblot analysis of key molecules implicated in OC differentiation and function on RAF265-treated OC precursors for indicated times. PBMCs were maintained in M-CSF and RANKL- supplemented osteoclastogenic medium, treated with RAF265 or vehicle, and analyzed for the expression of selected molecules after 4, 7 or 14 days. Equal protein loading was assessed by α-tubulin expression. **b.** αVβ3 integrin (CD51/61) and CCR1 (CD191) expression were evaluated by flow cytometry analysis in viable (7-AAD$^-$) pre-OCs after culture in the absence or presence of RAF265 for 2 weeks. Graphs represent mean values of the median fluorescence intensity (MFI) percentage from OCs derived from three healthy donors±SD (*bars*). *, $p<0.05$ indicates significant differences between RAF265 treated cultures and vehicle control. **c.** Relative expression of several molecules implicated in OC resorption after differentiation of PBMCs in the presence RAF265 for 17 days, as assessed by real-time RT-PCR. Expression of every gene at all doses of RAF265 was found to be significantly diminished from vehicle control (*, $p<0.05$) or very significantly diminished for uPA at doses≥250 nM (**, $p<0.05$). **d.** Effects of RAF265 on VEGFR2 phosphorylation were evaluated by immunoblot. Pre-OCs (generated from PBMCs in osteoclastogenic medium with M-CSF and RANKL for 14 days) were serum-deprived overnight, treated with RAF265 for 90 min and subsequently stimulated with 50 ng/ml $VEGF_{165}$ for 10 min prior to cell harvest. **e.** RAF265 inhibits OC resorption at low doses and similarly to an anti-VEGFR2 neutralizing antibody. PBMCs were seeded on calcium-phosphate coated wells and differentiated to OCs in M-CSF+RANKL containing medium. Either a neutralizing anti-VEGFR2 antibody (10–100 ng/ml) or different RAF265 doses were added from day 7 (upregulated VEGFR2 expression [14]) to day 17, when the area of resorbed lacunae was calculated for each condition. Graphs represent mean values of resorption from OCs derived from three healthy donors±SD (*bars*). *, $p<0.05$ indicates significant differences between RAF265 or anti-VEGFR2-treated cultures and positive control (M-CSF+RANKL)

as low as 10 nM) (Fig. 2c), likely accounting for the potent inhibitory effect of this agent on OC function.

To determine whether RAF265 inhibitory activity on VEGFR2 was implicated in the inhibition of OC function, we examined the effect of RAF265 pretreatment on $VEGF_{165}$-stimulated VEGFR2 activation. We observed that RAF265 was capable of diminishing VEGFR2 activation starting at doses between 10 and 50 nM (Fig. 2d). Accordingly, RAF265 also reduced OC resorption from M-CSF and RANKL-differentiated PBMCs to an extent similar to that of a neutralizing anti-VEGFR2 antibody; again, this effect being already evident at low doses (10 nM) of RAF265 (Fig. 2e).

Discussion

In this study, we characterize the effects of RAF265, a small molecule inhibitor of RAF kinase and VEGFR2 on formation

and function of primary human OCs. Under continuous treatment, RAF265 dose-dependently inhibits osteoclastogenesis from PBMC-derived precursors (IC_{50}=160 nM), which is accompanied by a potent inhibition of OC resorption even at low doses (IC_{50}≅20 nM). Relative to RAF265 mechanism of action, early commitment from myeloid precursors does not seem to be affected since PU.1 levels do not change (day 4) [15]. RAF265 rather seems to exert its effects at later stages of differentiation by down-regulation of c-fos and NFATc1 expression (day 7), which are major transcription factors implicated in RANKL-mediated osteoclastogenesis [7, 15]. Phosphorylation of Erk1/2 (which is a convergent molecule downstream RAF kinase [7] and VEGFR2 signaling [14]) is also inhibited, paralleling the dose inhibitory effect of this compound on OC formation. These effects of RAF265 closely resemble those of MEK inhibition on OCs [9, 10], indirectly suggesting that RAF265 activity is at least in part being mediated by inhibition of the RAS/RAF/MEK/ERK signaling pathway. At later stages of differentiation (14 days; pre-OCs), levels of cathepsin K, together with those of αVβ3 integrin and CCR1 are significantly diminished by RAF265 (100–500 nM); being cathepsin K the major cysteine protease implicated in degradation of organic cellular matrix in OCs [16], αVβ3 an essential molecule for OC survival and necessary for effective OC resorption [7, 17], and CCR1 the main receptor mediating CCL3 induction of osteoclastogenesis and stimulation of OC activity [18, 19], their reduced expression would further account for RAF265 inhibitory effects on OC differentiation and activity at high doses of the drug. Starting at low doses (10 nM), RAF265 also significantly diminished the expression of several molecules directly (MMP9) or indirectly (CAII, ATP6V1A, uPA, tPA, Rab7) implicated in bone matrix degradation [16, 20, 21], and therefore likely contributing to the potent abrogation of OC function of this agent.

We were also able to observe that RAF265 was capable of inhibition of VEGFR2 phosphorylation after ligand stimulation in pre-OCs at low doses (starting at 10–50 nM). Resorption of PBMCs differentiated in the presence of M-CSF and RANKL was inhibited by RAF265 (≥ 10 nM doses), and this resorptive inhibitory effect was similar to that of an anti-VEGFR2 neutralizing antibody, supporting that the observed potent inhibitory effects of RAF265 on resorption are mediated by VEGFR2 inhibition. The fact that RAF265 inhibits VEGFR2 phosphorylation and proliferation of endothelial cells within the same range of concentrations (IC_{50}=20–30 nM) [1], also indirectly supports our hypothesis. In addition, a switch from VEGFR1 to VEGFR2 expression has been reported to occur along osteoclastogenesis [14], allowing VEGFR2 to play increasingly important roles in resorption of more mature OCs [12, 14], which would further sustain the possibilities of RAF265 inhibitory effects through VEGFR2.

Collectively, our data support a new underappreciated potential therapeutic application of RAF265 for inhibition of osteoclastogenesis and OC resorption, mediated by both its RAF kinase and VEGFR2 inhibitory properties. In addition, our studies provide rationale to target VEGFR2 and RAF kinase to inhibit OC formation and also effectively impair OC function. Assessment of RAF265 anti-resorptive properties with adequate skeletal and extra-skeletal safety margins needs to be proven with appropriate *in vivo* models. Since many treatment strategies for skeletal disorders coursing with augmented OC numbers and increased bone resorption are based on antiresorptive therapies, it could be theoretically hypothesized that patients suffering from those disorders may benefit from RAF265 treatment. Moreover, increasing interest is emerging in the treatment of osteoporosis for the use of uncoupling anti-resorptives which may suppress OC function rather than OC viability, thus theoretically preserving osteoblast and OC physiological communication and maintaining bone formation [22]. It might be worthwhile to evaluate the potential of low doses of RAF265 to preserve the anti-resorptive effects of this compound and not to affect OC viability. Therefore, further studies are needed to test the possibility of RAF265 to be added to the armamentarium of anti-resorptive drugs.

In conclusion, RAF265, based on its RAF kinase and VEGFR2 inhibitory properties, significantly diminishes human OC formation and resorption. Our data also suggest the potential application of RAF265 in bone diseases characterized by augmented OC number and excessive bone resorption, such as osteoporosis, osteolytic tumor metastasis, Paget's disease and multiple myeloma.

Acknowledgements We thank the Fundación de Hemoterapia y Hemodonación de Castilla y León for supply of leuko-platelet concentrates. The authors are also indebted to Montserrat Martín, Irene Rodríguez and Sara González (CIC-IBMCC, Universidad de Salamanca-CSIC), for their excellent technical work and assistance.

This work was supported by grants from the Ministerio de Ciencia e Innovación – Instituto de Salud Carlos III (PI081825); the Fundación de Investigación Médica Mutua Madrileña (AP27262008); and the Centro en Red de Medicina Regenerativa y Terapia Celular de Castilla y León, Consejería Sanidad JCyL-ISCIII. AG-G was supported by the "Proyecto Centro en Red de Medicina Regenerativa y Terapia Celular de Castilla y León" and a Grant from the Fundación Española de Hematología y Hemoterapia 2012.

Conflicts of interest All authors state they have no conflicts of interest. No limitations on access to data or other materials critical to the work being reported are to be disclosed.

References

1. Amiri P, Aikawa ME, Dove J, Stuart DD, Poon D, Pick T, Ramurthy S, Subramanian S, Levine B, Costales A, Harris A, Paul R (2006) CHIR-265 is a potent selective inhibitor of c-Raf/B-Raf/mutB-Raf that effectively inhibits proliferation and survival of cancer cell lines

with Ras/Raf pathway mutations. Proc Amer Assoc Cancer Res 47:4855, Abstract
2. Arkenau HT, Kefford R, Long GV (2011) Targeting BRAF for patients with melanoma. Br J Cancer 104:392–398
3. Ramurthy S, Subramanian S, Aikawa M, Amiri P, Costales A, Dove J, Fong S, Jansen JM, Levine B, Ma S, McBride CM, Michaelian J, Pick T, Poon DJ, Girish S, Shafer CM, Stuart D, Sung L, Renhowe PA (2008) Design and synthesis of orally bioavailable benzimidazoles as Raf kinase inhibitors. J Med Chem 51:7049–7052
4. Chin L, Garraway LA, Fisher DE (2006) Malignant melanoma: genetics and therapeutics in the genomic era. Genes Dev 20:2149–2182
5. Garcia-Echeverria C (2009) Protein and lipid kinase inhibitors as targeted anticancer agents of the Ras/Raf/MEK and PI3K/PKB pathways. Purinergic Signal 5:117–125
6. Tseng JR, Stuart D, Aardalen K, Kaplan A, Aziz N, Hughes NP, Gambhir SS (2011) Use of DNA microarray and small animal positron emission tomography in preclinical drug evaluation of RAF265, a novel B-Raf/VEGFR-2 inhibitor. Neoplasia 13:266–275
7. Ross FP, Teitelbaum SL (2005) alphavbeta3 and macrophage colony-stimulating factor: partners in osteoclast biology. Immunol Rev 208:88–105
8. Yavropoulou MP, Yovos JG (2008) Osteoclastogenesis–current knowledge and future perspectives. J Musculoskelet Neuronal Interact 8:204–216
9. Kim K, Kong SY, Fulciniti M, Li X, Song W, Nahar S, Burger P, Rumizen MJ, Podar K, Chauhan D, Hideshima T, Munshi NC, Richardson P, Clark A, Ogden J, Goutopoulos A, Rastelli L, Anderson KC, Tai YT (2010) Blockade of the MEK/ERK signalling cascade by AS703026, a novel selective MEK1/2 inhibitor, induces pleiotropic anti-myeloma activity in vitro and in vivo. Br J Haematol 149:537–549
10. Tai YT, Fulciniti M, Hideshima T, Song W, Leiba M, Li XF, Rumizen M, Burger P, Morrison A, Podar K, Chauhan D, Tassone P, Richardson P, Munshi NC, Ghobrial IM, Anderson KC (2007) Targeting MEK induces myeloma-cell cytotoxicity and inhibits osteoclastogenesis. Blood 110:1656–1663
11. Aldridge SE, Lennard TW, Williams JR, Birch MA (2005) Vascular endothelial growth factor acts as an osteolytic factor in breast cancer metastases to bone. Br J Cancer 92:1531–1537
12. Aldridge SE, Lennard TW, Williams JR, Birch MA (2005) Vascular endothelial growth factor receptors in osteoclast differentiation and function. Biochem Biophys Res Commun 335:793–798
13. Nakagawa M, Kaneda T, Arakawa T, Morita S, Sato T, Yomada T, Hanada K, Kumegawa M, Hakeda Y (2000) Vascular endothelial growth factor (VEGF) directly enhances osteoclastic bone resorption and survival of mature osteoclasts. FEBS Lett 473:161–164
14. Yang Q, McHugh KP, Patntirapong S, Gu X, Wunderlich L, Hauschka PV (2008) VEGF enhancement of osteoclast survival and bone resorption involves VEGF receptor-2 signaling and beta3-integrin. Matrix Biol 27:589–599
15. Asagiri M, Takayanagi H (2007) The molecular understanding of osteoclast differentiation. Bone 40:251–264
16. Vaananen HK, Laitala-Leinonen T (2008) Osteoclast lineage and function. Arch Biochem Biophys 473:132–138
17. Nakamura I, le Duong T, Rodan SB, Rodan GA (2007) Involvement of alpha(v)beta3 integrins in osteoclast function. J Bone Miner Metab 25:337–344
18. Han JH, Choi SJ, Kurihara N, Koide M, Oba Y, Roodman GD (2001) Macrophage inflammatory protein-1alpha is an osteoclastogenic factor in myeloma that is independent of receptor activator of nuclear factor kappaB ligand. Blood 97:3349–3353
19. Tsubaki M, Kato C, Isono A, Kaneko J, Isozaki M, Satou T, Itoh T, Kidera Y, Tanimori Y, Yanae M, Nishida S (2010) Macrophage inflammatory protein-1alpha induces osteoclast formation by activation of the MEK/ERK/c-Fos pathway and inhibition of the p38MAPK/IRF-3/IFN-beta pathway. J Cell Biochem 111:1661–1672
20. Delaisse JM, Andersen TL, Engsig MT, Henriksen K, Troen T, Blavier L (2003) Matrix metalloproteinases (MMP) and cathepsin K contribute differently to osteoclastic activities. Microsc Res Tech 61:504–513
21. Everts V, Daci E, Tigchelaar-Gutter W, Hoeben KA, Torrekens S, Carmeliet G, Beertsen W (2008) Plasminogen activators are involved in the degradation of bone by osteoclasts. Bone 43:915–920
22. Rachner TD, Khosla S, Hofbauer LC (2011) Osteoporosis: now and the future. Lancet 377:1276–1287

Leukemia (2012), 1–11

www.nature.com/leu

ORIGINAL ARTICLE

The epoxyketone-based proteasome inhibitors carfilzomib and orally bioavailable oprozomib have anti-resorptive and bone-anabolic activity in addition to anti-myeloma effects

MA Hurchla[1,7], A Garcia-Gomez[2,3,4,7], MC Hornick[1], EM Ocio[2,4], A Li[1], JF Blanco[4], L Collins[5], CJ Kirk[6], D Piwnica-Worms[5], R Vij[1], MH Tomasson[1], A Pandiella[2,4], JF San Miguel[2,3,4], M Garayoa[2,3,4,8] and KN Weilbaecher[1,8]

Proteasome inhibitors (PIs), namely bortezomib, have become a cornerstone therapy for multiple myeloma (MM), potently reducing tumor burden and inhibiting pathologic bone destruction. In clinical trials, carfilzomib, a next generation epoxyketone-based irreversible PI, has exhibited potent anti-myeloma efficacy and decreased side effects compared with bortezomib. Carfilzomib and its orally bioavailable analog oprozomib, effectively decreased MM cell viability following continual or transient treatment mimicking *in vivo* pharmacokinetics. Interactions between myeloma cells and the bone marrow (BM) microenvironment augment the number and activity of bone-resorbing osteoclasts (OCs) while inhibiting bone-forming osteoblasts (OBs), resulting in increased tumor growth and osteolytic lesions. At clinically relevant concentrations, carfilzomib and oprozomib directly inhibited OC formation and bone resorption *in vitro*, while enhancing osteogenic differentiation and matrix mineralization. Accordingly, carfilzomib and oprozomib increased trabecular bone volume, decreased bone resorption and enhanced bone formation in non-tumor bearing mice. Finally, in mouse models of disseminated MM, the epoxyketone-based PIs decreased murine 5TGM1 and human RPMI-8226 tumor burden and prevented bone loss. These data demonstrate that, in addition to anti-myeloma properties, carfilzomib and oprozomib effectively shift the bone microenvironment from a catabolic to an anabolic state and, similar to bortezomib, may decrease skeletal complications of MM.

Leukemia advance online publication, 27 July 2012; doi:10.1038/leu.2012.183

Keywords: proteasome inhibitors; multiple myeloma; osteoblast; osteoclast; bone lesions

INTRODUCTION

Multiple myeloma (MM), a malignancy of plasma cells that reside within the bone marrow (BM), is associated with the development of osteolytic lesions (70–80% of patients) characterized by increased osteoclast (OC) numbers and resorption and suppressed osteoblast (OB) differentiation and bone formation. The interaction of myeloma cells with stromal and osteoprogenitor cells in the BM leads to the overexpression of multiple OC activating factors including RANKL, MIP1-α, interleukin (IL)-3, osteopontin, IL-6 and vascular endothelial growth factor.[1,2] In turn, OCs also support myeloma proliferation and survival by production of growth factors such as IL-6, osteopontin, BAFF and APRIL.[1] Conversely, OB formation and activity is significantly reduced by tumoral production of OB inhibitory factors such as DKK-1, sFRP-2, sFRP-3, IL-7 and IL-3, and by direct myeloma and OB cell-to-cell interactions.[3]

The first generation proteasome inhibitor (PI) bortezomib has proven highly efficacious in treating MM, with greatly improved response rates and overall survival in both newly diagnosed and relapsed/refractory myeloma patients.[4,5] Bortezomib, a dipeptide boronic acid,[6] primarily inhibits the chymotrypsin-like activity of the 20S proteasome with slowly reversible binding kinetics.[7] The therapeutic success of bortezomib relies on pleiotropic effects, which decrease both the growth and survival of myeloma cells and the interactions between myeloma cells and the BM microenvironment (reviewed in Hideshima and Anderson[8]). Bortezomib treatment has been associated with clinically beneficial effects on myeloma bone disease,[9] with reports of increase in bone formation markers and decrease in markers of bone resorption (reviewed in Trepos *et al.*[10]). This effect of bortezomib on bone remodeling is not only the consequence of reduced tumor burden, but also due to direct effects on bone cells with the promotion of osteoblastogenesis and reduction of OC numbers reported in both myelomatous and non-myelomatous *in vivo* models[11,12] as well as in numerous *in vitro* studies.[13–18]

Although results obtained with bortezomib are encouraging, a substantial proportion of myeloma patients are refractory to this agent or develop drug resistance.[19] Peripheral neuropathy is a major and dose-limiting adverse effect of bortezomib treatment,[19,20] prompting the development of next-generation PIs with safer toxicity profiles, better tissue distribution and/or oral bioavailability. Within these new PIs, carfilzomib and oprozomib (both from Onyx Pharmaceuticals, San Francisco, CA, USA) are

[1]Department of Medicine, Division of Oncology, Washington University School of Medicine, St Louis, MO, USA; [2]Centro de Investigación del Cáncer, IBMCC (Universidad de Salamanca-CSIC), Salamanca, Spain; [3]Centro en Red de Medicina Regenerativa y Terapia Celular de Castilla y León, Salamanca, Spain; [4]Hospital Universitario de Salamanca-IBSAL, Salamanca, Spain; [5]BRIGHT Institute and Molecular Imaging Center, Mallinkrodt Institute of Radiology, Washington University School of Medicine, St Louis, MO, USA and [6]ONYX Pharmaceuticals, South San Francisco, CA, USA. Correspondence: Dr KN Weilbaecher, Department of Medicine, Division of Oncology, Washington University School of Medicine, Campus Box 8069, 660 S. Euclid Avenue, St Louis, MO 63110, USA.
E-mail: kweilbae@dom.wustl.edu
[7]These authors contributed equally to this work.
[8]These authors contributed equally to this work.
Received 21 October 2011; revised 1 June 2012; accepted 28 June 2012; accepted article preview online 5 July 2012

peptide epoxyketones[6] with selective and irreversible binding to the proteasome chymotrypsin-like subunit.[7] In preclinical studies, carfilzomib exhibits anti-myeloma activity with IC_{50} values and pleiotropic cellular effects comparable to those of bortezomib.[21–23] Furthermore, carfilzomib has been reported to overcome acquired resistance to bortezomib, melphalan and dexamethasone.[21] Phase II and III studies are ongoing in patients with relapsed or refractory myeloma with no serious adverse reports of peripheral neuropathy.[24,25] Oprozomib (formerly known as ONX 0912 and PR-047) is an orally bioavailable analog of carfilzomib, which has been reported to have anti-tumor activity equivalent to carfilzomib in xenograft models of non-Hodgkin's lymphoma and colorectal cancer,[26] and also to exert anti-MM activity *in vitro* and in myeloma animal models.[27] Its favorable pharmacologic profile and tolerability supports its further clinical development and Phase I clinical trials are underway.[28]

While epoxyketone-based PIs have been shown to stimulate bone formation[29] and inhibit osteoclastogenesis,[30] the specific bone effects of carfilzomib and oprozomib are unknown. In this report, we show that both compounds promote OB differentiation and function and inhibit OC formation and resorption equivalently to bortezomib *in vitro* and *in vivo*. Both drugs were effective at reducing myeloma burden and osteolytic bone destruction in mice bearing BM-disseminated myeloma. Collectively, our data demonstrate that carfilzomib and oprozomib effectively inhibit myeloma growth and shift the bone microenvironment from a catabolic to an anabolic state, with reduced toxicity[24,28] and oral administration (in the case of oprozomib)[26,27] being significant advantages to patients.

MATERIALS AND METHODS

Animals

C57Bl/6 and NOD.SCID.IL2R$\gamma^{-/-}$ mice were obtained from The Jackson Laboratory (Bar Harbor, ME, USA). C57Bl/KaLwRij mice were obtained from Dr G Mundy (Vanderbilt University, Nashville, TN, USA). All mice were bred in-house under specific pathogen-free conditions according to guidelines of the Washington University Division of Comparative Medicine. The Animal Ethics Committee approved all experiments.

Drugs

Bortezomib was purchased from Selleckem (Houston, TX, USA). Carfilzomib and oprozomib were supplied by Onyx Pharmaceuticals.

Cell lines

Human myeloma cell lines were obtained from the American Type Culture Collection or other origins[31] and modified to express firefly luciferase. The 5TGM1-GFP murine myeloma line was obtained from Dr G Mundy.[32]

Viability assays

A total of 5×10^4 cells/ml were plated and standard MTT assay (Sigma-Aldrich, St Louis, MO, USA) was performed. For transient dosing experiments, cells were washed twice with phosphate-buffered saline and replaced with drug-free media after 1 h (bortezomib, carfilzomib) or 4 h (oprozomib).

MM.1S-luc co-cultures

Primary human CD138-negative BM stromal cells (BMSCs) from MM patients were plated at 1×10^4 cells/well in 96-well plates for 24 h, serum-starved for 12 h and then MM.1 S-luc cells (1×10^5 cells per well) were added and co-cultured for an additional 48 h. Pre-OCs were generated under osteoclastogenic conditions and 4×10^3 MM.1S-luc cells per well were added, with co-cultures maintained in medium supplemented with 0.5% fetal bovine serum for 5 days. MM.1S-luc viability was assessed by luciferase activity.

In vitro OC differentiation and resorption

Peripheral blood mononuclear cells (PBMCs) from healthy donors were differentiated as in Garcia-Gomez *et al.*[33] Briefly, adherent cells were maintained in osteoclastogenic medium (50 ng/ml RANKL and 25 ng/ml M-CSF (Peprotech, London, UK) for 14 days (pre-OCs) or 21 days (mature OCs). TRAP + (Sigma-Aldrich) multinucleated (⩾3 nuclei) OCs were enumerated. To measure resorption, PBMCs were seeded on calcium-coated wells (BD Biosciences, Bedford, MA, USA) in osteoclastogenic medium for 17 days (with 1 μM dexamethasone the first week), and resorption pit area was calculated.

Nuclear factor-κB (NF-κB) translocation and actin ring formation

Pre-OCs received a 3 h pulse of PIs followed by stimulation with 50 ng/ml RANKL for 30 min. Cells were fixed in 4% paraformaldehyde, permeabilized with 0.1% Triton X-100, and incubated with a mouse anti-p65 antibody (Santa Cruz Biotechnology, Santa Cruz, CA, USA) and a secondary rhodamine-conjugated antibody. Pre-OC F-actin microfilaments were stained using rhodamine-conjugated phalloidin (Invitrogen, Carlsbad, CA, USA).

In vitro OB differentiation, alkaline phosphatase (ALP) activity and mineralization

Primary mesenchymal stem cells (MSCs) from BM aspirates of healthy donors ($n = 6$) and MM patients with ($n = 6$) or without osteolytic bone lesions ($n = 3$) were generated and assayed as described.[33] The human MSC line (hMSC-TERT) was a generous gift from Dr D Campana (St Jude Children's Research Hospital, Memphis, TN, USA). Briefly, the hMSC-TERT and primary MSCs (passage 3) were cultured in osteogenic medium (containing 5 mM β-glycerophosphate, 50 μg/ml ascorbic acid and 80 nM dexamethasone) for 11 (early OBs; ALP activity), 14 (pre-OBs) or 21 days (mature OBs; matrix mineralization). ALP activity was quantified by hydrolysis of *p*-nitrophenylphosphate into *p*-nitrophenol (Sigma-Aldrich) and mineralization assessed by alizarin red staining.

Real-time reverse transcription-PCR analysis

TaqMan Gene Expression Assays (Applied Biosystems, Foster City, CA, USA) were performed according to manufacturer's instructions. Assay IDs were: *Runx2*, Hs01047976_m1, *Osterix*, Hs00541729_m1, *Osteopontin*, Hs00959010_m1, *Osteocalcin*, Hs01587814_g1, *DKK-1*, Hs00183740_m1, *Osteoprotegerin*, Hs00900358_m1, *RANKL*, Hs00243522_m1_ and *IRE1α*, Hs00176385_m1. Relative quantification of the target gene expression was calculated by the comparative threshold cycle method. Samples were performed in duplicate with GAPDH used for normalization.

Reporter Assay

MC3T3-E1 murine pre-OB cells were transfected with Cignal Finder dual-luciferase reporter constructs (SABiosciences, Valencia, CA, USA) using X-tremeGENE HP reagent (Roche, Indianapolis, IN, USA). Twenty-four hours after transfection, cells were drug treated for 24 h in OptiMEM (Invitrogen) containing 1% fetal bovine serum and assayed using the Dual-Glo Luciferase Assay System (Promega, Madison, WI, USA). As the CMV promoter driving the Renilla reporter construct used for normalization was modulated itself by PIs, firefly luciferase activity is presented as a ratio over the average of vehicle group. The assay was repeated twice with six replicates per condition to partially account for the lack of normalization.

Western blot

Protein isolation and western blot analyses were performed as in Garcia-Gomez *et al.*[33] using antibodies against IRE1α (Cell Signaling Technology, Danvers, MA, USA) and α-tubulin (Calbiochem, Damstadt, Germany).

Gene silencing

hMSC-TERT cells were transfected with either ON-TARGETplus SMARTpool siRNA targeting human IRE1 or ON-TARGETplus non-targeting pool as negative control (Dharmacon, Lafayette, CO, USA), using SAFEctin-STEM (Deliverics, Edinburg, UK) following supplierś instructions. Minimal toxicity of transfection reagent allowed repeated siRNA transfections (three times per week for 3 weeks).

In vivo drug treatment

PIs were administered to mice on the following weekly schedules: bortezomib (1 mg/kg intravenously days 1 and 4); carfilzomib (5 mg/kg for C57Bl/6, 3 mg/kg for KaLwRij, intravenously days 1 and 2); oprozomib

(30 mg/kg by oral gavage once daily for 5 consecutive days followed by 2 days of rest). Vehicle mice were administered both oral 1% carboxymethylcellulose (oprozomib schedule) and intravenous 10% Captisol in 10 mM citrate buffer, pH 3.5 (carfilzomib schedule). In Figure 5f, following 14 days of drug treatment, three doses of 1 mg/kg of RANKL were given intraperitoneally at 24 h intervals as described in Tomimori *et al.*[34] Serum was collected 90 min after the final RANKL injection.

Micro-computed tomography (microCT)

Tibial metaphyses were scanned with a microCT-40 system (Scanco Medical, Wayne, PA, USA) as described previously.[35] A three-dimensional cubical voxel model of bone was built and calculations were made for relative bone volume per total volume and trabecular number.

Bone turnover markers

Carboxy-terminal telopeptide collagen crosslinks (CTX) and N-terminal propeptide of type I procollagen (P1NP) were measured in fasting serum using ELISA systems (Immunodiagnostic Systems, Scottsdale, AZ, USA).

In vivo bone formation rate

Mice were injected with 20 mg/kg calcein (Sigma-Aldrich) in 2% sodium bicarbonate 7 days and 2 days prior to sacrifice. Bone formation rate (BFR/BS) in femoral trabeculae was calculated as previously described[36] using Bioquant Osteo software (Bioquant, Nashville, TN, USA).

Mouse models of BM disseminated MM

A total of 1×10^6 murine 5TGM1-GFP cells were injected intravenously into 8-week-old female KaLwRij mice.[32] Clonal tumor expansion was monitored by serum murine IgG2b ELISA (Bethyl Laboratories, Montgomery, TX, USA). Drug treatment was initiated 14 days following tumor injection. At sacrifice, GFP+ tumor burden was assessed by flow cytometry. In separate experiments, 2×10^6 human RPMI-8226-luc were injected intravenously into NOD-SCID-IL2R$\gamma^{-/-}$ mice and tumor development was monitored by non-invasive bioluminescence imaging with an IVIS 100 system (Caliper, Hopkinton, MA, USA; exposure time 300 s, binning 16, field of view 12, f/stop 1, open filter) following intraperitoneal injection of 150 μg/g D-luciferin (Biosynth, Naperville, IL, USA).[37] Serum human Igλ was measured by ELISA (Bethyl Laboratories).

Statistical analyses

Assays were performed at least three times using cells from at least three different individuals and duplicates (reverse transcription-PCR) or triplicates were measured. Statistical comparisons were performed on *in vitro* experiments (Figures 1 and 4) using the non-parametric Mann–Whitney *U* test (2 groups) and Kruskal–Wallis with Mann–Whitney *U post-hoc* test with Bonferroni's adjustment (⩾3 groups); *in vivo* studies (Figures 5 and 7) used the Student's *t*-test (2 groups) or one-way ANOVA with Tukey's multiple comparison test (⩾3 groups): $^*P<0.05$; $^{**}P<0.01$; $^{***}P<0.001$.

RESULTS

Continuous or physiologic transient administration of carfilzomib or oprozomib is cytotoxic to human MM cells *in vitro*

Under 48 h of continual drug incubation, carfilzomib and oprozomib exerted a cytotoxic effect on a panel of 10 human MM cell lines similar to bortezomib. In agreement with previous reports, the IC_{50} was approximately 2 nM for bortezomib,

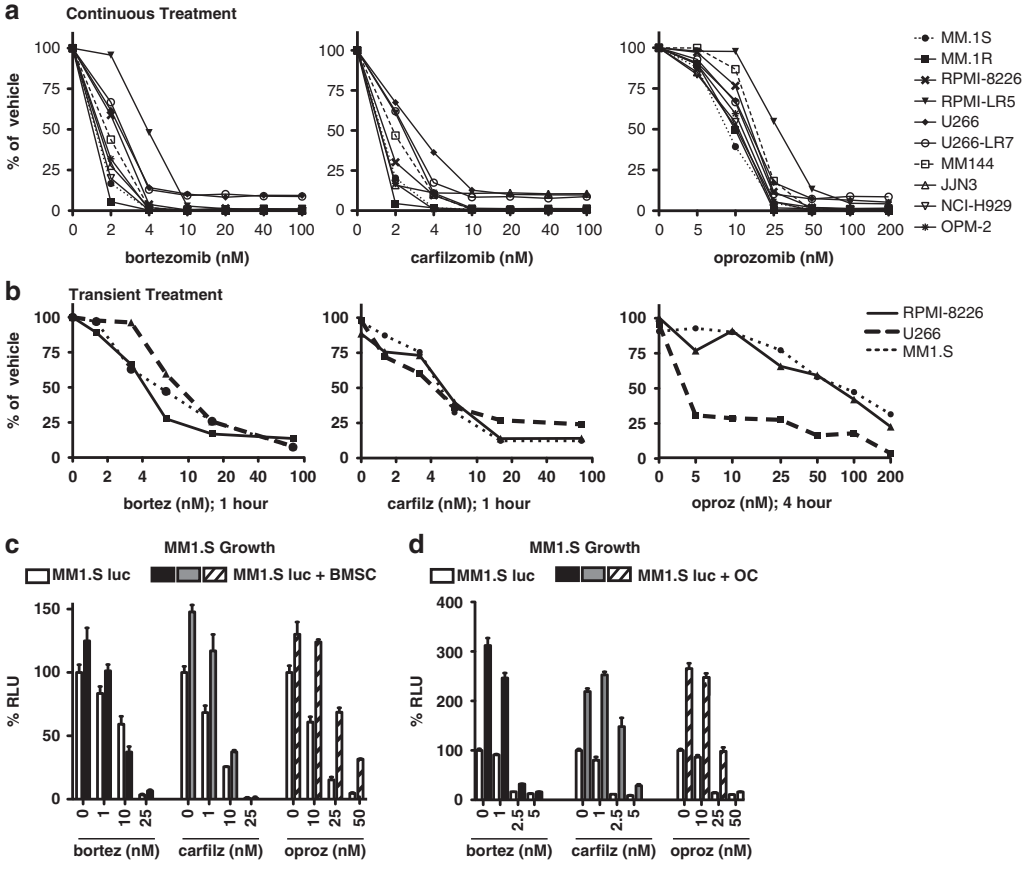

Figure 1. Continuous or physiologic transient administration of carfilzomib or oprozomib is cytotoxic to human MM cells *in vitro*. (**a**) A panel of 10 human MM cell lines were treated with the indicated doses of bortezomib, carfilzomib or oprozomib continuously for 48 h and subjected to MTT assay for viability. (**b**) MM cell lines were treated with indicated drug doses on day 0 for 1 h (bortezomib, carfilzomib) or 4 h (oprozomib). Cells were then washed and cultured in drug-free media for 48 additional h and viability assessed by MTT assay. (**c**, **d**) PIs overcome the proliferative and protective effects of bone microenvironment cells. MM.1S cells labeled with firefly luciferase (MM.1S-luc) were cultured in the presence (filled bars) or absence (open bars) of human (**c**) $CD138^-$ BMSCs or (**d**) OCs. Cultures were treated with indicated doses of drugs for 48 h (BMSC) or 5 days (OC) and MM cell viability readout by luciferase activity. Results are expressed as mean ± s.d. RLU, relative luminescence units.

3 nM for carfilzomib[22] and 25 nM for oprozomib[27] (Figure 1a). However, pharmacokinetic data indicate that *in vivo* exposure to drug is approximately 4 h following oral delivery of oprozomib[28] and approximately 1 h with intravenous administration of carfilzomib or bortezomib.[22,38] To more accurately replicate this physiological situation *in vitro*, cells were transiently treated with oprozomib for 4 h and with carfilzomib or bortezomib for 1 h followed by an additional 48 h culture in drug-free media. Myeloma cell lines remained susceptible to proteasome inhibition under short treatment conditions (Figure 1b), although increased doses were required to achieve similar efficacy (8 nM bortezomib, 6 nM carfilzomib and 50 nM oprozomib). Effective transient doses were still well below the maximum serum levels (C_{max}) attained in patients (bortezomib: 0.162 μM (1.3 mg/m^2 intravenous)[39]; carfilzomib: 0.95 μM (20 mg/m^2 intravenous);[40] oprozomib: 3.8 μM (30 mg per os)[28]). The decrease in MM viability by carfilzomib and oprozomib was attributed to both inhibition of proliferation and apoptosis induction (data not shown), consistent with previous reports examining these PIs.[21,27]

Cells within the BM microenvironment, specifically BMSCs and OCs, produce factors that support the growth and survival of myeloma cells[1] while protecting them from chemotherapy-induced apoptosis.[41] Under experimental settings resembling the protective environment of bone, all PIs remained effective at inhibiting MM.1S survival, although co-culture with human MM BMSCs (Figure 1c) or OCs (Figure 1d) required approximately twofold dose increases to reach similar cytotoxic efficacy (Figure 1c). Notably, the required doses remained well within the range achievable *in vivo*.[28,39,40] In summary, similarly to bortezomib, carfilzomib and oprozomib exert potent cytotoxic effects on myeloma cells under continuous and physiological dosing conditions, even in the presence of protective BMSCs and OCs.

Oprozomib and carfilzomib inhibit OC differentiation and function *in vitro*

Similar to bortezomib, carfilzomib and oprozomib strongly inhibited the *in vitro* differentiation and formation of mature, multinucleated OCs of human (Figure 2a) and murine (Supplementary Figure 1A) origin. Under continuous treatment, osteoclastogenesis was abrogated by 50% at concentrations similar to doses exerting myeloma cell cytotoxicity (bortezomib = 1.21 nM, carfilzomib = 2.43 nM; oprozomib = 25.88 nM). Importantly, this inhibitory effect was evident under both continuous and physiological transient drug treatment conditions, though transient treatment required approximately fivefold higher doses. Notably, oprozomib and carfilzomib did not exert cytotoxic effects on OCs, as cell densities in cultures for IC_{50} doses were not markedly reduced (Figure 2a and Supplementary Figure 1A). Murine macrophages (OC progenitors) were also resistant to the cytotoxic effects of PIs, with IC_{50}'s greater than 1 μM, approximately 50–100-fold higher than doses required to kill myeloma cells (Supplementary Figures 1B and C). Thus, under physiological conditions and at concentrations cytotoxic to myeloma cells, carfilzomib and oprozomib inhibited OC differentiation without exerting cytotoxic effects on their precursor cells.

To test the ability of the new PIs to inhibit osteoclastic bone resorption, OC cultures from human PBMCs were established on calcium substrate-coated slides. Similarly to bortezomib,[17,18,42] a dose-dependent reduction in resorption pit area was observed following continuous incubation with carfilzomib or oprozomib (Figure 2b). The concentration of each drug required to inhibit resorption was less than that required to inhibit OC differentiation, most notably for oprozomib (Figures 2a and b, left), suggesting that these PIs may independently affect OC resorptive function. Both preservation of the F-actin ring and expression of the αVβ3 integrin are necessary for maintenance of OC structural polarization, adhesion to bone matrix and formation of a sealing zone for effective bone resorption.[43,44] Treatment with all PIs resulted in a partial or complete disruption of the F-actin ring (Figure 2c) and reduced expression of αVβ3 integrin (Supplementary Table 1). OC-mediated resorption also requires functional signaling through a complex pathway involving mitogen-activated protein kinase (MAPK) and NF-κB[45]. PI treatment of human pre-OCs prevented RANKL-induced NF-κB activation, with the p65 subunit being retained in the cytoplasm (Figure 2d). This effect is consistent with impaired proteasomal degradation of I-κB, suggesting that, similar to bortezomib,[17,18] carfilzomib and oprozomib-mediated inhibition of *ex vivo* OC activity may partially act through disruption of RANKL-induced NF-κB signaling. Together, these data demonstrate that epoxyketone-based PIs are capable of inhibiting OC resorptive function through multiple mechanisms.

Carfilzomib and oprozomib promote osteogenic differentiation and mineralization *in vitro*

While the inhibition of pathological bone resorption through anti-catabolic agents is inarguably crucial for the control of myeloma bone disease, anabolic treatments capable of stimulating new bone formation are important for reversing damage. As several PIs including bortezomib[13–16] and epoxomicin[29] are recognized to enhance OB formation and function, we tested whether the same held true for carfilzomib and oprozomib. Murine mesenchymal stem cells (MSC), the OB progenitors, were resistant to cytotoxic effects (Supplementary Figure 2A) and alterations in proliferation (Supplementary Figure 2B) at clinically relevant doses of PIs. When differentiating primary human MM patient MSCs (Figure 3a) or murine MSCs (Supplementary Figure 2C) into OBs *in vitro*, carfilzomib and oprozomib increased matrix mineralization and calcium deposition under both continuous (days 0–21) and transient (1–4 h dose on day 0) dosing conditions. Furthermore, both drugs dose-dependently increased ALP activity, a surrogate marker of early osteoblastic activation, in human myeloma patient OBs (Figure 3b). Increased ALP activity and mineralization were also observed when treating MSCs from healthy donors (data not shown), suggesting that such effects are not isolated to myelomatous stroma. Likewise, markers of OB differentiation were significantly elevated in PI-treated OBs derived from the hMSC-TERT cell line compared with vehicle-treated controls (Figure 3c). Of note, at equimolar concentrations, carfilzomib induced a significantly higher expression of Osterix and osteopontin as compared with bortezomib. In addition, all PIs induced modest but significant reductions in mRNA levels of the OB inhibitory protein Dkk-1 in pre-OBs (Figure 3c).

In reporter assay systems, 24 h treatment of MC3T3-E1 osteoprogenitor cells with PIs enhanced the activity of Smad2/3/4, serum response element (SRE) and AP1 transcription factors (Figure 4a). Although transforming growth factor β signaling exerts inhibitory effects in mature OBs,[46] activity of Smad2/3 together with Smad4 promotes early osteoprogenitor commitment and differentiation by inducing OB-specific gene transcription.[47] Likewise, MAPK signaling cascades through ERK (extracellular-signal-regulated kinase) (SRE) and JNK (c-Jun N-terminal kinase) (AP1) have been reported to upregulate Runx2 and Osterix, supporting osteogenic differentiation.[48,49] Conversely, the activation of the unfolded protein response (UPR) is of particular importance in cells specialized to secrete proteins, such as plasma cells, endocrine cells and OBs. The IRE1-XBP1 pathway has been recently shown to promote OB differentiation by driving transcription of Osterix.[50] Treatment of hMSC-TERT cells with carfilzomib or oprozomib resulted in upregulation of the IRE1α component of the UPR (Figure 4b). IRE1α inhibition by siRNA significantly diminished PI-enhanced mineralization (Figures 4c and d), underscoring the crucial role of IRE1α in the promotion of OB activity by PIs. In MM,

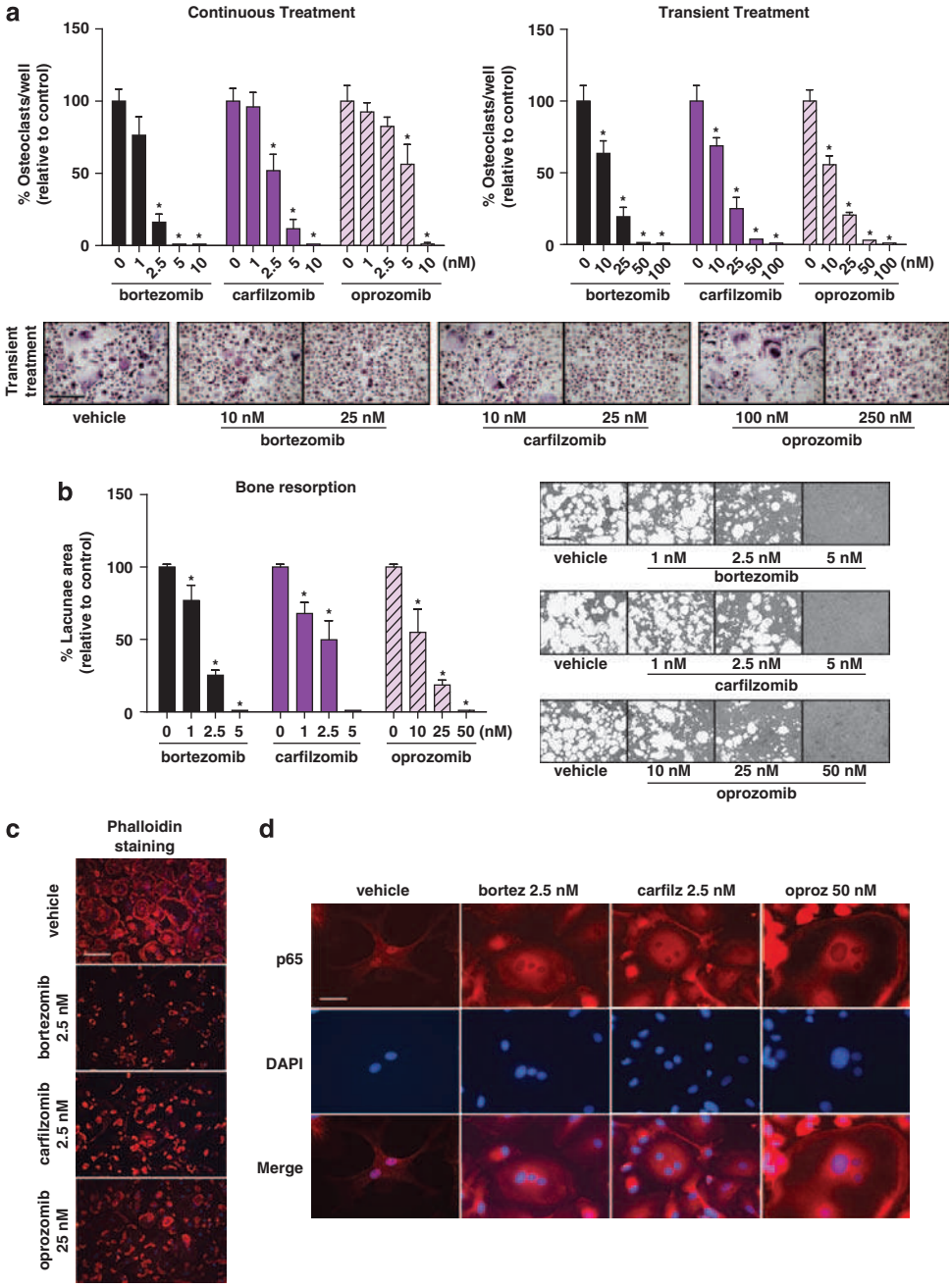

Figure 2. Oprozomib and carfilzomib inhibit OC differentiation and function *in vitro*. (**a**) Human OCs were generated from PBMCs cultured in osteoclastogenic medium for 21 days in the presence or absence of indicated concentrations of the PIs (continuous treatment, left panel); alternatively, PIs were present only for the initial 4 h of differentiation (transient treatment, right panel). OCs were identified as multinucleated ($\geqslant$3 nuclei) TRAP+ cells. Representative micrographs of differentiated OCs after transient treatment are shown. (**b**) To assess inhibition of mineralized matrix resorption, PBMCs were seeded on calcium-coated slides and maintained in osteoclastogenic medium for 17 days with or without indicated concentrations of the drugs. Graphs represent mean values of samples from OCs derived from three healthy donors ± s.d. *$P<0.05$ between treated cultures and vehicle control. Bar = 50 μm. (**c**) PIs disrupted the integrity of the actin ring in multinucleated pre-OCs (14 days in osteoclastogenic medium under continuous PI-treatment). Actin = phalloidin–rhodamine, DAPI = nuclei; representative micrographs are reported. Bar = 50 μm. (**d**) Pre-OCs were treated with indicated concentrations of PIs for 3 h prior to stimulation with RANKL for 30 min. In absence of PIs (vehicle), RANKL induces p65 translocation to the nucleus, whereas in PI-treated cells the p65 subunit of NF-κB is retained in the cytoplasm. p65 subunit = visualized in red, DAPI = nuclei; representative micrographs for each PI are shown (Bar = 12.5 μm).

osteoclastogenesis and OC activity is partially modulated by OB expression of membrane-bound RANKL and secreted osteoprotegerin.[1] The presence of PIs during OB differentiation inhibited RANKL expression, yet only a modest trend toward increase of osteoprotegerin mRNA levels was observed (Figure 4e). In summary, PIs directly stimulated the transforming growth factor β and MAPK pathways and increased the activity of the UPR resulting in enhanced OB differentiation and matrix mineralization, while indirectly hindering OC stimulation through decreased OB expression of RANKL.

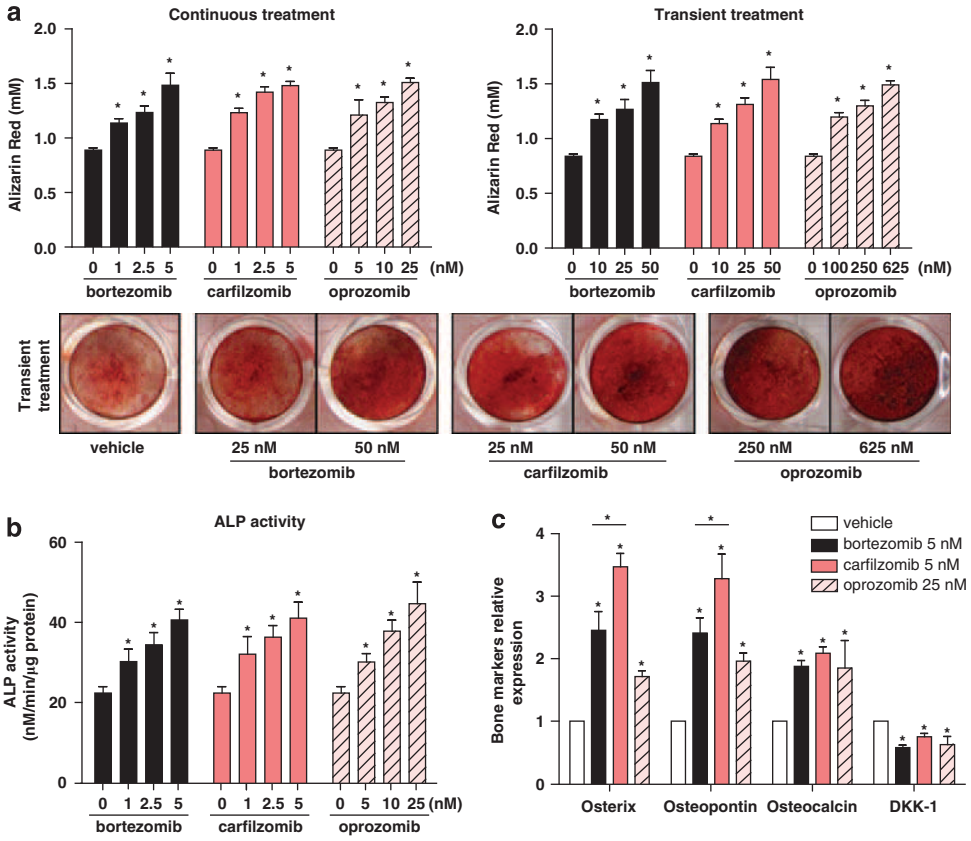

Figure 3. PIs promote osteogenic differentiation and mineralization *in vitro*. (**a**) Primary MSCs from MM patients (6/9 with osteolytic lesions) were cultured in osteogenic medium either in the continuous presence of PIs (left panel) or transiently treated on day 0 for 4 h (right panel). Mineralization was analyzed by alizarin red staining and subsequent dye quantification in OBs differentiated for 21 days; representative images of alizarin red staining following transient treatment are shown. Results are expressed as the mean ± s.d. (**b**) In the presence of PIs and at day 11 of osteogenic differentiation, ALP activity was measured in OBs derived from MSCs from five MM patients (3/5 with osteolytic lesions). Graphs illustrate mean values ± s.e.m. (**c**) Total RNA from the hMSC-TERT cell line was isolated at day 14 of differentiation in the presence of PIs at indicated doses, and expression of osteogenic-related markers (Osterix, osteopontin, osteocalcin) and DKK-1 were evaluated using real-time reverse transcription-PCR. Expression levels for each gene were normalized with respect to GAPDH expression and referred to vehicle control. Data are represented as the mean ± s.d. from three different experiments. In all panels: $*P<0.05$, versus vehicle control or between indicated groups.

Epoxyketone-based PIs exert bone anabolic effects on non-tumor bearing mice.

In vitro evidence suggests that PIs exert cell-autonomous effects on both OCs and OBs. To examine their effects on non-myelomatous bone, PIs were administered to non-tumor bearing immunocompetent C57Bl/6 mice for two weeks. Similar to bortezomib, treatment with carfilzomib or oprozomib increased trabecular bone parameters (Figures 5a and b). All three PIs comparably inhibited OC function as measured by decreased serum levels of collagen breakdown products (carboxy-terminal telopeptide collagen crosslinks) resulting from bone resorption (Figure 5c). Furthermore, all drugs significantly increased OB activity as measured by increased serum levels of N-terminal propeptide of type I procollagen, a marker of bone formation, compared with controls (Figure 5d). Notably, carfilzomib exerted an increase in N-terminal propeptide of type I procollagen that was significantly greater than that obtained with bortezomib. In agreement, double calcein labeling demonstrated that PIs increased bone formation rate (Figure 5e). These data demonstrate that the epoxyketone-based PIs carfilzomib and oprozomib enhance bone volume in healthy mice through both anabolic and anti-catabolic properties that are equipotent to or even superior to that of bortezomib.

Following treatment with anti-cancer agents, it is difficult to discern whether protection from tumor-associated bone loss is due to direct effects on bone cells or indirectly to a decrease in overall tumor burden. To examine the efficacy of PIs in decreasing pathological OC activation without the confounding factor of tumor burden, *in vivo* injection of RANKL (three doses over 50 h[34]) was used to mimic OC stimulation by myeloma cell-derived RANKL. We found that all PIs prevented a RANKL-induced increase in carboxy-terminal telopeptide collagen crosslinks (Figure 5f), demonstrating that this class of compounds exerts direct effects on the activity of pathologically activated OCs.

Carfilzomib and oprozomib decrease MM tumor burden and protect mice from bone destruction

To examine the combined anti-tumor and bone-preserving effects of carfilzomib and oprozomib for therapeutic treatment of established myeloma, we utilized two *in vivo* mouse models. Intravenous injection of 5TGM1-GFP murine myeloma cells into immunocompetent, syngeneic C57Bl/KaLwRij mice yields disseminated tumors with significant bone destruction within 28 days.[51,52] 5TGM1 tumors were established for 14 days after which bortezomib, carfilzomib, or oprozomib were administered on schedules correlating with each drug's clinical dosing (see Materials and Methods). All PIs significantly decreased tumor burden as measured by serum levels of the clonotypic antibody IgG2b (Figure 6a) or by percentage of BM or spleen

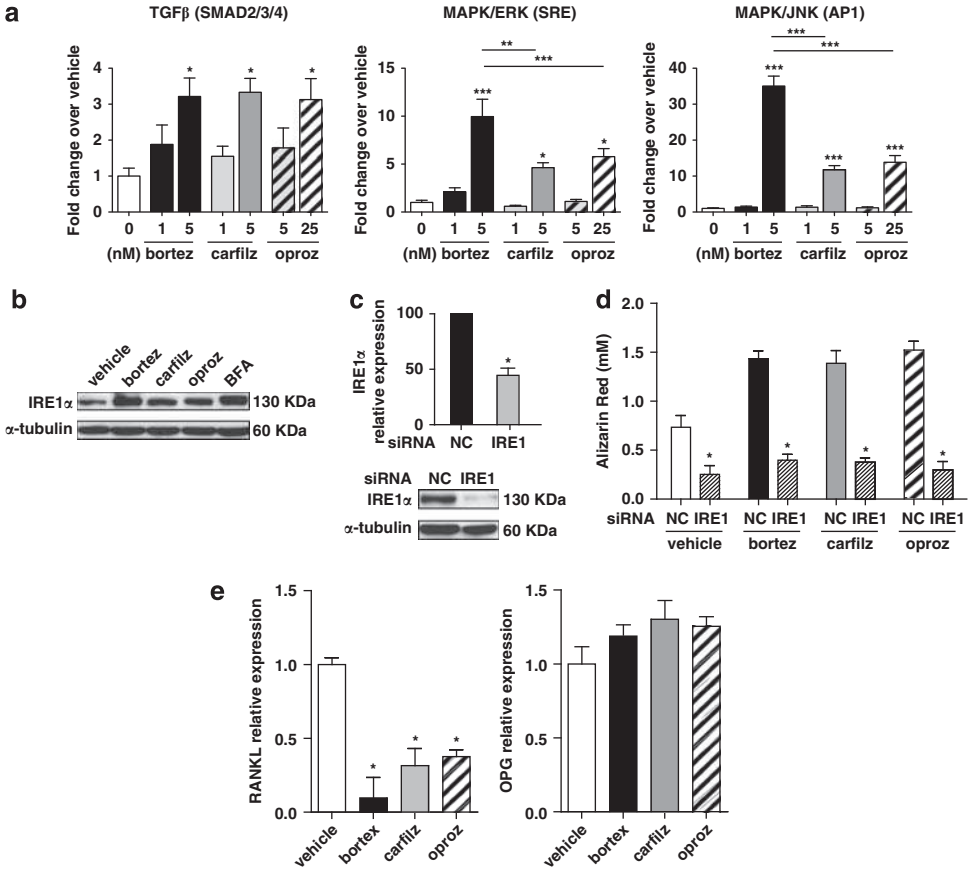

Figure 4. PI treatment diminishes RANKL expression in OBs and promotes osteogenic differentiation and function through activation of the transforming growth factor β (TGFβ), MAPK and UPR pathways. (**a**) Reporter assays demonstrated that the activity of the Smad2/3/4, MAPK/ERK (serum response element; SRE) and MAPK/JNK (AP1) pathways were increased in MC3T3-E1 OB-progenitor cells following 24 h of continuous treatment with PIs; results are expressed as mean ± s.e.m. (**b**) Western blot for the IRE1α component of the UPR in hMSC-TERT cells treated with PIs for 24 h (25 nM bortezomib and carfilzomib, 250 nM oprozomib). Brefeldin A (600 ng/ml) was used as a positive control. (**c**) Expression of IRE1α was reduced at the mRNA and protein levels 48 h after transfection with IRE1 targeting siRNAs. (**d**) The hMSC-TERT cell line was maintained for 14 days in osteogenic medium with PIs (5 nM bortezomib/carfilzomib or 25 nM oprozomib) and transfected 3 times/week with IRE1 targeting or non-targeting (NC) siRNAs. Mineralization was greatly reduced when IRE1α was silenced even in the presence of PIs. (**e**) The hMSC-TERT cell line was maintained in osteogenic medium for 21 days in the presence of PIs and expression of RANKL and osteoprotegerin was assessed by real-time reverse transcription-PCR. Maximal effect on the relative expression of RANKL (day 14) or osteoprotegerin (day 7) is shown; results are expressed as mean ± s.d. In all panels: $*P<0.05$, $**P<0.01$, $***P<0.001$ versus vehicle or between indicated groups.

comprised of GFP-expressing tumor cells (Figures 6b and c). Protection from tumor-induced bone loss was evident by microCT in all PI-treated groups (Figures 6d and e), with serum markers of bone turnover showing significant anti-resorptive (Figure 6f) and bone anabolic (Figure 6g) effects. Notably, although differences within PIs were not statistically significant, a trend toward increased N-terminal propeptide of type-I procollagen activity with carfilzomib and oprozomib versus bortezomib was observed.

Finally, the efficacy of oprozomib was examined in NOD-SCID-IL2Rγ$^{-/-}$ mice bearing established human RPMI-8226-luc myeloma cells. Oprozomib treatment decreased tumor burden as measured by bioluminescent imaging (Figure 7a) and serum levels of human Igλ secreted by RPMI-8226-luc cells (Figure 7b). MicroCT analysis demonstrated marked tumor-associated bone loss in vehicle-treated mice. By contrast, oprozomib-treated mice presented significant increases in trabecular bone parameters (Figures 7c and d). Serum markers of bone turnover showed that oprozomib inhibited bone resorption (Figure 7e) while enhancing bone formation (Figure 7f). In summary, these data demonstrate that orally administered oprozomib exerts *in vivo* anti-myeloma activity along with bone anti-catabolic and anabolic effects in mice bearing human MM.

DISCUSSION

In this report, we have demonstrated that the next generation epoxyketone-based PIs carfilzomib and oprozomib exerted potent anti-myeloma growth effects, inhibited osteoclastogenesis, and resorption, and enhanced OB formation and function *in vitro* under clinically relevant doses and exposure periods. Consistently, these PIs decreased bone resorption and increased bone formation in non-tumor bearing mice while decreasing tumor growth and pathologic bone loss in models of BM-disseminated myeloma. Notably, in both *in vitro* and *in vivo* models, carfilzomib consistently appeared to enhance OB activity to a greater extent than bortezomib (Figures 3c, 5d and 6f), suggesting that this compound may offer an additional benefit to patients by enhancing the extent to which lost bone can be rebuilt.

These data also demonstrate that proteasome inhibition with the orally bioavailable compound, oprozomib, has similar efficacy to intravenously delivered PIs. Although effects were achieved at

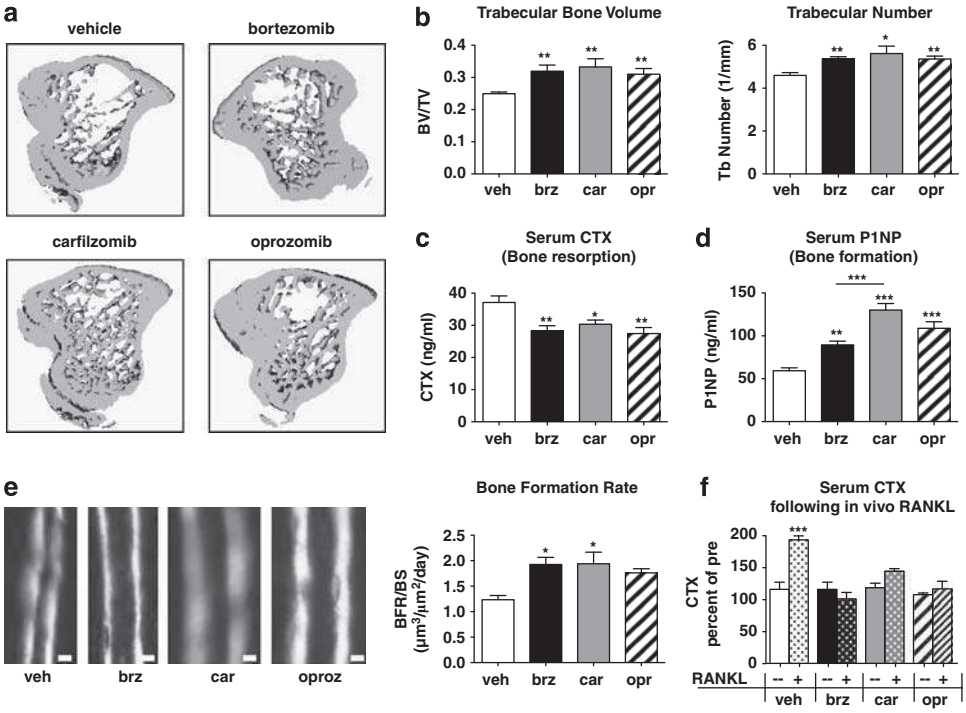

Figure 5. Epoxyketone-based PIs exert bone anabolic effects on non-tumor bearing mice. C57Bl/6 mice ($n = 10$/group) were treated for 2 weeks with vehicle, bortezomib, carfilzomib or oprozomib on dosing schedules outlined in Materials and Methods. (**a**, **b**) MicroCT analyses show that all PIs induced an equivalent increase in trabecular bone volume and number. (**c**) Bone resorption (serum carboxy-terminal telopeptide collagen crosslinks (serum CTX)) was significantly and equivalently decreased with each PI. (**d**) OB function (serum N-terminal propeptide of type I procollagen (serum P1NP)) was significantly increased in all PI-treated animals compared with vehicle-treated. Notably, P1NP levels in carfilzomib-treated mice were significantly greater than those of bortezomib-treated mice. (**e**) Trabecular bone formation rate was measured by double calcein labeling; calcein incorporates into actively mineralizing bone with the distance between labels being proportional to the amount of newly formed bone within the 5-day interlabel period. PI treatment increased the bone formation rate per bone surface (BFR/BS) as assessed by dynamic histomorphometry (Bar = 10 μm). (**f**) PIs inhibited RANKL-induced pathological bone resorption in the absence of tumor. After 2 weeks of PI treatment as above, mice were given three doses of purified RANKL ($n = 5$/drug) or PBS vehicle ($n = 5$) to stimulate OC activity. Serum CTX measured 90 min following the final RANKL dose is expressed as a percent of the same mouse prior to RANKL stimulation. All results are expressed as mean ± s.e.m. $^*P < 0.05$, $^{**}P < 0.01$, $^{***}P < 0.001$ versus vehicle or between indicated groups.

higher concentrations, pharmacokinetic data demonstrate that concentrations well surpassing these doses are readily obtained following oral dosing of oprozomib.[28,40] Importantly, peptide epoxyketones such as carfilzomib and oprozomib, specifically inhibit N-terminal threonine active proteasome subunits in contrast to dipeptide boronates that can also inhibit serine proteases. This difference may account for the favorable toxicity profiles and relatively low rates of peripheral neuropathy associated with epoxyketone PIs.[24,53] This could permit more prolonged and intense dosing regimens, potentially increasing the efficacy of the drug. Bortezomib is dosed on a day 1, day 4 schedule, allowing for full recovery of proteasome activity between doses.[38] In ongoing clinical trials, carfilzomib is dosed intravenously on two subsequent days; experimental evidence suggests that daily dosing is similarly well tolerated, although the necessity for intravenous delivery limits this use in practice.[22,24,25] In current trials, oprozomib is dosed orally on five continuous days. While we demonstrate that single *in vitro* pulse treatments of oprozomib effectively exert anti-tumor, anti-OC, and pro-OB effects, the QDx5 repeated dosing schedule increases the overall period during which proteasome activity is inhibited. Therefore, the continuous treatment of cell cultures *in vitro* may more closely mimic the *in vivo* activity of oprozomib under this regimen. Furthermore, we have observed these effects below the maximal tolerated dose of oprozomib, reported to exceed 50 mg/kg.[27]

The BM microenvironment supports MM cell growth and certain drugs are unable to overcome this protection.[54] In addition to their direct effects on tumor cell survival, PIs also exert indirect anti-tumor effects by rendering the host microenvironment less hospitable. In agreement with data in Waldenstrom's macroglobulinemia,[55] we found that both carfilzomib and oprozomib remained cytotoxic to MM cells co-cultured with BMSCs or OCs. Furthermore, tumor-produced factors can unbalance normal bone turnover resulting in pathological osteolysis, which in turn further stimulates tumor growth.[45] Shifting the bone microenvironment to an anabolic or bone-building state, would then negatively impact myeloma progression.[3] Comparably to bortezomib and other PIs, our data demonstrate that oprozomib and carfilzomib exert direct effects on OCs in part through disruption of RANKL-induced NF-κB signaling,[17,18,30,56] together with reduced expression of integrin αVβ3 and F-actin ring disruption.[30,42] Carfilzomib and oprozomib also modulate OB differentiation and function *in vitro* similarly to bortezomib,[14–16] augmenting bone formation marker expression and increasing ALP activity and bone nodule formation. We have identified the UPR as a novel pathway impacted by PIs that results in enhanced osteoblastogenesis. This is of particular interest as induction of a pro-apoptotic UPR has been shown to be a mechanism by which PIs induce cytoxicity in myeloma cells.[57,58] Thus, agents inducing the UPR may prove beneficial in myeloma owing to both direct anti-tumor[59] and OB-stimulatory effects, similar to PIs. In differentiating OBs, bortezomib,[42] carfilzomib and oprozomib also reduced RANKL expression, therefore diminishing their OC stimulating ability. Other groups have reported that oprozomib may block migration of MM to the bone and decrease angiogenesis.[27] Of note, epoxyketone-based PIs also modulated

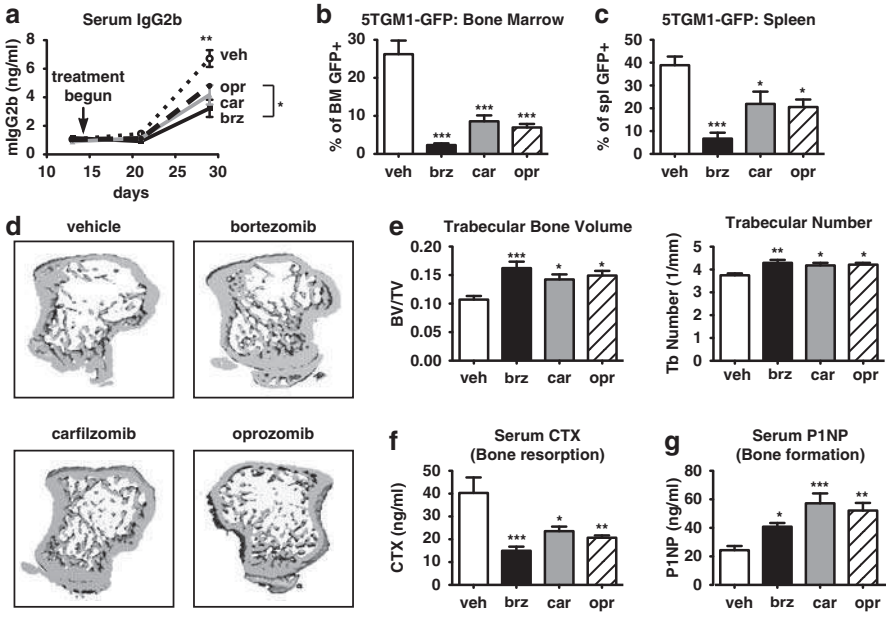

Figure 6. PIs decrease myeloma burden and associated bone destruction in an immunocompetent murine model. 5TGM1-GFP murine myeloma cells were injected into syngeneic C57Bl/KaLwRij mice. After 14 days, mice were randomized into PI treatment groups ($n \geqslant 7$/group) and dosed for an additional 2 weeks. All PIs decreased tumor burden as measured by (**a**) levels of serum IgG2b (clonotype of 5TGM1 cells) and (**b**, **c**) percent of GFP + tumor cells within the BM or spleen upon sacrifice at day 28. (**d**, **e**) MicroCT analysis demonstrated that treatment with PIs protected animals from myeloma-induced loss of trabecular bone volume and number. (**f**) Serum carboxy-terminal telopeptide collagen crosslinks (serum CTX) was significantly decreased and (**g**) serum N-terminal propeptide of type I procollagen (serum P1NP) was significantly increased in all PI-treated animals compared with vehicle-treated animals. All results are expressed as mean ± s.e.m. $^{*}P<0.05$, $^{**}P<0.01$, $^{***}P<0.001$ versus vehicle or between indicated groups.

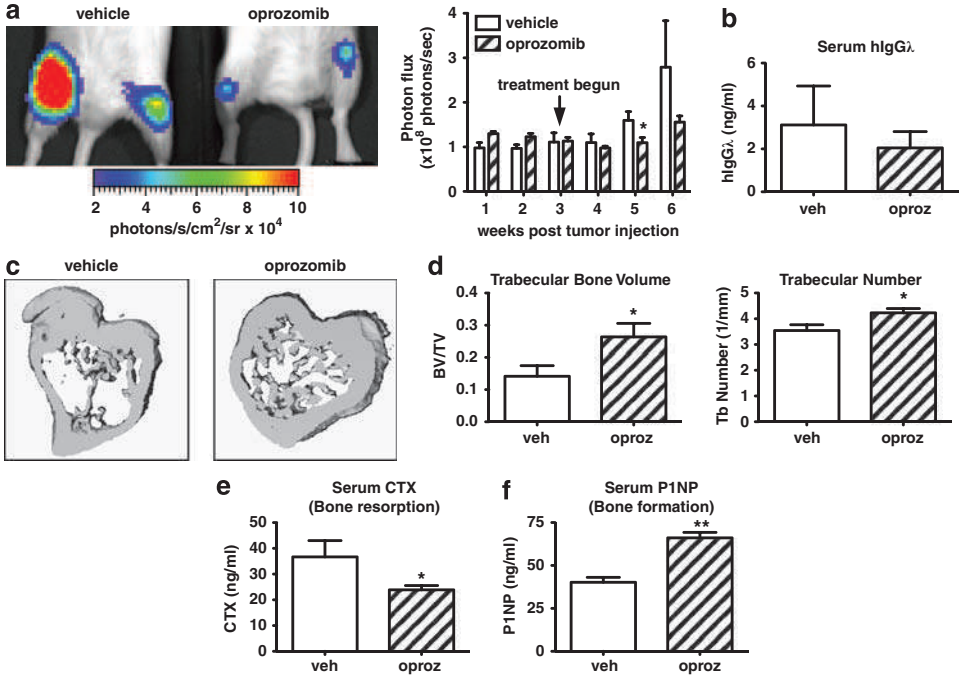

Figure 7. Oprozomib decreases human MM tumor burden and protects mice from bone destruction. Immunocompromised NOD-SCID-IL2R$\gamma^{-/-}$ mice ($n = 5$/group) were intravenously injected with RMPI-8226 human MM cells stably labeled with firefly luciferase. Tumors were allowed to establish for 3 weeks after which mice were randomized into treatment groups. During weeks 3–6 animals were treated with oprozomib ($n = 5$) or vehicle ($n = 5$). (**a**) Tumor burden was monitored weekly by *in vivo* bioluminescence imaging. Mice treated with oprozomib had decreased tumor burden compared with those in the vehicle treated group. Representative image of hind limb tumor burden as visualized on week 6. (**b**) Serum human Igλ (secreted by RPMI-8226 cells) was decreased in oprozomib-treated mice at the time of killing, indicating decreased tumor burden. (**c**, **d**) Although tumor-associated bone loss was evident in vehicle-treated mice, trabecular bone was preserved with oprozomib treatment as measured by micro CT. (**c**) Representative 3D reconstructions. (**d**) Oprozomib significantly increased trabecular bone volume and number. Oprozomib treatment decreased serum carboxy-terminal telopeptide collagen crosslinks (serum CTX) (**e**) and increased serum N-terminal propeptide of type I procollagen (serum P1NP) (**f**). Results are expressed as mean ± s.e.m. $^{*}P<0.05$, $^{**}P<0.01$.

OC and OB activity in non-tumor bearing mice, suggesting that they may be equally effective as an adjuvant therapy in other pathologic bone diseases, including rheumatoid arthritis and osteoporosis.

In summary, the next generation PIs carfilzomib and oprozomib are effective at decreasing both myeloma growth and myeloma-associated bone disease by: (i) direct killing of myeloma cells; (ii) inhibition of OC differentiation and resorption; and (iii) enhancement of OB formation and function. As these drugs progress through clinical trials, prospective studies of bone turnover markers, bone mineral density and documentation of skeletal events would be of particular value to determine whether these new PIs obtain meaningful combined benefits on myeloma and associated bone disease.

CONFLICT OF INTEREST

CJK is an employee of Onyx Pharmaceuticals. All other authors declare no conflict of interest.

ACKNOWLEDGEMENTS

We are grateful to the Washington University MM/MGUS Research Program and Tissue Bank and to Lindsay Goddard, Montserrat Martín, Isabel Isidro, Teresa Prieto and Almudena Martín for their excellent technical work. This research was supported by grants from the National Institutes of Health (T32CA113275:MAH; P01CA100730:KNW; P50CA94056:DP-W), the St Louis Men's Group Against Cancer (KNW), the Holway Myeloma Fund (KNW), the Spanish MICINN-ISCIII (PI081825), the Fundación de Investigación Médica Mutua Madrileña (AP27262008), the Centro en Red de Medicina Regenerativa y Terapia Celular de Castilla y León, the Spanish Myeloma Network Program (RD06/0020/0006 and RD06/0020/0041) and Spanish FIS (PS09/01897). MicroCT services were provided by the WU musculoskeletal core (P30AR057235).

REFERENCES

1 Basak GW, Srivastava AS, Malhotra R, Carrier E. Multiple myeloma bone marrow niche. *Curr Pharm Biotechnol* 2009; **10**: 345–346.
2 Esteve FR, Roodman GD. Pathophysiology of myeloma bone disease. *Best Pract Res Clin Haematol* 2007; **20**: 613–624.
3 Yaccoby S. Osteoblastogenesis and tumor growth in myeloma. *Leuk Lymphoma* 2010; **51**: 213–220.
4 Kumar SK, Rajkumar SV, Dispenzieri A, Lacy MQ, Hayman SR, Buadi FK *et al.* Improved survival in multiple myeloma and the impact of novel therapies. *Blood* 2008; **111**: 2516–2520.
5 Kyle RA, Rajkumar SV. Multiple myeloma. *Blood* 2008; **111**: 2962–2972.
6 de Bettignies G, Coux O. Proteasome inhibitors: Dozens of molecules and still counting. *Biochimie* 2010; **92**: 1530–1545.
7 Dick LR, Fleming PE. Building on bortezomib: s-generation proteasome inhibitors as anti-cancer therapy. *Drug Discov Today* 2010; **15**: 243–249.
8 Hideshima T, Anderson KC. Preclinical studies of novel targeted therapies. *Hematol Oncol Clin North Am* 2007; **21**: 1071–1091viii-ix.
9 Terpos E, Sezer O, Croucher P, Dimopoulos MA. Myeloma bone disease and proteasome inhibition therapies. *Blood* 2007; **110**: 1098–1104.
10 Terpos E, Dimopoulos MA, Sezer O, Roodman D, Abildgaard N, Vescio R *et al.* The use of biochemical markers of bone remodeling in multiple myeloma: a report of the International Myeloma Working Group. *Leukemia* 2010; **24**: 1700–1712.
11 Mukherjee S, Raje N, Schoonmaker JA, Liu JC, Hideshima T, Wein MN *et al.* Pharmacologic targeting of a stem/progenitor population *in vivo* is associated with enhanced bone regeneration in mice. *J Clin Invest* 2008; **118**: 491–504.
12 Pennisi A, Li X, Ling W, Khan S, Zangari M, Yaccoby S. The proteasome inhibitor, bortezomib suppresses primary myeloma and stimulates bone formation in myelomatous and nonmyelomatous bones *in vivo*. *Am J Hematol* 2009; **84**: 6–14.
13 Oyajobi BO, Garrett IR, Gupta A, Flores A, Esparza J, Munoz S *et al.* Stimulation of new bone formation by the proteasome inhibitor, bortezomib: implications for myeloma bone disease. *Br J Haematol* 2007; **139**: 434–438.
14 Giuliani N, Morandi F, Tagliaferri S, Lazzaretti M, Bonomini S, Crugnola M *et al.* The proteasome inhibitor bortezomib affects osteoblast differentiation *in vitro* and *in vivo* in multiple myeloma patients. *Blood* 2007; **110**: 334–338.
15 Qiang YW, Hu B, Chen Y, Zhong Y, Shi B, Barlogie B *et al.* Bortezomib induces osteoblast differentiation via Wnt-independent activation of beta-catenin/TCF signaling. *Blood* 2009; **113**: 4319–4330.
16 De Matteo M, Brunetti AE, Maiorano E, Cafforio P, Dammacco F, Silvestris F. Constitutive down-regulation of Osterix in osteoblasts from myeloma patients: *in vitro* effect of Bortezomib and Lenalidomide. *Leuk Res* 2010; **34**: 243–249.
17 von Metzler I, Krebbel H, Hecht M, Manz RA, Fleissner C, Mieth M *et al.* Bortezomib inhibits human osteoclastogenesis. *Leukemia* 2007; **21**: 2025–2034.
18 Boissy P, Andersen TL, Lund T, Kupisiewicz K, Plesner T, Delaisse JM. Pulse treatment with the proteasome inhibitor bortezomib inhibits osteoclast resorptive activity in clinically relevant conditions. *Leuk Res* 2008; **32**: 1661–1668.
19 Orlowski RZ, Kuhn DJ. Proteasome inhibitors in cancer therapy: lessons from the first decade. *Clin Cancer Res* 2008; **14**: 1649–1657.
20 Richardson PG, Briemberg H, Jagannath S, Wen PY, Barlogie B, Berenson J *et al.* Frequency, characteristics, and reversibility of peripheral neuropathy during treatment of advanced multiple myeloma with bortezomib. *J Clin Oncol* 2006; **24**: 3113–3120.
21 Kuhn DJ, Chen Q, Voorhees PM, Strader JS, Shenk KD, Sun CM *et al.* Potent activity of carfilzomib, a novel, irreversible inhibitor of the ubiquitin-proteasome pathway, against preclinical models of multiple myeloma. *Blood* 2007; **110**: 3281–3290.
22 Demo SD, Kirk CJ, Aujay MA, Buchholz TJ, Dajee M, Ho MN *et al.* Antitumor activity of PR-171, a novel irreversible inhibitor of the proteasome. *Cancer Res* 2007; **67**: 6383–6391.
23 Parlati F, Lee SJ, Aujay M, Suzuki E, Levitsky K, Lorens JB *et al.* Carfilzomib can induce tumor cell death through selective inhibition of the chymotrypsin-like activity of the proteasome. *Blood* 2009; **114**: 3439–3447.
24 Singhal SB, DSd Siegel, Martin T, Vij R, Wang M, Jakubowiak AJ *et al.* Pooled safety analysis from phase (Ph) 1 and 2 studies of carfilzomib (CFZ) in patients with relapsed and/or refractory multiple myeloma (MM). *Blood* 2010; **116**: abstract 1954.
25 Vij R, Wang M, Kaufman JL, Lonial S, Jakubowiak AJ, Stewart AK *et al.* An open-label, single-arm, phase 2 (PX-171-004) study of single-agent carfilzomib in bortezomib-naive patients with relapsed and/or refractory multiple myeloma. *Blood* e-pub ahead of print 3 May 2012, doi:10.1182/blood-2012-03-414359.
26 Zhou HJ, Aujay MA, Bennett MK, Dajee M, Demo SD, Fang Y *et al.* Design and synthesis of an orally bioavailable and selective peptide epoxyketone proteasome inhibitor (PR-047). *J Med Chem* 2009; **52**: 3028–3038.
27 Chauhan D, Singh AV, Aujay M, Kirk CJ, Bandi M, Ciccarelli B *et al.* A novel orally active proteasome inhibitor ONX 0912 triggers *in vitro* and *in vivo* cytotoxicity in multiple myeloma. *Blood* 2011; **116**: 4906–4915.
28 Papadopoulos KP, Mendelson DS, Tolcher AW, Patnaik A, Burris HA, Rasco DW *et al.* A phase I, open-label, dose-escalation study of the novel oral proteasome inhibitor (PI) ONX 0912 in patients with advanced refractory or recurrent solid tumors. *J Clin Oncol* 2011; **29**: abstract 3075.
29 Garrett IR, Chen D, Gutierrez G, Zhao M, Escobedo A, Rossini G *et al.* Selective inhibitors of the osteoblast proteasome stimulate bone formation *in vivo* and *in vitro*. *J Clin Invest* 2003; **111**: 1771–1782.
30 Ang E, Pavlos NJ, Rea SL, Qi M, Chai T, Walsh JP *et al.* Proteasome inhibitors impair RANKL-induced NF-kappaB activity in osteoclast-like cells via disruption of p62, TRAF6, CYLD, and IkappaBalpha signaling cascades. *J Cell Physiol* 2009; **220**: 450–459.
31 Carvajal-Vergara X, Tabera S, Montero JC, Esparis-Ogando A, Lopez-Perez R, Mateo G *et al.* Multifunctional role of Erk5 in multiple myeloma. *Blood* 2005; **105**: 4492–4499.
32 Garrett IR, Dallas S, Radl J, Mundy GR. A murine model of human myeloma bone disease. *Bone* 1997; **20**: 515–520.
33 Garcia-Gomez A, Ocio EM, Crusoe E, Santamaria C, Hernandez-Campo P, Blanco JF *et al.* Dasatinib as a bone-modifying agent: anabolic and anti-resorptive effects. *PLoS One* 2012; **7**: e34914.
34 Tomimori Y, Mori K, Koide M, Nakamichi Y, Ninomiya T, Udagawa N *et al.* Evaluation of pharmaceuticals with a novel 50-hour animal model of bone loss. *J Bone Miner Res* 2009; **24**: 1194–1205.
35 Lane NE, Yao W, Nakamua MC, Humphrey MB, Kimmel D, Huang X *et al.* Mice lacking the integrin beta5 subunit have accelerated osteoclast maturation and increased activity in the estrogen-deficient state. *J Bone Miner Res* 2005; **20**: 58–66.
36 Hapidin H, Othman F, Soelaiman IN, Shuid AN, Luke DA, Mohamed N. Negative effects of nicotine on bone-resorbing cytokines and bone histomorphometric parameters in male rats. *J Bone Miner Metab* 2007; **25**: 93–98.
37 Gross S, Piwnica-Worms D. Real-time imaging of ligand-induced IKK activation in intact cells and in living mice. *Nat Methods* 2005; **2**: 607–614.
38 Papandreou CN, Daliani DD, Nix D, Yang H, Madden T, Wang X *et al.* Phase I trial of the proteasome inhibitor bortezomib in patients with advanced solid tumors with observations in androgen-independent prostate cancer. *J Clin Oncol* 2004; **22**: 2108–2121.
39 Moreau P, Coiteux V, Hulin C, Leleu X, van de Velde H, Acharya M *et al.* Prospective comparison of subcutaneous versus intravenous administration of bortezomib in patients with multiple myeloma. *Haematologica* 2008; **93**: 1908–1911.

40 O'Connor OA, Stewart AK, Vallone M, Molineaux CJ, Kunkel LA, Gerecitano JF *et al.* A phase 1 dose escalation study of the safety and pharmacokinetics of the novel proteasome inhibitor carfilzomib (PR-171) in patients with hematologic malignancies. *Clin Cancer Res* 2009; **15**: 7085–7091.
41 Abe M, Hiura K, Wilde J, Shioyasono A, Moriyama K, Hashimoto T *et al.* Osteoclasts enhance myeloma cell growth and survival via cell-cell contact: a vicious cycle between bone destruction and myeloma expansion. *Blood* 2004; **104**: 2484–2491.
42 Breitkreutz I, Raab MS, Vallet S, Hideshima T, Raje N, Mitsiades C *et al.* Lenalidomide inhibits osteoclastogenesis, survival factors and bone-remodeling markers in multiple myeloma. *Leukemia* 2008; **22**: 1925–1932.
43 Vaananen HK, Laitala-Leinonen T. Osteoclast lineage and function. *Arch Biochem Biophys* 2008; **473**: 132–138.
44 Nakamura I, Duong le T, Rodan SB, Rodan GA. Involvement of alpha(v)beta3 integrins in osteoclast function. *J Bone Miner Metab* 2007; **25**: 337–344.
45 Weilbaecher KN, Guise TA, McCauley LK. Cancer to bone: a fatal attraction. *Nat Rev Cancer* 2011; **11**: 411–425.
46 Matsumoto T, Abe M. TGF-beta-related mechanisms of bone destruction in multiple myeloma. *Bone* 2011; **48**: 129–134.
47 Chen G, Deng C, Li Li YP.. TGF-beta and BMP signaling in osteoblast differentiation and bone formation. *Int J Biol Sci* 2012; **8**: 272–288.
48 Choi YH, Gu YM, Oh JW, Lee KY. Osterix is regulated by Erk1/2 during osteoblast differentiation. *Biochem Biophys Res Commun* 2011; **415**: 472–478.
49 Lee KS, Hong SH, Bae SC. Both the Smad and p38 MAPK pathways play a crucial role in Runx2 expression following induction by transforming growth factor-beta and bone morphogenetic protein. *Oncogene* 2002; **21**: 7156–7163.
50 Tohmonda T, Miyauchi Y, Ghosh R, Yoda M, Uchikawa S, Takito J *et al.* The IRE1alpha-XBP1 pathway is essential for osteoblast differentiation through promoting transcription of Osterix. *EMBO Rep* 2011; **12**: 451–457.
51 Dallas SL, Garrett IR, Oyajobi BO, Dallas MR, Boyce BF, Bauss F *et al.* Ibandronate reduces osteolytic lesions but not tumor burden in a murine model of myeloma bone disease. *Blood* 1999; **93**: 1697–1706.
52 Edwards CM, Lwin ST, Fowler JA, Oyajobi BO, Zhuang J, Bates AL *et al.* Myeloma cells exhibit an increase in proteasome activity and an enhanced response to proteasome inhibition in the bone marrow microenvironment *in vivo*. *Am J Hematol* 2009; **84**: 268–272.
53 Arastu-Kapur S, Anderl JL, Kraus M, Parlati F, Shenk KD, Lee SJ *et al.* Nonproteasomal targets of the proteasome inhibitors bortezomib and carfilzomib: a link to clinical adverse events. *Clin Cancer Res* 2011; **17**: 2734–2743.
54 Chauhan D, Auclair D, Robinson EK, Hideshima T, Li G, Podar K *et al.* Identification of genes regulated by dexamethasone in multiple myeloma cells using oligonucleotide arrays. *Oncogene* 2002; **21**: 1346–1358.
55 Roccaro AM, Sacco A, Aujay M, Ngo HT, Azab AK, Azab F *et al.* Selective inhibition of chymotrypsin-like activity of the immunoproteasome and constitutive proteasome in Waldenstrom macroglobulinemia. *Blood* 2010; **115**: 4051–4060.
56 Zavrski I, Krebbel H, Wildemann B, Heider U, Kaiser M, Possinger K *et al.* Proteasome inhibitors abrogate osteoclast differentiation and osteoclast function. *Biochem Biophys Res Commun* 2005; **333**: 200–205.
57 Lee AH, Iwakoshi NN, Anderson KC, Glimcher LH. Proteasome inhibitors disrupt the unfolded protein response in myeloma cells. *Proc Natl Acad Sci USA* 2003; **100**: 9946–9951.
58 Obeng EA, Carlson LM, Gutman DM, Harrington Jr WJ, Lee KP, Boise LH. Proteasome inhibitors induce a terminal unfolded protein response in multiple myeloma cells. *Blood* 2006; **107**: 4907–4916.
59 Davenport EL, Moore HE, Dunlop AS, Sharp SY, Workman P, Morgan GJ *et al.* Heat shock protein inhibition is associated with activation of the unfolded protein response pathway in myeloma plasma cells. *Blood* 2007; **110**: 2641–2649.

Supplementary Information accompanies the paper on the Leukemia website (http://www.nature.com/leu)